High resolution seismic reflection to characterize small scale mechanisms of large scale natural dissolution in the Hutchinson Salt Member

by

Brett E. Judy

Submitted to the Department of Geology
and the Faculty of the Graduate School of the University of Kansas
in partial fulfillment of the requirements for the degree of
Master of Science

Advisory Committee:

_____

Richard D. Miller, Chairman

_____

Don W. Steeples

_____

J. Douglas Walker

Date Defended: _____02-13-2015_____

The Thesis Committee for Brett E. Judy certifies that this
is the approved version of the following thesis:

High resolution seismic reflection to characterize
small scale mechanisms of large scale natural
dissolution in the Hutchinson Salt Member

_____

Richard D. Miller, Chairman

Date approved: _____02-13-2015_____

Abstract

High resolution seismic reflection imaging of the local scale processes along the eastern natural dissolution front of the Hutchinson Salt Member were correlated with its regional scale progression to define a more complete dissolution model that accounts for all observations along the front. 2-D high resolution seismic reflection imaging suggests dissolution along the eastern margin has resulted in a complex system of dissolution channels that have intruded westward into the salt body. Anomalous thinning of the rock salt and resulting sinkholes imaged between 8-20 km from the dissolution front provide evidence to support protruding dissolution has extended west into the salt body in a very irregular fashion. Subsidence features along the eastern margin appear to increase in width (>700 m) due to episodic re-activation of subsidence after long periods of dormancy. Time varying access to unsaturated water continues to expand these dissolution corridors and is forming expansive solution networks that grossly make up the dissolution front. It is suggested that dissolution is predominantly progressed horizontally through the salt interval driven by both hydrologic and geologic influences. Geometric distortion of reflections from the salt interval indicate recent activity (e.g. Brandy Lake) and dormant paleo dissolution networks that discontinuously span a zone approximately 6 km wide along the eastern margin of the Hutchinson salt.

High resolution seismic imaging of subsidence related to Brandy Lake is indicative of the complex dissolution history along the front. This dynamic dissolution zone has resulted in the formation of four seismically identified and interpreted subsidence episodes that directly correspond to recent road subsidence along the western flank of Brandy Lake. This unique growth structure represents the continued westward encroachment of horizontally driven dissolution channels into the salt.

Acknowledgments:

I would like to acknowledge and thank everyone on my thesis committee: Rick Miller who provided me with a great opportunity, imparted his knowledge to me and who helped me through revisions of a very rough first draft; Don Steeples for both revisions and his past research which was often consulted during the processing of my data; Doug Walker for his support and work through the revision process

I would also like to thank my co-workers: Shelby Peterie for her direction and guidance throughout my time in Kansas; Julian Ivanov for his knowledge and assistance during processing (and dietary council); Mary Brohammer for her assistance with software licenses and figure creation; all the students who I have worked with at the Kansas Geological Survey for their advice and assistance (and donuts). I would also like to thank my wife Cynthia who has been a support throughout my academic career and for her aid in the creation of figures.

Table of Contents

List of Figures

List of Tables

Introduction

A multitude of studies have attempted to accurately describe the mechanisms and progression of dissolution induced subsidence of the Hutchinson Salt Member in central Kansas. No previous study has accounted for all observations along the eastern dissolution margin of the Hutchinson Salt. This is the first study to shed light on all the processes responsible for the westward progressing natural dissolution front. This is also the first study to attempt to correlate the regional scale progression with that of local scale processes imaged using the high resolution seismic reflection method, to provide a more complete model of the front. The development scheme outlined in this work accounts for all observations along the dissolution front, many not described before and some previously without explanation.

Dissolution of bedded rock salt can result in sinkholes and confinement breaches that degrade valuable freshwater aquifers with brackish waters. Sinkholes pose a threat to transportation, infrastructure, property and human safety (Beck et al, 1999). Contamination of fresh water aquifers with salt water due to breaches in confining layers affects the suitability of water for public use (Leonard and Kleinschmidt, 1976; Gogel, 1981). Surface subsidence and associated water contamination in central Kansas is often associated with leaching of the Lower Permian Hutchinson Salt Member (Walters, 1978) (Figure 1). Leaching episodes within the Hutchinson Salt Member can be natural occurring or proceed fully by anthropogenic activity such as breached brine disposal wells or salt mining. The most active zone of natural induced dissolution in Kansas is located along the eastern edge of the Hutchinson Salt Member and commonly referred to as the natural dissolution front (Walters, 1978; Watney and Paul, 1980; Anderson et al., 1995; Miller, 2002; Miller, 2003) (Figure 1). The risks associated with the

westward progressing natural dissolution front and the resulting surface subsidence necessitates a thorough delineation and understanding of its processes and progression.

Over the last 50 years researchers at the Kansas Geological Survey have used seismic reflection data, well data, elevation data and surface subsidence to try and piece together the progression and processes associated with the dissolution front and natural induced surface subsidence (Walters, 1978; Watney and Paul, 1980; Anderson et al., 1994; Anderson et al., 1995; Miller, 2007; Herrs, 2010). Well data and segments of 2-D seismic reflection data have provided the majority of the information about the dissolution front (Walters, 1978; Watney and Paul, 1980; Miller, 2002; Nissen and Watney, 2003; Miller et al., 2005). The high resolution seismic reflection method has proven to be an effective tool imaging stratigraphic and structural features related to salt dissolution in Kansas.

Early seismic reflection investigations relating to salt leaching in Kansas were used to establish the utility of the reflection method and to improve the understanding of the relationship between surface expression and subsurface processes (Steeples, 1980; Steeples et al., 1986; Knapp et al., 1989). The success of these initial studies led to methodology development and further seismic reflection investigations focused on understanding the stress fields and dissolution extent associated with voids and the subsidence failure processes (Anderson et al., 1995; Miller et al., 1997; Miller, 2007). Continued advancements in processing methodologies, source bandwidth, and signal-to-noise over the past 30 years were driven by near surface seismic studies (Coruh and Costain, 1983; Knapp and Steeples, 1986; Miller, 1992; Steeples and Miller, 1998). These improvements have resulted in higher resolution and improved clarity of subsidence structures that has facilitated considerable increases in understating of their failure

mechanics, development stages and predictions for future growth (Miller et al., 1997; Miller, 2002; Lambrecht, 2006).

Past seismic investigations have focused on single or closely grouped subsidence features and not on the large scale mechanisms of natural dissolution along the eastern margin of the Hutchinson Salt. Some of these studies have attempted to extrapolate the progression of the dissolution front from these seismically imaged structures (Anderson, et al., 1994; Anderson, et al., 1998) However, these studies were limited by the narrow scope of the seismic data and have been shown to possess questionable seismic interpretations due to processing flows that lacked tuning (Miller, 2007). This is the first study to utilize the high resolution seismic reflection method to create an extensive (22 km) profile of the eastern margin of the Hutchinson Salt.

Research Focus

For the past 40 years the prevailing concept about the eastern margin of the salt is that a distinct and relatively continuous (north to south) main dissolution front exists (Walters, 1978, Anderson et al., 1994; Anderson et al., 1998; Herrs, 2010) (Figure 2). The main front has been characterized by a gradual stepwise thinning of the salt interval towards the east over a zone ranging from 5 – 10 km in width with the hypothesis that the salt is being leached in a relatively continuous westward progression (Anderson et al., 1994). The dissolution process related to this model is suspected to be mostly driven by geologic flow systems (faults and fracture zone) and overburden collapse that has resulted from salt removal (Anderson et al., 1994; Watney et al., 2003). Unsaturated surficial waters are thought to then access the salt through these vertical conduits resulting in leaching of the upper salt interval. It has also been suggested that natural

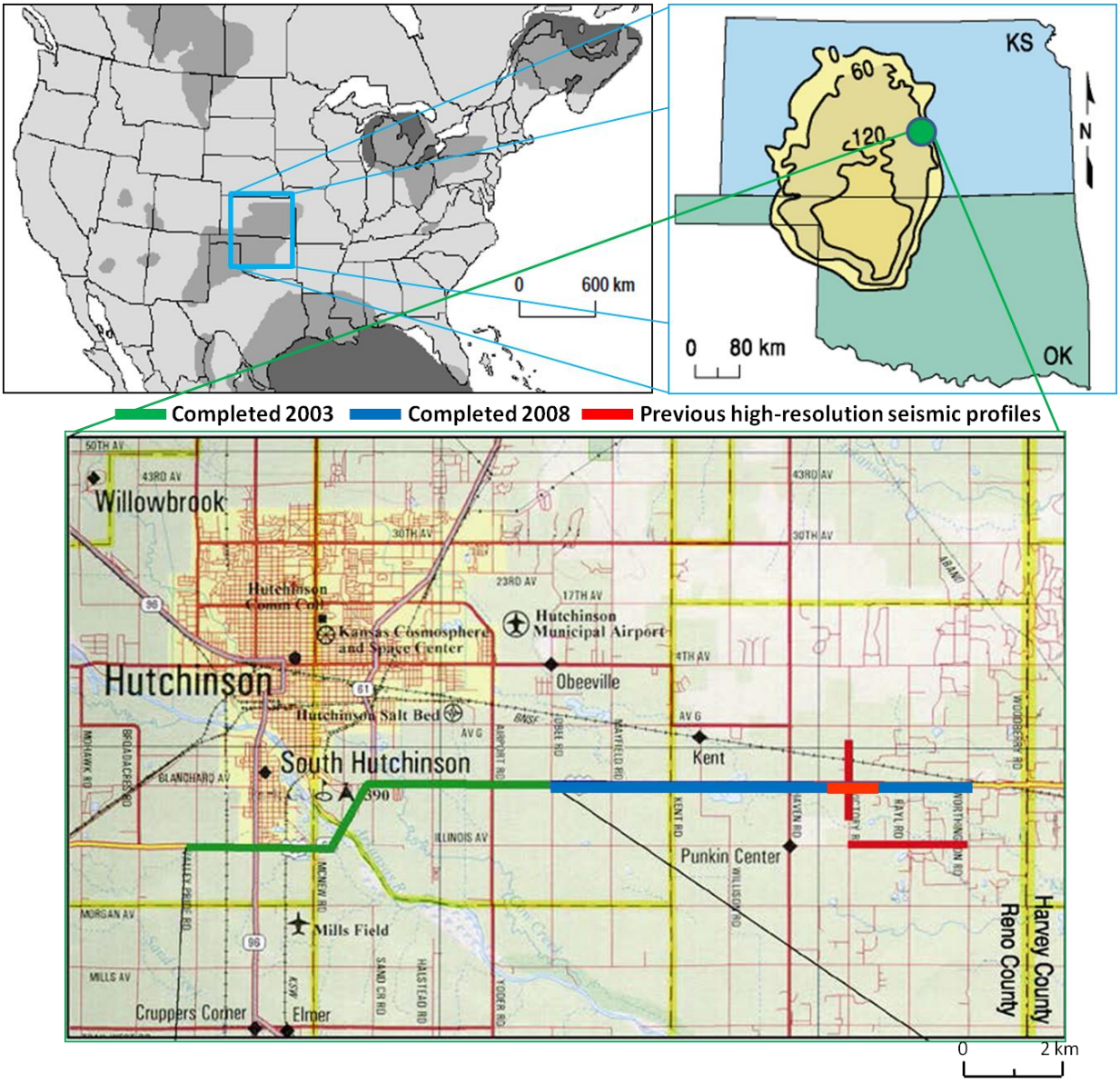

Figure 1: (top-left) Locations of salt basins in North America, indicated by dark shading (Ege, 1984). (top-right) Isopach of the Permian aged Hutchinson Salt member in meters. The high gradient eastern edge is the result of the westward progressing natural dissolution front (modified from Walters, 1978). (bottom) Seismic survey lines completed by the Kansas Geological Survey in 2003 and 2008 along U.S. highway 50. Red lines depict locations of previous high-resolution seismic data acquisition (Modified from Miller, 2006).

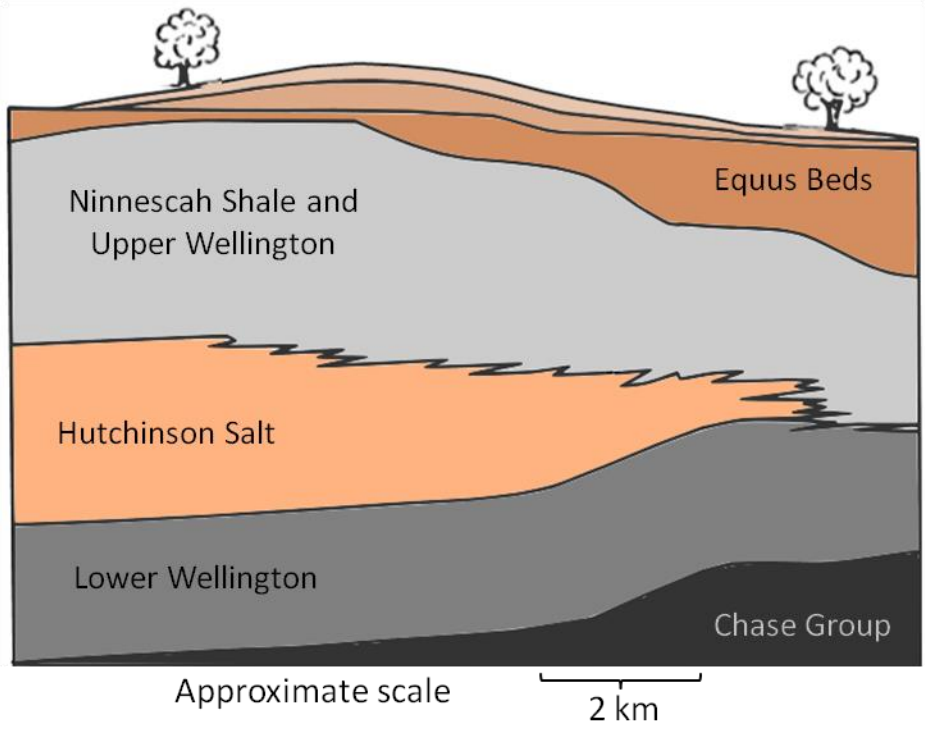

Figure 2: Generalized depiction of the currently accepted dissolution model of the eastern dissolution front of the Hutchinson Salt. This gradual ramp-style dissolution front has been the accepted model for more than 40 years. However, this model is over simplified and not consistent with observations along the dissolution front.

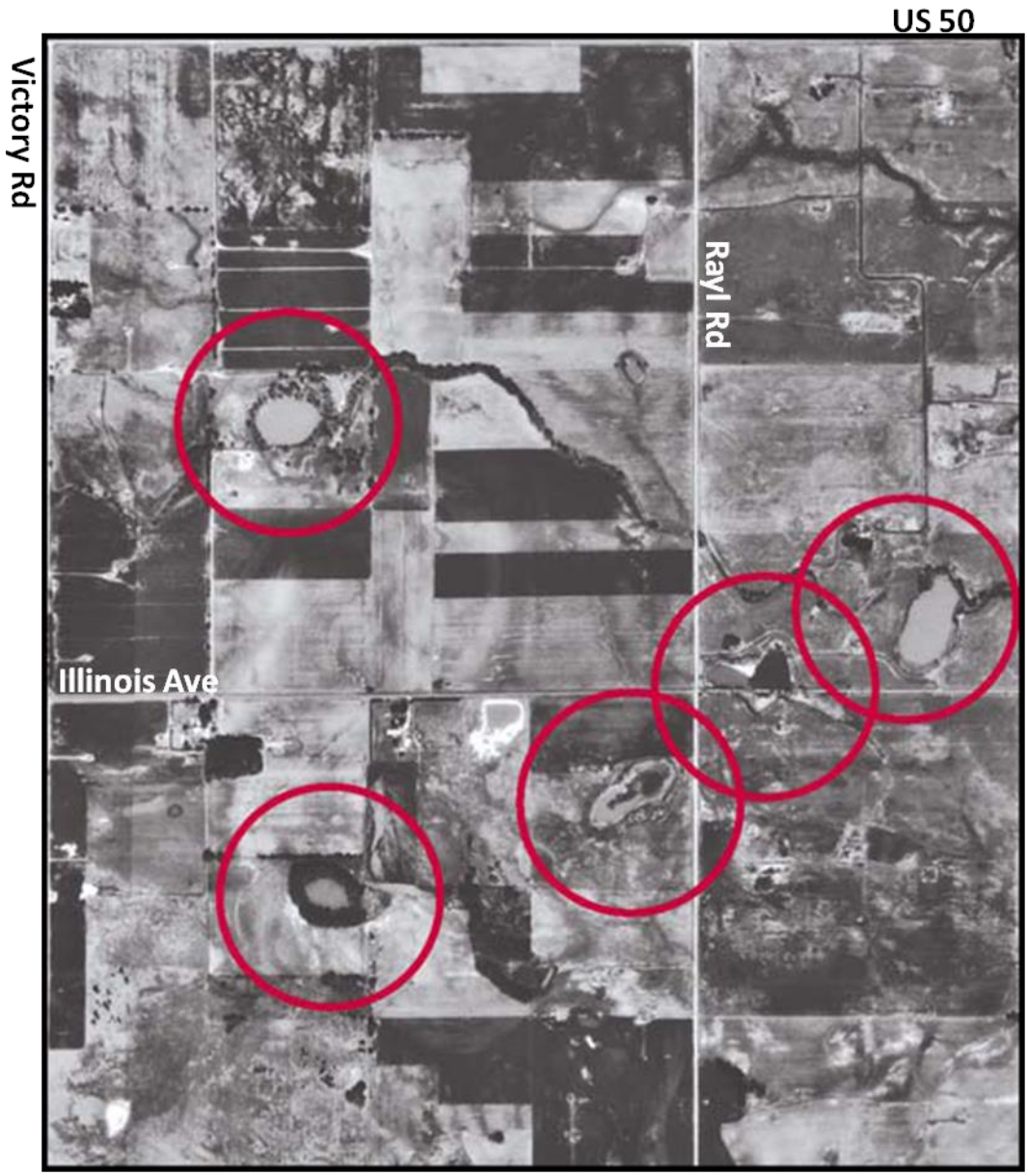

Figure 3: Ortho-photo showing a suspected pattern of dissolution near the front in Reno County, Kansas. This is located just south of U.S. 50.

dissolution is relatively confined to within the span of this ramp-style dissolution front (Anderson et al., 1994).

Several observations and recent evidence appear to not be fully accounted for in this dissolution model such as paleo-sinkholes inadvertently imaged on seismic data ranging over 20 km west of the front, the lack of subsidence events occurring along fault and fracture systems throughout the main body of the Hutchinson Salt, and patterns of dissolution indicated by surface expressions extending away from the front (Miller and Henthorne, 2004) (Figure 3). With the long-term goal of identification and delineation of potential hazards associated with the dissolution front, further clarity of the fronts natural dissolution patterns are investigated along a recently active 2-D seismic reflection profile.

In 2003 the Kansas Geological Survey acquired seismic data over a 10-km stretch of U.S. Highway 50 in Reno County, Kansas (Figure 1). The survey was collected over a region where ground stability has been a concern in recent history due to abandoned and unmapped solution mining activities within close proximity of the roadway (Miller and Henthorne, 2004). The primary objectives of the study were to identify and seismically characterize the Hutchinson Salt Member beneath a proposed alignment of the U.S. 50 bypass around the city of Hutchinson (Miller et al., 2005). A 12-km eastward continuation of the 2003 survey was collected in the summer of 2008 and is the focus of this study (Figure 1). The purpose of the 2008 survey was to study the Hutchinson Salt Member across the most disturbed section of the salt along the eastern dissolution edge with a particular focus on natural processes. This 12 km extension of the seismic survey was to delineate at high spatial resolution the natural dissolution features and the characteristics driving the westward progression of the front.

Current and past surface subsidence at Brandy Lake is also very diagnostic of the progression and hydrology of dissolution along the front. This lake was crossed during the 2008 survey and is one of the focus areas of this research (Figure 4). The lake is located 9 km east of Hutchinson and is a sinkhole, or combination of sinkholes, that resulted from subsidence that occurred prior to construction of U.S. 50 (Miller, 2007; Herrs, 2010). Subsidence reactivated since the last re-surfacing along its western edge in the late 1990s (Herrs, 2010). Lidar data collected by Herrs (2010) from February 2009 to November 2009 in response to the recent surface subsidence indicates this depression along U.S.50 has affected over 350 m of road with a maximum subsidence magnitude over 1.25 m (Figure 4). Analysis of the time-lapse LiDAR data indicates surface subsidence was dormant over the 10 month span of intermittent data collection (Herrs, 2010). Unlike the characteristic bowl shaped depression common with some single episode sinkholes, the depression along the road surface is asymmetric suggesting a complex (multi-episode) subsidence progression. Uncovering the leaching process along this dynamic dissolution zone can provide unique insight into its growth process that may be analogous to the eastern margin of the Hutchinson Salt.

The continuous 22 km seismic profile along U.S. 50 is the only seismic line that extends from undisturbed salt through the borehole-mapped dissolution front (Watney and Paul, 1980). Primary objectives of this study were:

- Delineation and mapping of subsidence structures defining the westward encroachment of the Permian Hutchinson Salt dissolution front
- Identify changes in the reflection characteristics (amplitude, geometry) within the Hutchinson Salt that may indicate the progression and extent of dissolution along this cross section

- Delineate the recently active subsurface expression that has posed a threat to highway stability west of Brandy Lake

These seismic data will provide a snapshot of the current expression and processes associated with the westward thinning of the Hutchinson Salt Member along this cross section, its relationship to recent subsidence and some geologic time frame of the dissolution process.

Geologic Background of Reno County, Kansas

During the Permian, Kansas was part of a shallow marine shelf sloping to the south providing an inlet to the sea. Alternating open marine and stranded sea depositional environments persisted throughout the period (Merriam, 1963). The material deposited during the cyclic sea level change consisted of some sand and silt deposits originating inland but mostly resulted from a cyclic Permian sea. The stranded nature of the sea resulted in thick evaporate deposits with the open inlet providing new brackish fluid during high sea levels. (Merriam, 1963; West, et al., 2010).

The interval of interest for this survey is within the Permian-aged Sumner Group in Reno County that consists of the Wellington Formation and the Ninnescah Shale (Norton, 1939). . Currently this sedimentary sequence dips gently to the west within the study area at approximately 6 m/km (Watney et al., 2003). The Wellington Formation can be divided into three contacts identifiable on the seismic data. These contacts are between the lower Wellington member, the Hutchinson Salt member, and the upper Wellington member (Gogel, 1981). The lower Wellington is largely composed of gray shale but has been described as the “anhydrite beds” (Ver Wiebe, 1937) due to the many cyclical anhydrite layers interbedded within the shale

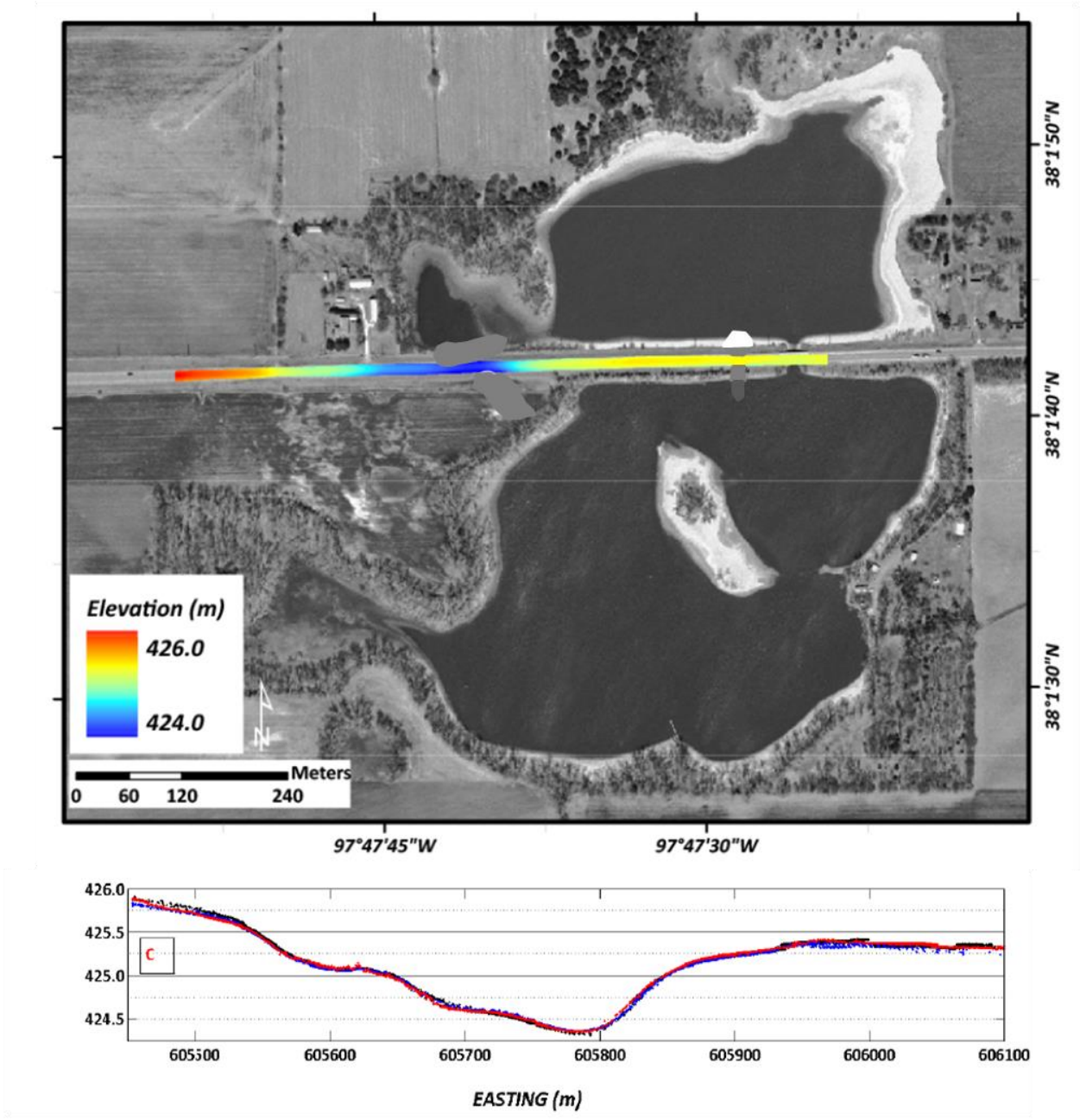

Figure 4: (top) Arial view image of Brandy Lake. LiDAR elevation profile was completed along U.S. 50 due to recent road deformation along the western edge of Brandy Lake. A maximum surface subsidence of 1.25 meters was identified. (modified from Herrs, 2010)(bottom) Elevation profile from LiDAR data corresponding to the road surface west of Brandy Lake.

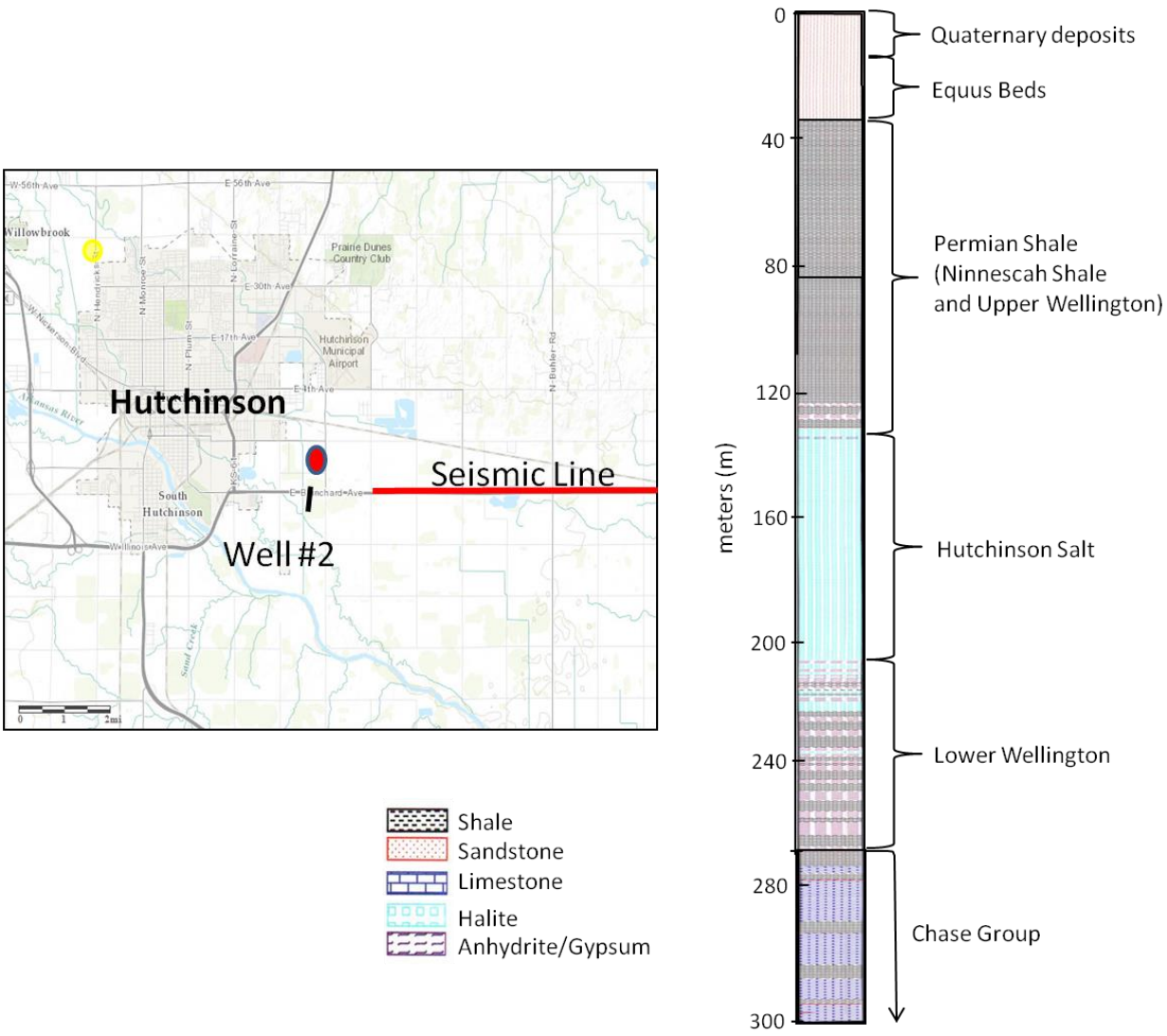

Figure 5: (right) Geology log from well WD#2 owned by the City of Hutchinson indicating depths to Lower Permian units near the area of interest. (left) Map showing well proximity to the 2008 U.S. 50 seismic survey.

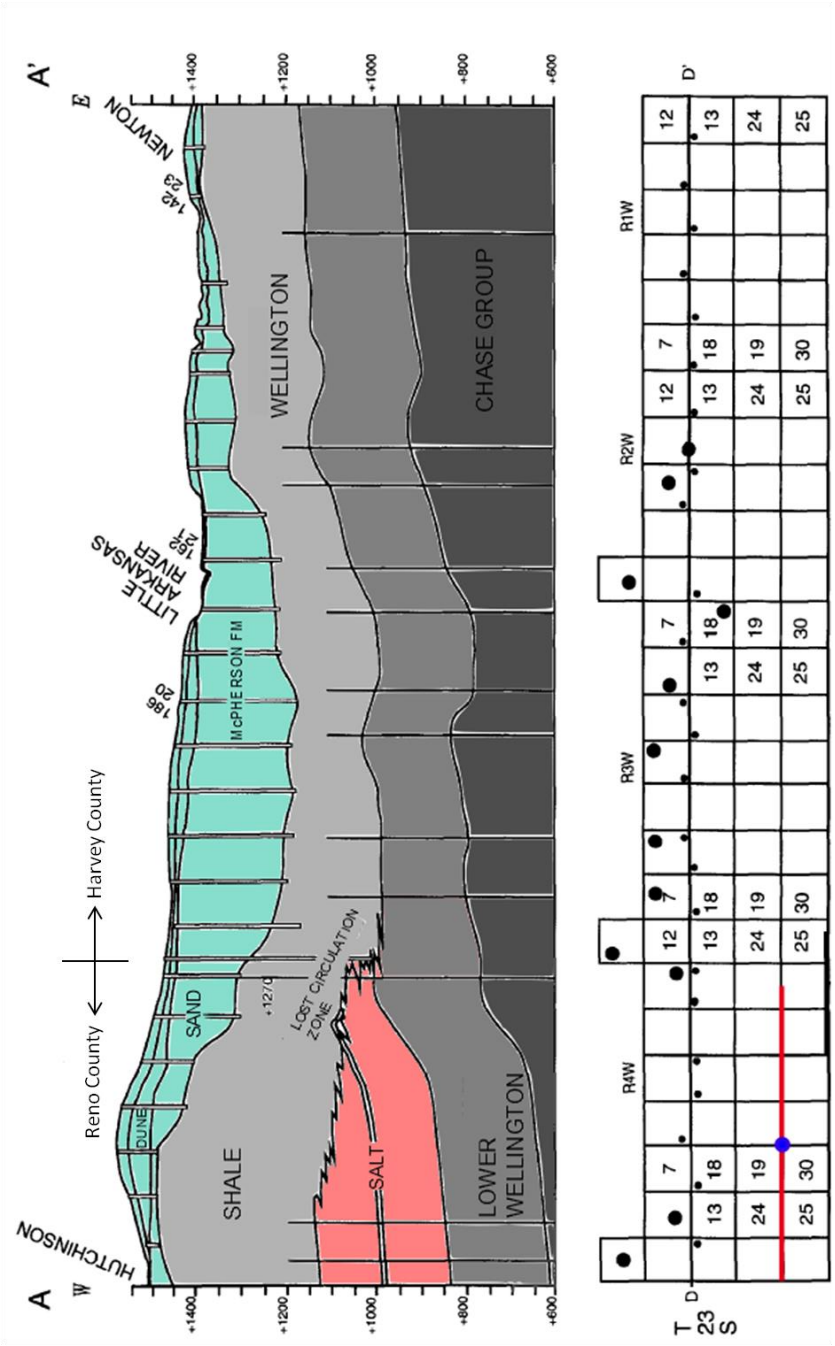

Figure 6: West to east cross-section between Hutchinson and Newton depicting the salt dissolution front and the highly deformed Permian beds above the salt interval. Equus Bed deposits thicken as a result of increased accommodation space caused by subsidence (McPherson Channel). Location of the seismic line (red line), wells (shallow, small dots; deep, large dots) and Brandy Lake (blue dot) are indicated (Modified from Walters, 1980)**.**

interval. The lower Wellington is largely composed of gray shale with thin anhydrite and gypsum beds (Bayne, 1956; Gogel, 1981). The upper Wellington also is predominantly gray shale with intermittal gypsum, anhydrite, and dolomite (Gogel, 1981). Overlying the Wellington Formation is the Ninnescah Shale which is considered the bedrock within the study area and is composed of red to reddish-brown shale with some interbedded anhydrite and gypsum (Gogel, 1981). Geology logs from a borehole located immediately west (≈1.5 km) of the 2008 seismic survey place the top of the Chase Group at 265 m, the top of the Hutchinson Salt at 133 m, the top of the Upper Wellington at 80 m and the top of the Ninnescah Shale at 35 m (Figure 5). A cross section (Walters, 1980) created from well log data 4 km to the north of the seismic line indicates significant depth variability along the eastern dissolution margin (Figure 6).

Throughout much of the Tertiary, south and central Kansas was subjected to heavy erosion which removed any Mesozoic and Tertiary deposits (Bayne, 1956). This has resulted in the Permian rocks within the study area being unconformably overlain by Pliocene-Pleistocene deposits. Known as the Equus beds aquifer, these Pliocene-Pleistocene deposits are the primary groundwater supply for the region and are predominantly composed of unconsolidated accumulations of silt, clay, sand and gravel (Spinazola, et al., 1985). The Equus Beds are overlain by Quaternary deposits that make up the current surface sediments. Combined the Equus Beds and Quaternary deposits make up roughly the upper 35 m below the ground surface (Spinazola, et al., 1985).

Hutchinson Salt Member

The extent of the Hutchinson Salt has been mapped as a product of oil and gas exploration through penetration and logging data from over 80,000 boreholes throughout the state (Walters, 1978). This laterally persistent member is present in the subsurface through a

significant portion of south-central and central Kansas, extending over an area of approximately 95,830 km^2 (Watney et al., 1988). The thickness of the Hutchinson Salt Member varies with an average net thickness of 75 m and maximum thickness reaching over 120 m in the south-central part of the basin (Walters, 1978) (Figure 1).

The Hutchinson Salt is composed of halite beds ranging from 0.15 to 3 m thick interbedded with laterally discontinuous insoluble beds of shale, anhydrite and dolomite (Walters, 1978). The salt interval has wide lateral continuity in south-central Kansas; however the lateral continuity of individual salt beds is less extensive, generally only continuous for a few miles (Dellwig, 1971).

The margins of the Hutchinson Salt to both the west and the north are depositional, whereas the eastern margin is dissolutional (Watney and Paul, 1980). Along the eastern up-dip margin the salt interval is relatively shallow (typically less than 125 m) and characterized by an abruptly thinning salt interval over a span of 6-8 km (Figure 7). This pronounced change in thickness is broadly referred to as the dissolution front and extends from near the city of Salina in the north to Wichita in the south, approximately 150 km in length (Watney and Paul, 1980; Anderson et al., 1994) (Figure 7).

Evaporite Dissolution

The solubility of halite is 7,500 times greater than limestone (Waltham, et al., 2005). Due to its relatively high solubility, surficial deposits of halite globally are limited to very arid environments (Johnson, 1981). Buried halite deposits, such as the Hutchinson Salt Member, are vulnerable to dissolution even beneath thick sedimentary sections if water can gain access

through overlying rock via high permeability and/or fracturing. There are three requirements for dissolution of an evaporite to occur; these are described by Johnson, 1981:

1) A fresh water supply
2) An outlet for saturated waters to escape.
3) Groundwater to flow through the system.

Water chemistry, access to the salt interval by these waters, and the hydrology are key factors affecting the dissolution process. Flow characteristics of water within the Hutchinson salt highly influence the patterns of leaching. Under natural pressure, a brine-density flow can occur when fresh water increases in density from contact with salt (Anderson and Kirkland, 1980). The density contrast between the fresh water and the higher density brine cause the brine to sink and flow along separate pathways from the fresh water. The lower density fresh water replaces the brine at the top of the water column (Anderson and Kirkland, 1980). This type of gravity drive system creates more proficient salt removal near the uppermost section of the salt. The rate of dissolution is bottlenecked by the exchange rate of fresh water and brine through the systems inlet and outlet. This rate slows or halts when the recharge of fresh water slows/ceases or saturated fluids cannot exit the system.

Hydrology and Dissolution along the Eastern Margin

As discussed previously, the eastern margin of the Hutchinson Salt Member has been described as a dissolutional boundary (Walters, 1978). Leaching along the eastern edge of the Hutchinson salt began in earnest at least as early as the Tertiary based on previous seismic reflection investigations (Anderson et al., 1994, Miller, 2002). Unsaturated ground water from surficial deposits is believed to have initially penetrated the salt along the shallow up-dip, eastern

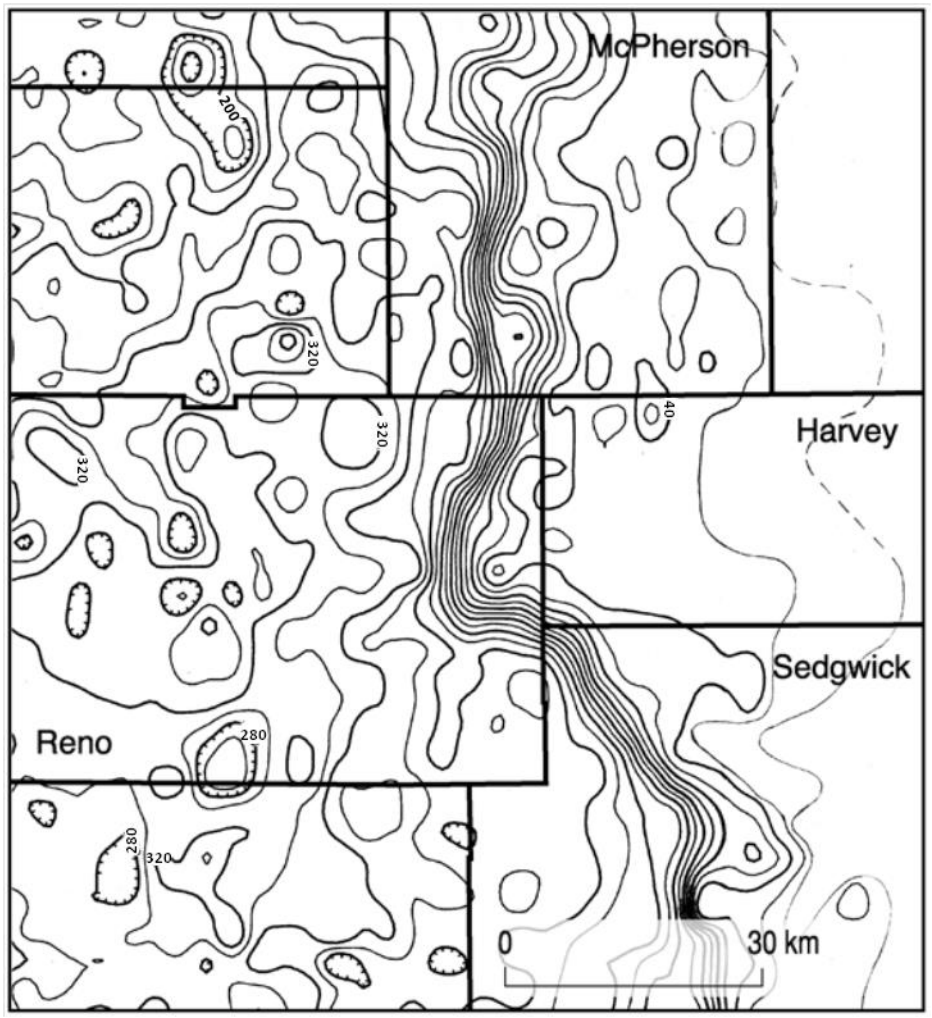

Figure 7: Net salt isopach map of the Hutchinson Salt Member. Eastern margin is considered to be a dissolution boundary which extends from the north near Salina to the south of Wichita (from Watney and Paul, 1980). Contour intervals are 40 ft.

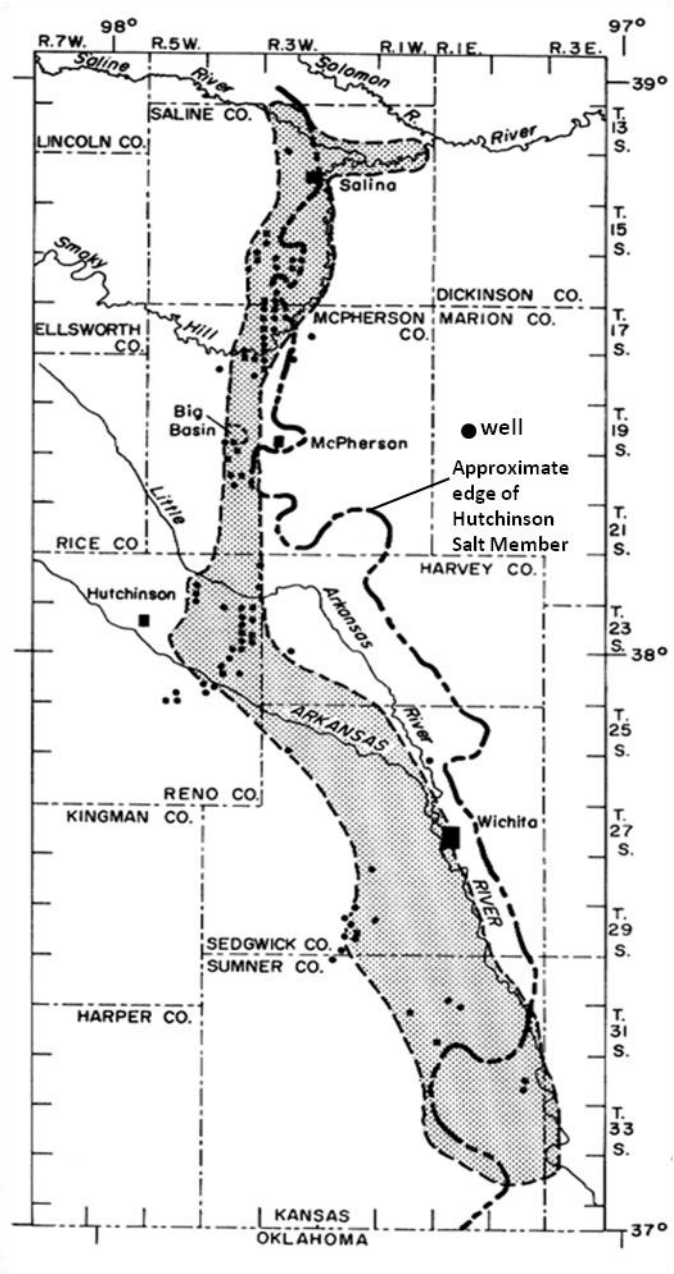

Figure 8: Outline of the Wellington aquifer (grey) defined by sinkholes, undrainded depressions, and lost circulation during drilling (from Gogel, 1981). Notice the correlation between the Wellington aquifer and the high gradient contours of the net salt isopach (Figure 7)

depositional edge and resulted in a gradual removal of the salt (Walters, 1978). This has resulted in the Hutchinson Salt's eastern boundary migrating westward approximately 30 km (Walters, 1978) (Figure 6).

Seismic reflection imaging interpreted and discussed below suggests that dissolution occurring along the eastern margin is not consistent with a continuous east to west progression along a relatively well defined main front. Alternately, leaching along the eastern margin is hypothesized to have resulted in a complex network of dissolution channels following bounded salt intervals that are gradually intruding westward into the salt driven by hydrologic and geologic factors. These channel systems have been described by drillers as the "lost-circulation zone" due to the loss of drilling fluids observed when penetrating the highly permeable solution cavities located at the stratigraphic depth of the Hutchinson Salt (Leonard and Kleinschmidt, 1976). The lost circulation zone has not been mapped on a regional scale and has been described as erratic with local variability of drilling into the zone occurring over spans of only 15 m (Walters, 1978).

Dissolution along the eastern margin is envisioned to be the result of a complex hydrologic system. Unsaturated water is likely accessing the salt from both above and east of the eastern salt face. Extensive subsidence and collapse zones above sections where the majority of the salt has been removed, such as beneath the McPherson channel, have transformed impermeable rock into permeable units allowing fluid to be transmitted (Walters, 1978) (Figure 6). These collapse zones are collectively referred to as the Wellington aquifer (lost circulation zone) and act as conduits for fluid to move vertically under hydrostatic head from the fresher Equus Beds aquifer and progress into the Wellington aquifer (Gogel, 1981) (Figure 8). This recharge process allows the Wellington aquifer to be a source and storage for waters that drive

the dissolution front (Spinazola et al., 1985). This eastern recharge zone is the source for unsaturated water that is intruding westward into the salt body into regions where minimal or no communication exists between the Wellington and fresh water aquifers. Fluid pathways within the aquifer are highly complex with hydraulic connectivity tests through observation wells demonstrating its discontinuity (Gogel, 1981).

Natural dissolution has been suggested to typically occur from the top of the salt interval and possess a horizontally preferential leaching pattern channeled by less soluble bounding layers (Anderson et al, 1995; Watney et al., 2003; Miller, 2007). This is considered to be driven by gravity and associated with time varying pressure gradients within the Wellington aquifer (Gogel, 1981). This system is analogous to both naturally and anthropogenic created solution tunnels identified in salt intervals in the Windsor – Detroit region. During borehole and cross-well seismic studies, complex solution caverns within the salt intervals beneath Detroit, Michigan were uncovered and suspected to be the complex artifacts of both natural processes and solution mining operations from the early 1900's (Terzaghi, 1970; Russell, 1993). It was found that laterally driven dissolution was vertically constrained by insoluble shale layers creating cavity systems within the salt (Boone, et al. 2008). In the Hutchinson Salt, vertical propagation of dissolution is confined by the shale/salt cap rock and less soluble beds within the salt that guide the horizontal dissolution process (Walters, 1978) (Figure 19). Discontinuities within interbedded insoluble layers of the Hutchinson Salt could increase the susceptibility of the salt to vertical leaching.

Fault systems have been well documented to have influenced leaching patterns in evaporite dissolution systems throughout the world (Anderson, 1981; Black, 2003; Shalev et al., 2006; Johnson, 2013). Fault and fracture systems formed through the episodic re-activation of

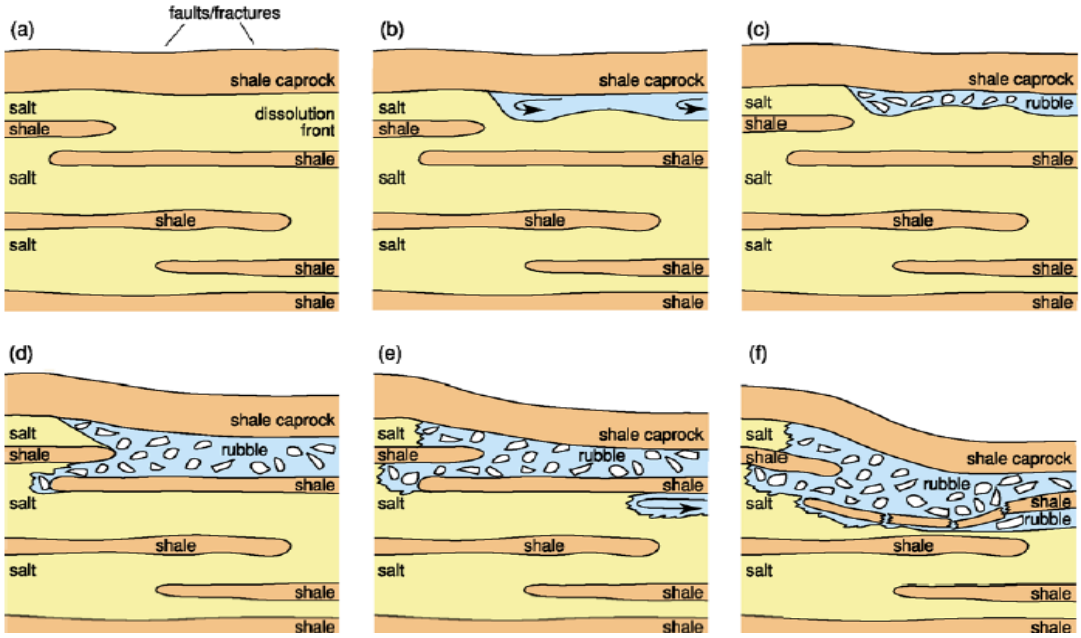

Figure 9: Conceptual cartoon depicting possible natural dissolution progression. Fluid can be guided by the overlying shale contact and interbedded insoluble layers. Failure of the overburden and interbedded layers can divert and halt dissolution (Miller, 2007).

regional and local basement structures have been inferred to have created high permeability conduits for fresh water to penetrate the salt interval. It has been suggested that this has affected the leaching pattern of the Hutchinson Salt dissolution front (Anderson et al., 1994; Watney et al., 2003). However, dissolution along fracture lineaments would likely result in expansive linear elongated surface expressions which are not present along the eastern margin of the salt (Black, 2003). There has also been no evidence in previous seismic investigations within the region to suggest dissolution is being driven by fault systems (Miller, 2002; Miller and Henthorne, 2004; Rice, 2008).

Sinkhole Formation and Subsidence Mechanics

Leaching of the Hutchinson Salt Member can result in voids, rubble zones and solution altered rock within the subsurface that become areas of weakness within a rock mass. Sinkholes or dolines are the result of a void that has migrated to the surface through overburden failure (Galloway et al., 2000). This process can vary from gradual to abrupt and is controlled by failure mechanism associated with void geometry and material properties. Within the Hutchinson Salt Member, salt removed through natural driven processes typically result in gradual or incremental failure rates (Anderson et al., 1995; Miller, 2002). These types of sinkholes are generally characterized by surface depressions with bowl shaped geometries and low angle settlement slopes with the angle of draw defining the extent of subsidence along the ground surface. This is the most common type of subsidence encountered along the eastern margin of the Hutchinson Salt.

Subsidence mechanics and progression are directly related to void geometry, material properties, and lithostatic load. Prior to formation of a void, the components of stress acting on

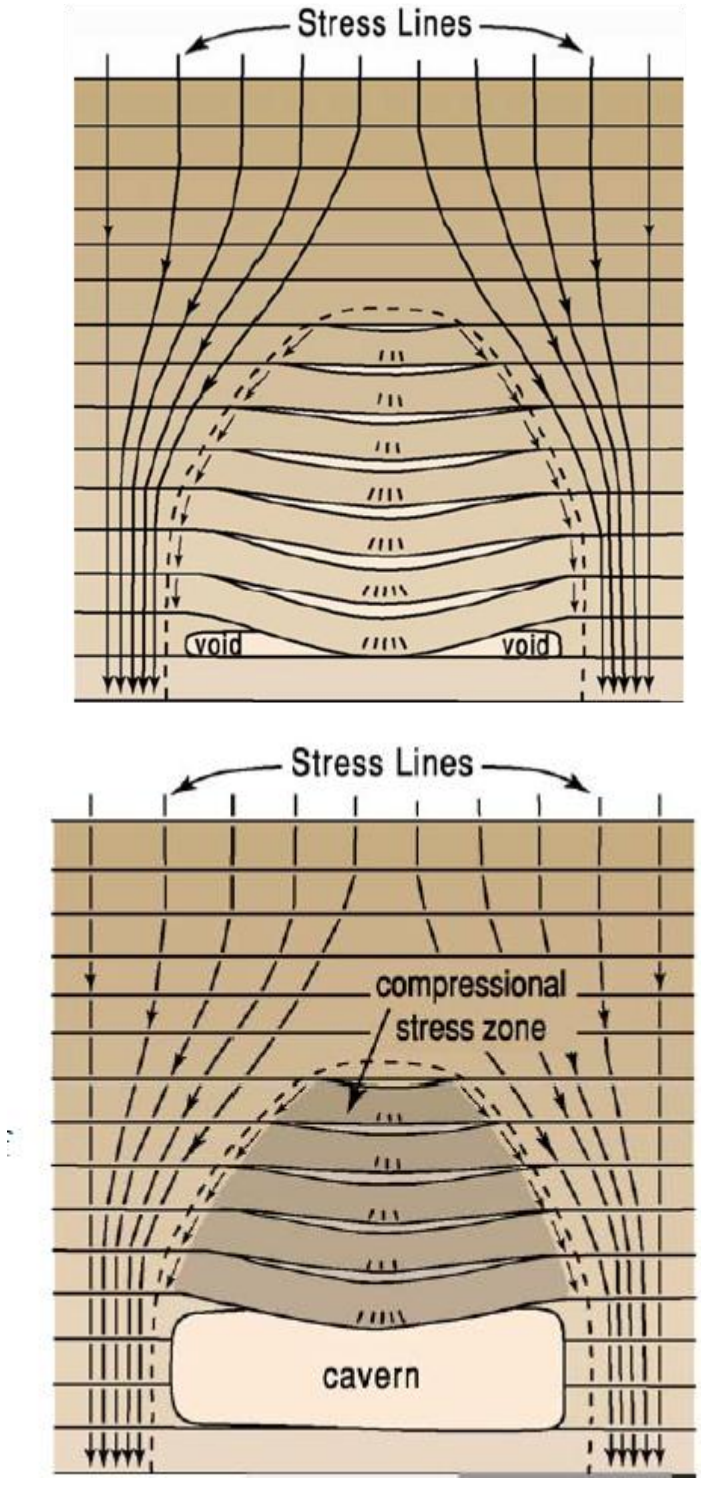

Figure 10: (top) Overburden failure for small horizontal dimensions of a void results in a more plastic appearing subsidence structure. (bottom) Depiction of the tensional dome and distribution of stress lines around a cavern opening in horizontal strata (Davies, 1951) (modified Miller 2007).

any point in the subsurface are in equilibrium (Miller et al., 2005). After void movement, the vertical and horizontal stress components lose equilibrium and a new stress field forms. If leaching continues and the roof rock of the void expands, the stress field will enlarge consistent with a tensional dome (Davies, 1951) (Figure 10). Within the tensional dome, a zone of compressional stress forms in the roof rock directly above the void. Strain is manifest through drape in the unsupported roof rock as a product of increasing compressional stress. Structural failure will generally occur within the unsupported roof rock centered on the location of greatest stress.

Compressional stress continues until the void migrates through the entire section of the overburden. Once failure has migrated to the surface, compressional stress will cease across the structure and an extensional stress regime will begin (Miller et al., 1997). The zone of compressional failure in subsidence features is defined by reverse faulting originating from and centered on the initial failure. Extensional failure is in the form of normal faulting and is the result of gravity slumping towards the center of the subsidence volume. Previous seismic interpretations of collapse features along the dissolution front suggest that they can experience many episodes of compressional and extensional failure during vertical migration (Miller, 2002).

Seismic Reflection Characteristics

Seismic reflections occur as a result of acoustic impedance contrasts at interfaces between geologic layers. Acoustic impedance is a property of rock layers determined by the product of the compressional wave velocity and density of the traveled medium. The energy and polarity of the reflection is determined by the contrast in impedances; where materials with a small acoustic impedance overlying materials with large acoustic impedance will result in a

positive reflectivity and vice versa (Yilmaz, 1987). Rock properties of typical geologic units encountered in the region of study are listed in Table 1.

A key aspect to the "high resolution" seismic reflection method is the collection of higher frequencies that can increase the resolution of the data over that of conventional reflection data (Widess, 1973). Seismic resolution typically refers to the bed thickness uniquely discernible on the seismic data and it depends on the wavelength of the data and seismic velocities within the earth. Conventional data generally do not possess useable frequencies above 50-60 Hz; useable upper frequencies above 80 Hz are considered to be high resolution (Sheriff, 2002).

Summary of 2003 Seismic Data Interpretation (Miller and Henthorne, 2004)

The western 10 km of the 22 km seismic profile were of excellent quality (high signal to noise ratio) and provided a relatively continuous lateral view of the Permian Wellington group and Hutchinson Salt (Miller and Henthorne, 2004) (Figure 1). Reflections from rock unit contacts were flat across the majority of the profile with only two dissolution features identified. A paleosinkhole located over 20 km west of the eastern margin of the salt was imaged on these seismic sections (Figure 11). This feature appears to be a single activation event and has resulted in a relatively symmetric depression in the overburden rock. The formation of this feature suggests that unsaturated water was able to penetrate the salt interval at this location and that brine was able to escape to create the necessary flow process to instigate leaching. The inadvertent imaging of paleo-sinkholes away from the dissolution front is evidence to support the suggestion that dissolution channels are intruding west into the salt interval away from the eastern margin. This would provide both the unsaturated water access into the salt and the needed flow paths for exiting brine.

A previously unknown fault was also imaged on this data near CMP 4420 and is located approximately 15 km from the dissolution front (Miller and Henthorne, 2004) (Figure 12). This fault is seismically indicated by the clear change in reflection characteristics across it. This fault is suspected to be a strike slip fault as there is minimal offset interpretable across it within this stacked section. The salt interval around this fault appears to be undisturbed with no evidence of dissolution. Though faults have long been inferred to provide fluid access into the salt interval, it does not mean they are indicative of dissolution nor are they required. A possible scenario that has prohibited dissolution may be that slippage along this fault has sealed up or reduced porosity and is not providing the suspected conduit for fresh water access to the salt interval. Alternatively, water may have access into the salt but the brine does not have the means to flow out of the system to continue the leaching process.

Material	P-wave Velocity (m/s)	Density (kg/m³)	Acoustic Impedance (kg/m²s)*
Dry sand/gravel	750	1800	$1.35 * 10^6$
Clay	900	2000	$1.80 * 10^6$
Saturated sand	1500	2100	$3.15 * 10^6$
Saturated clay	1800	2200	$3.96 * 10^6$
Shale	3500	2500	$8.75 * 10^6$
Limestone	4000	2600	$10.4 * 10^6$
Anhydrite	4100	2900	$11.89 * 10^6$
Halite**	5500	2200	$12.1 * 10^6$

Velocites are mean for a range appropriate for the material.

*Acoustic impedance is velocity multiplied by density, specifically for compressional waves.

**Velocity and density will decrease when water is within the halite.

Table 1: Rock properties of typical units found in Reno County, Kansas (modified from Lambrecht, 2006)

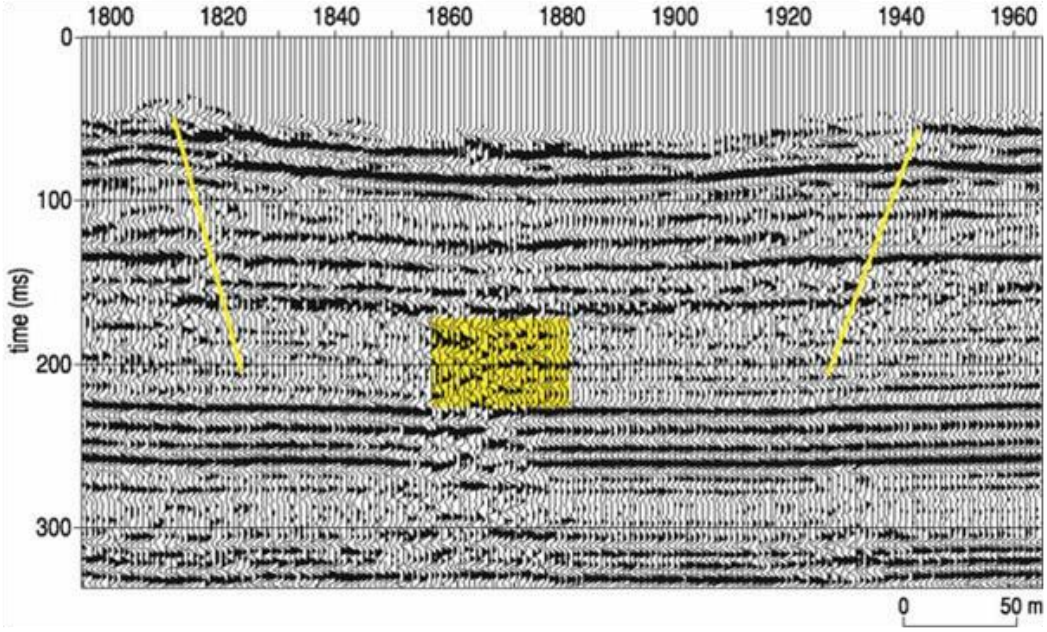

Figure 11: Paleosinkhole imaged along U.S. 50 in 2003. This feature is located over 20 km west of the dissolution front. This feature supports the suggestion that leaching is intruding west into the salt interval and that dissolution is not isolated to close proximity of the dissolution front.

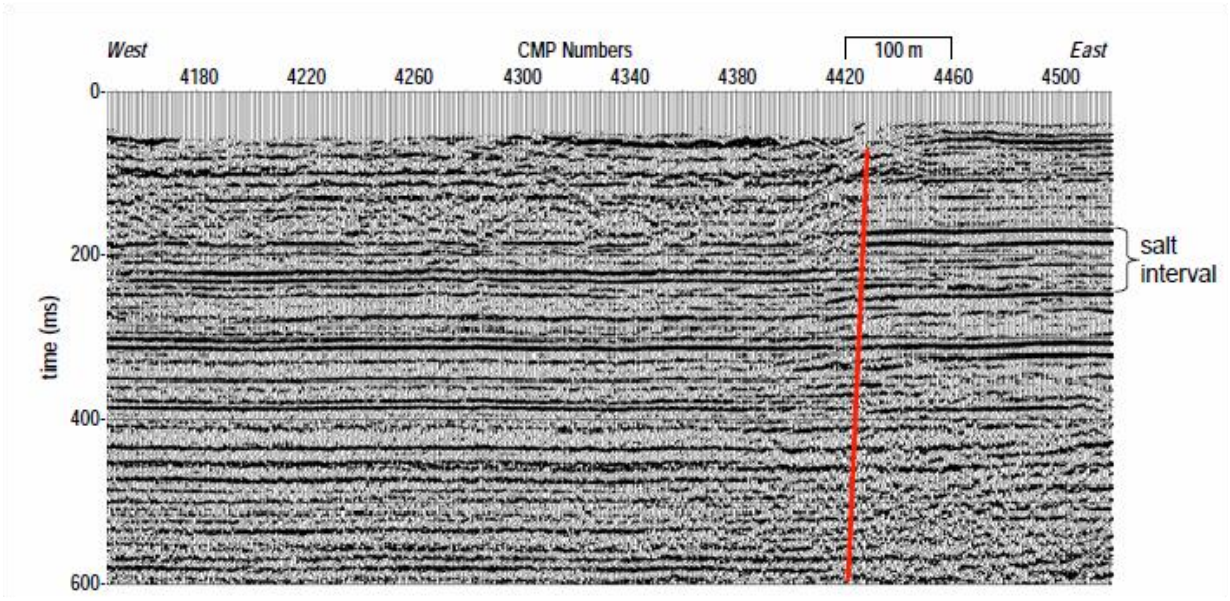

Figure 12: Fault located approximately15 km from the dissolution front. Minimal offset suggests this is a strike-slip fault. Faults have been suggested to be conduits for fluid that provide access to the salt interval, however there is no evidence of dissolution within the salt interval around this feature.

Methods

Data acquisition along U.S. Highway 50

The 12 km 2008 survey was acquired using a 240-channel rolling fixed-spread geometry. Data were collected using two Mark Products L28E 40 Hz geophones at each station with receiver stations set at 2.5-m intervals (Figure 13). The two geophones planted at each receiver station formed approximately 1-m arrays to reduce ground roll on the data. Geophones were planted in hard soil in the south roadside ditch using 14-cm spikes for improved coupling to the surface (Figure 14). Source stations were set at 5 m intervals along the paved south highway shoulder. An IVI Minivib 1 was used for the source, which delivered three, 10-second, 25-300 Hz linear up-sweeps at each source station (Figure 15). Data from each sweep were recorded with four, networked 60-channel Geometrics Strata View seismograph systems resulting in 240 recorded channels per shot gather. The ground force pilot for each sweep was telemetried from the vibrator to the seismograph and recorded as the first trace of each shot record and used for quality control of the source performance. Each sweep was recorded by the 240 channels and stored uncorrelated to allow pre-correlation processing and correlation methods.

After the Minivib sequentially occupied the central 60 source stations (120 receiver stations), the back 120 receiver stations would roll to the front to define the next fixed spread (Figure 16). This process continued through the approximately 12 km span of the survey. The rolling fixed spread design allowed for a sustained high fold data within the optimized offset range along the length of the line, and extended the far offset ranges accessible during processing for improved velocity control. All data were collected along the heavily travelled U.S. Route 50 with coordination of traffic flow by the Kansas Department of Transportation. A real time

kinematic (RTK) global positioning system recorded locations of seismic stations at random intervals along the seismic line.

Vibroseis Method

The vibroseis method was advantageous for this survey due to its low cultural impact, facilitated mobility, high repeatability, frequency control, and ability to extract reasonable signals in regions of high cultural noise. The vibroseis method utilizes a source that imparts an amplitude and frequency variant sweep across a given time interval into the ground (Yilmaz, 2001). The uncorrelated seismogram $x(t)$ is the result of the convolution $(*)$ between the vibroseis sweep $s(t)$ and the acoustic impulse response or reflectivity $r(t)$ of the earth summed with any uncorrelated noise $n(t)$ represented by the equation:

$$x(t) = r(t) * s(t) + n(t)$$

The recorded trace resulting from a vibroseis source will have the sweep embedded in the data. Removal of the sweep may be accomplished through cross correlation (♦) of the raw trace with the vibroseis drive/synthetic/pilot, resulting in a collapse of the frequency modulated sweep and replacement with a zero phase Klauder wavelet $k(t)$ convolved onto the reflectivity sequence (Yilmaz, 2001). The cross-correlation method can be represented by the equation:

$$x_{cc}(t) = r(t) * s(t) \blacklozenge s(t) = r(t) * k(t)$$ (Brittle, et al., 2001)

High-resolution seismic reflection data processing

A 2-D high resolution vibroseis common-midpoint (CMP) processing flow was utilized (Figure 17) (Steeples and Miller, 1998; Miller, 2007). Data processing was accomplished using software packages developed by the Kansas Geological Survey, Winseis and SeisUtilities. The

Figure 13: Receiver station with two 40 Hz geophones planted in approximate 1 m arrays

Figure 14: Receiver stations located along the south roadside ditch of U.S. Route 50

Figure 15: Photograph of the IVI Minivib I.

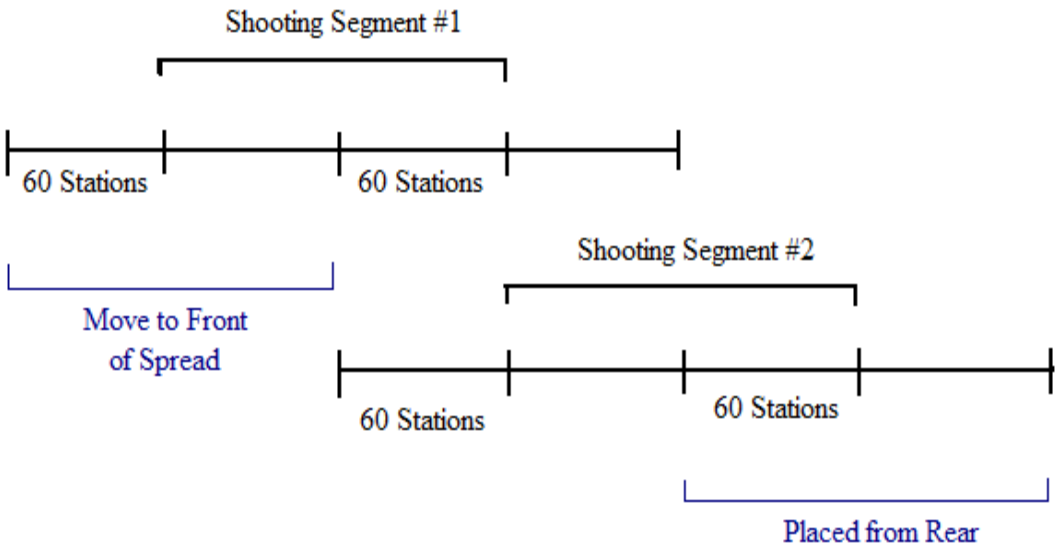

Figure 16: Rolling-fixed spread survey design (Modified from Rice, 2008)

2008 U.S. 50 data were collected in SEG2 format and were converted to a modified SEGY format for processing.

Vibroseis whitening (VSW) proved to be an effective early step in the processing flow (VSW) (Coruh, and Costain, 1983). This signal conditioning step was accomplished using a 1-sec automatic gain control (AGC) prior to cross correlation. VSW helps reduce high amplitude energy and recover small-amplitude components of the data trace through the application of time-varying amplitude scaling prior to cross correlation (Coruh, and Costain, 1983). Near-surface seismic data can often be plagued by high ambient noise and narrow bandwidth source-generated coherent noise. This can result in decreased coherency across reflections and a drop in resolution (Doll and Coruh, 1995). Application of floating gain control over the duration of the frequency modulated sweep allows for equalization of low and high amplitudes which can dramatically improve waveform continuity from trace to trace and apparent resolution (Klemperer, 1987; Lambrecht et al., 2004). Bandwidth balancing, increased S/N and improved trace-to-trace waveform correlation, particularly in reflections concealed by ground roll, were the result of VSW being applied to the U.S. 50 data (Figure 18).

Each raw recorded trace that results from the vibroseis source represents the convolution between the vibroseis sweep and the acoustic impulse response (reflectivity) of the earth. The sweep needs to be extracted from the recorded trace to expose the reflectivity series (Brittle, et al., 2001). This is done through cross-correlation of the recorded trace with the vibroseis drive signal/pilot/synthetic. For this processing flow a synthetic sweep was generated that matched the vibrator's drive signal. The synthetic sweep was then cross-correlated with each sweep record to produce the reflectivity series.

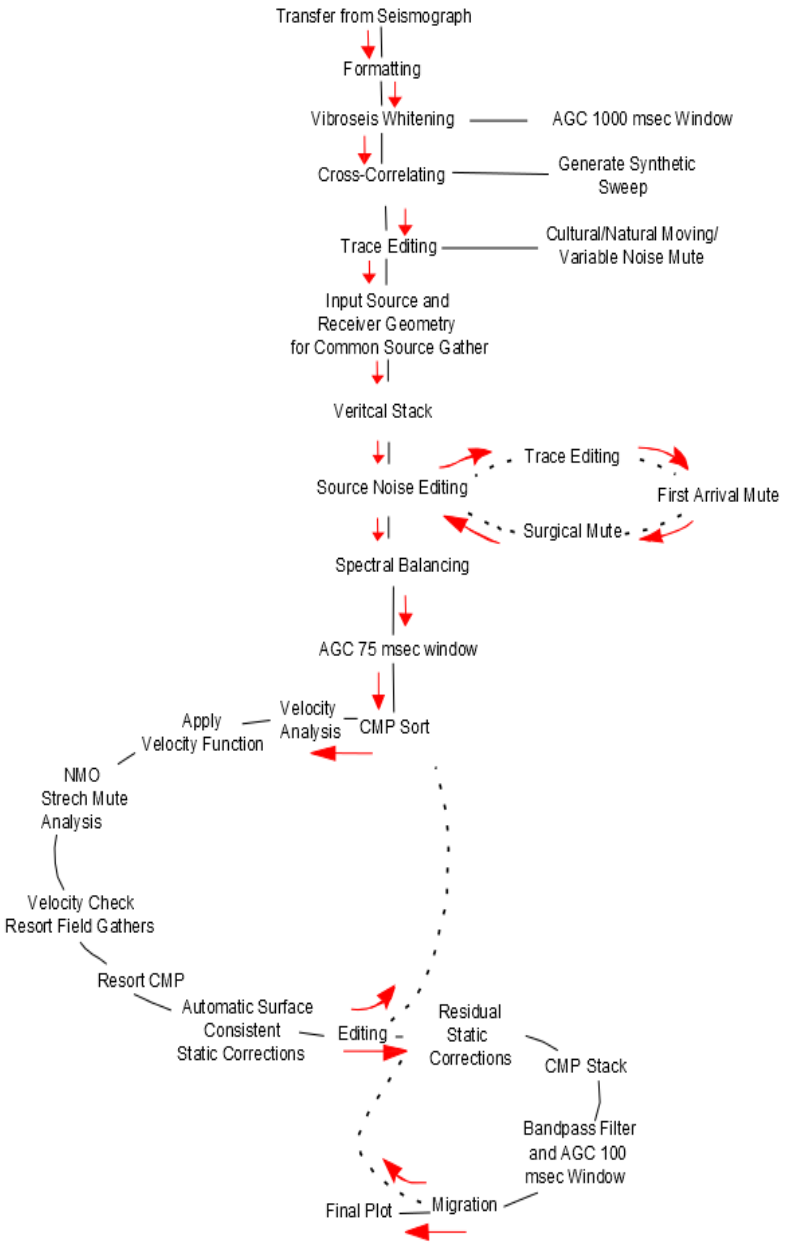

Figure 17: Processing flow

Common with near surface data, a heavy emphasis was placed on noise suppression/removal (Baker, 1999). Noise suppression was primarily focused on highway vehicles, the survey crew, power-lines, surface waves, first arrival energy, and air-coupled waves. Stacking, muting and filtering techniques were utilized for noise suppression and provided significant S/N improvements. Trace editing was used to mute traces with S/N below a qualitative threshold and dead traces on each individual shot gather.

Once trace editing and filtering were completed, the three shot records obtained at each source station were vertically stacked. Vertical stacking is the summation of each shot record located at the same source station to create one shot gather for that source point and spread. The intent is to take advantage of the repeatability and consistency of the seismic wavefield relative to cultural and environmental noise. Through vertical stacking, coherent reflected signal from each record constructively adds while record-to-record dissimilar arrivals will be reduced in amplitude. This process can attenuate random or non-source noise in each record not attributed to true reflection signal, while increasing the amplitudes of sweep to sweep coherent events (Klemperer, 1987).

Spectral balancing was applied to the data set to enhance the higher frequencies and flatten the spectrum, thereby suppressing the more dominant low frequencies. High frequency components of a propagating wave are more rapidly attenuated than low frequencies generally through energy dissipation and absorption losses, resulting in a narrow-band, low-frequency spectrum. Spectral balancing is similar to band-limited spiking deconvolution and effectively boosts the high frequency energy in the seismic data while retaining the originally high amplitudes and lower frequencies but at more equivalent amplitude to the high frequency energy.

This is a result of flattening the spectrum and compresses the waveform. Ideally this approach can enhance shallow reflections and improve the apparent resolution (Figure 19).

First arrival mutes were uniquely designed for each shot record to remove direct wave and refraction noise from the vertically stacked gathers (Figure 20). Direct arrivals and refractions can stack coherently on CMP stacked sections resulting in erroneous interpretations of first arrival energy as reflections (Steeples and Miller, 1998). Therefore, first arrival energy needs to be distinguishable from shallow reflections after correlating the shot records, and if not removed, tracked throughout the processing flow (Steeples and Miller, 1998; Miller, 2007). Reflections shallower than 50 ms are keenly susceptible to linear source noise interference and have proven essential to determining the sequence of subsidence events and/or periods of activity. All reflections on the CMP stacked sections need to be correlated to reflection hyperbolae on shot records.

Surgical mutes were designed and implemented here to remove the noise cone of the seismic data (Figure 21). The noise cone is principally comprised of the ground roll and air wave. Though some coherent reflection signal is observable within the noise cone, f-k and frequency filtering proved relatively ineffective at attenuating/eliminating those noise arrivals. It was determined necessary to use a surgical mute to remove the cone to increase the S/N of the stacked section.

High frequency noise was observed on shot gathers at two way travel times greater than 200 ms and therefore deeper than 250 m below ground surface. This noise masked the trace to trace coherency of reflections making it difficult to identify deep reflecting events. A time-variant high cut filter and migration was useful in reducing the noise.

Common-Midpoint (CMP) Sort Processing

Once noise suppression processing steps were completed on the shot gathers, the data were sorted to CMP gathers. The data were again evaluated in the CMP domain for noisy traces and identification of reflection hyperbolae relative to any coherent noise. Velocity analysis was accomplished using constant-velocity stacks. The velocity function was determined for coinciding groupings of 25 CMPs with a minimum of 5 velocity pairs defined within the upper 200 ms (Figure 22 and 23). Stacking velocities ranged from 1200 to 3500 m/s which were reasonable considering the geologic units. The highly disturbed near-surface setting resulted in lateral velocity variations causing the data to be inundated with inter-spread static problems. Trace-to-trace reflection arrival times could vary up to 10 milliseconds in highly disturbed areas. Iterations of automatic surface consistent statics and residual static corrections were applied after NMO corrections.

After NMO corrections the data was re-sorted into shot gathers for quality checks on the effectiveness and accuracy of the velocity function and NMO parameters. Shot gather sorts are useful for verifying how effectively hyperbolic reflections are flattened and determining the degree of wavelet distortion caused by the NMO stretch allowed during NMO corrections (Miller, 1992). An optimized severe stretch mute limit of 25% resulted in removal of longer offsets and increase in the apparent frequency of the stacked section at the expense of decreased fold and a lower signal to noise ratio in shallow reflections (upper 150 ms). After NMO quality checks, the data were resorted into CMP gathers and stacked with a final bandpass filter applied.

Migration was applied to the data to collapse diffractions and correct for distortions in the stacked section caused by complex subsidence structures in the upper 200 ms. The migration method utilized was a single velocity F-K migration (Stolt, 1978). Lateral changes in velocity

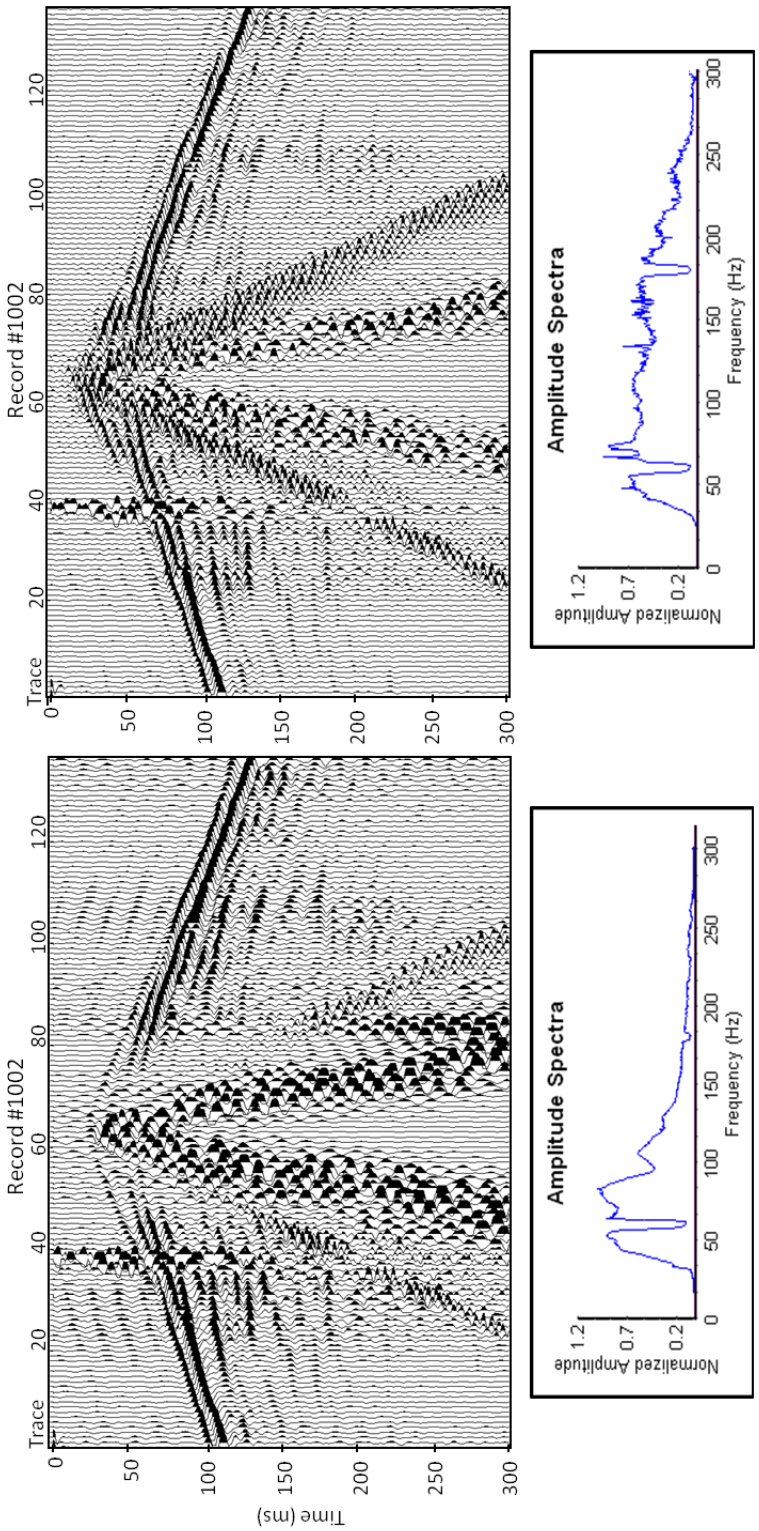

Figure 18: (left) Correlated shot record and amplitude spectra without pre-correlation whitening applied. (right) Correlated shot record and amplitude spectra with pre-correlation whitening (1000 ms AGC) applied. Pre-correlation whitening reduces noise and improves the apparent resolution through bandwidth enrichment. Notch filters are applied at 60 and 180 Hz to reduce electronic signal for a visual representation of the normalized amplitudes.

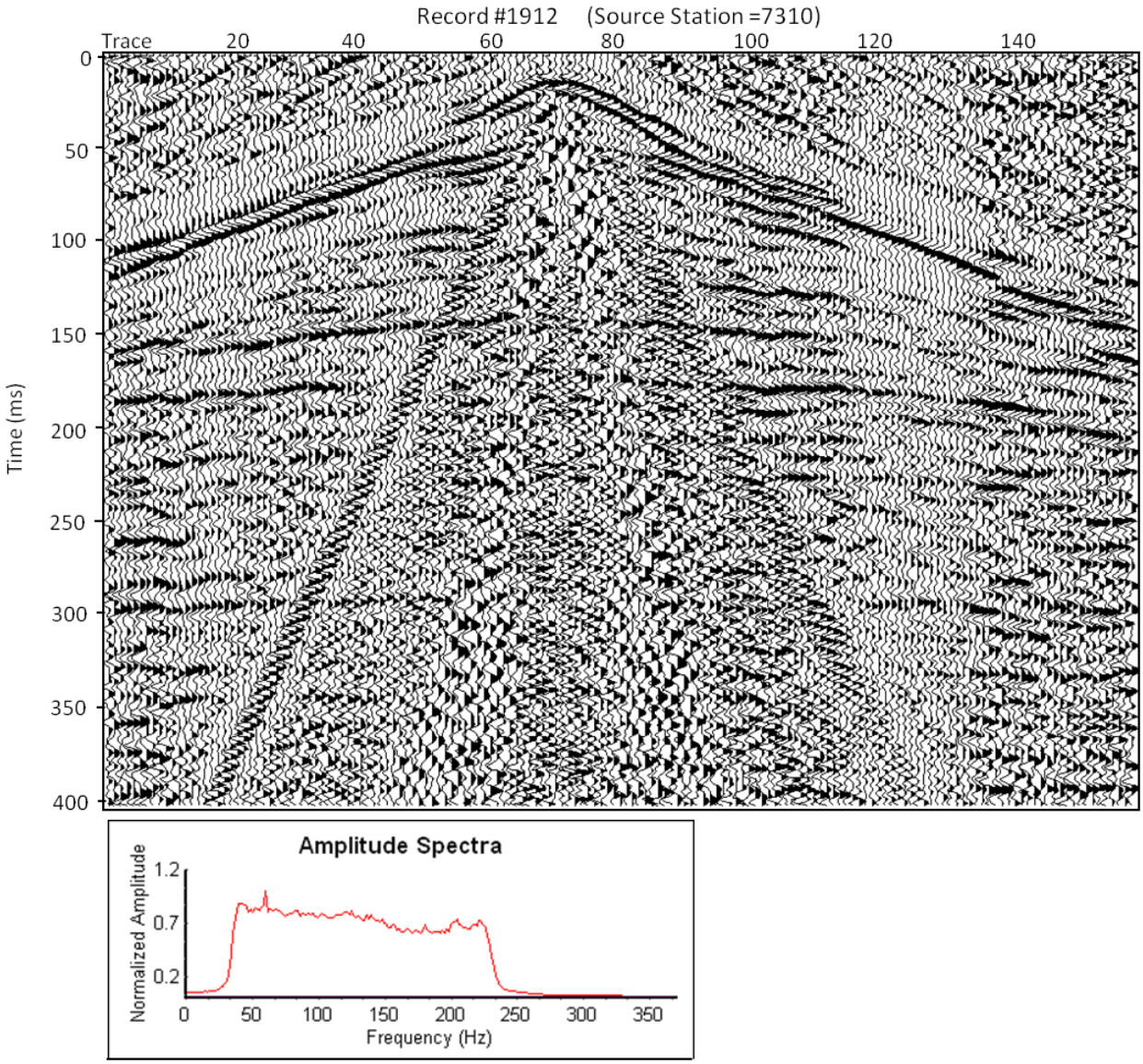

Figure 19: Representative shot gather that has been vertically stacked and spectrally balanced. 75 ms scaling applied.

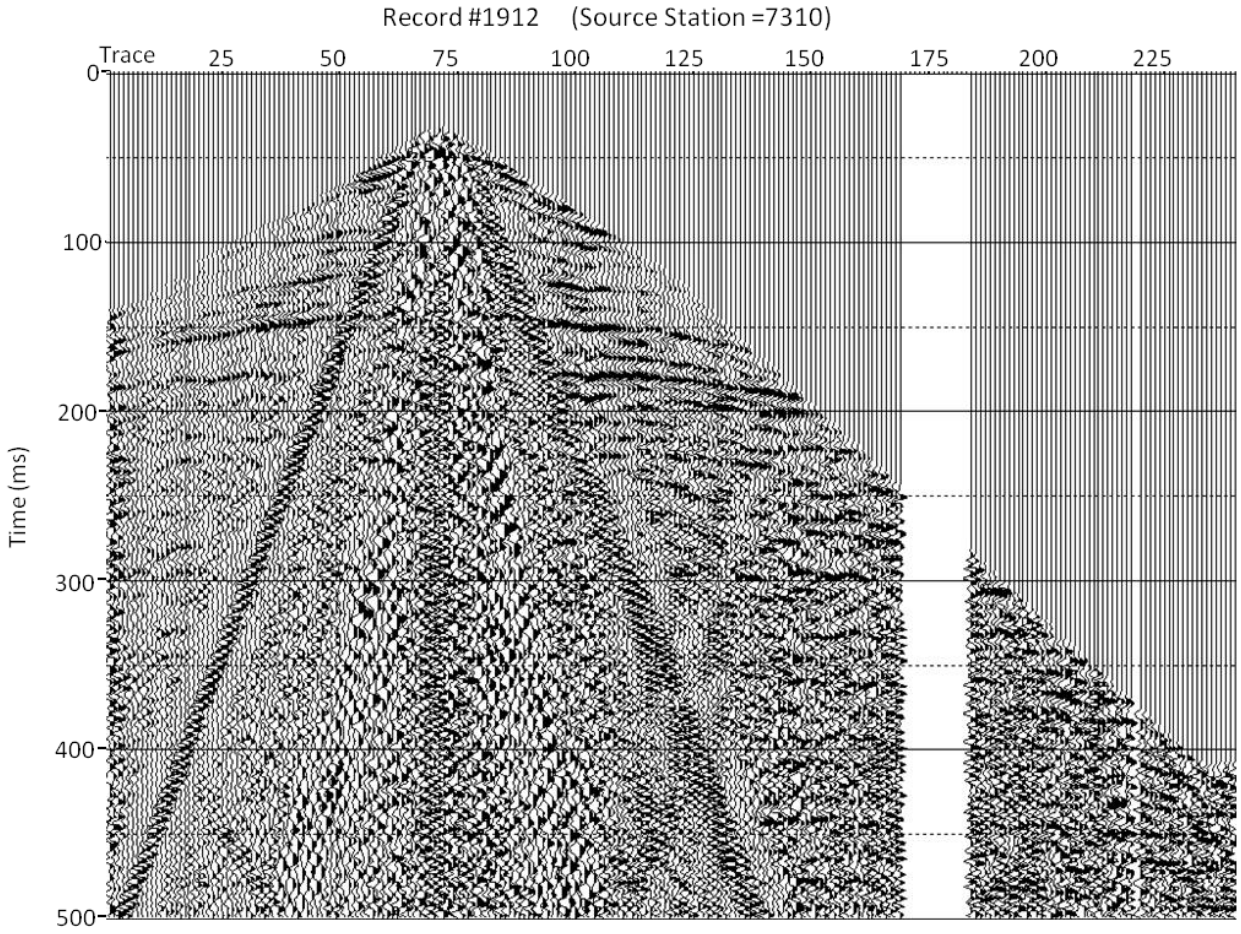

Figure 20: Representative shot gather with first arrival mute applied

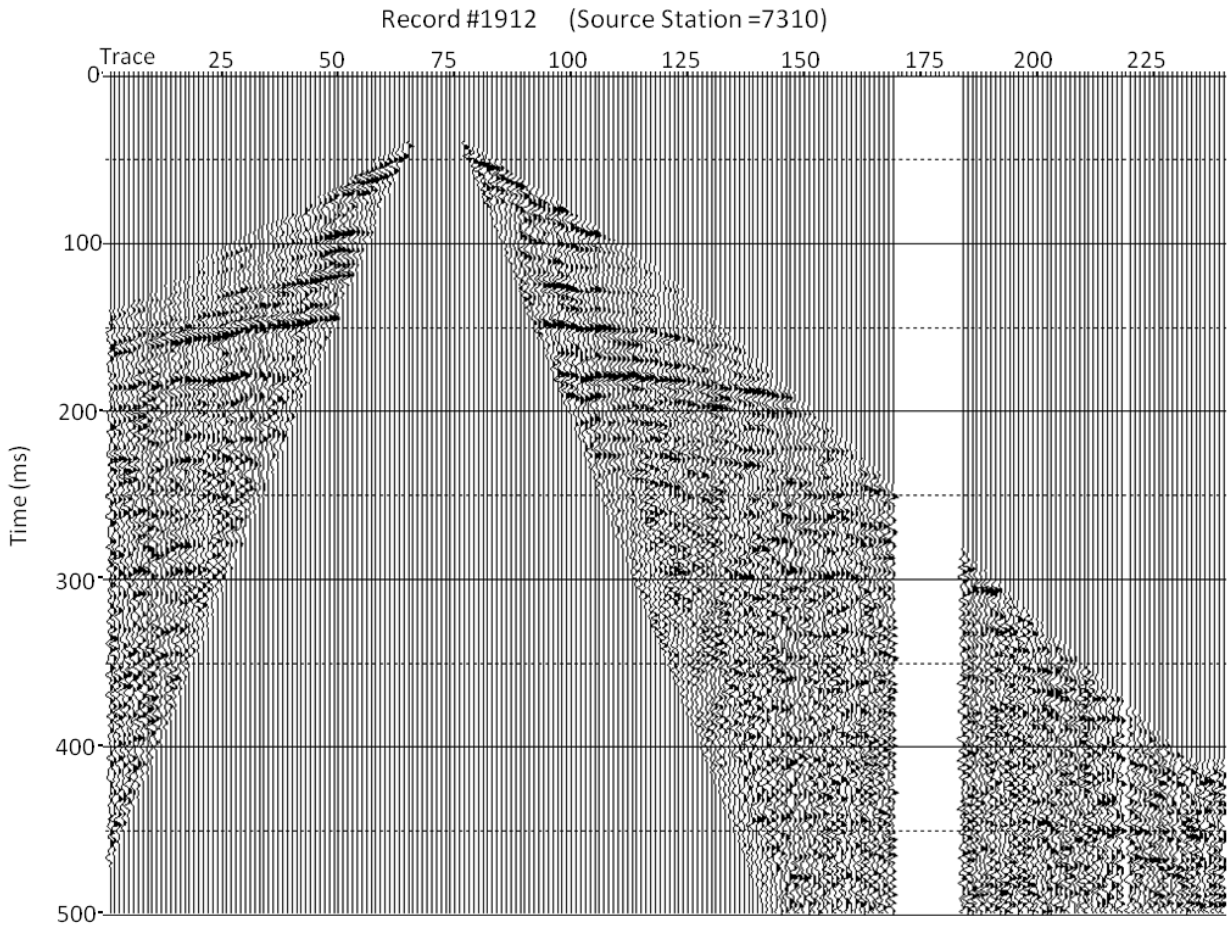

Figure 21: Shot gather with first arrival mute and noise cone mute applied.

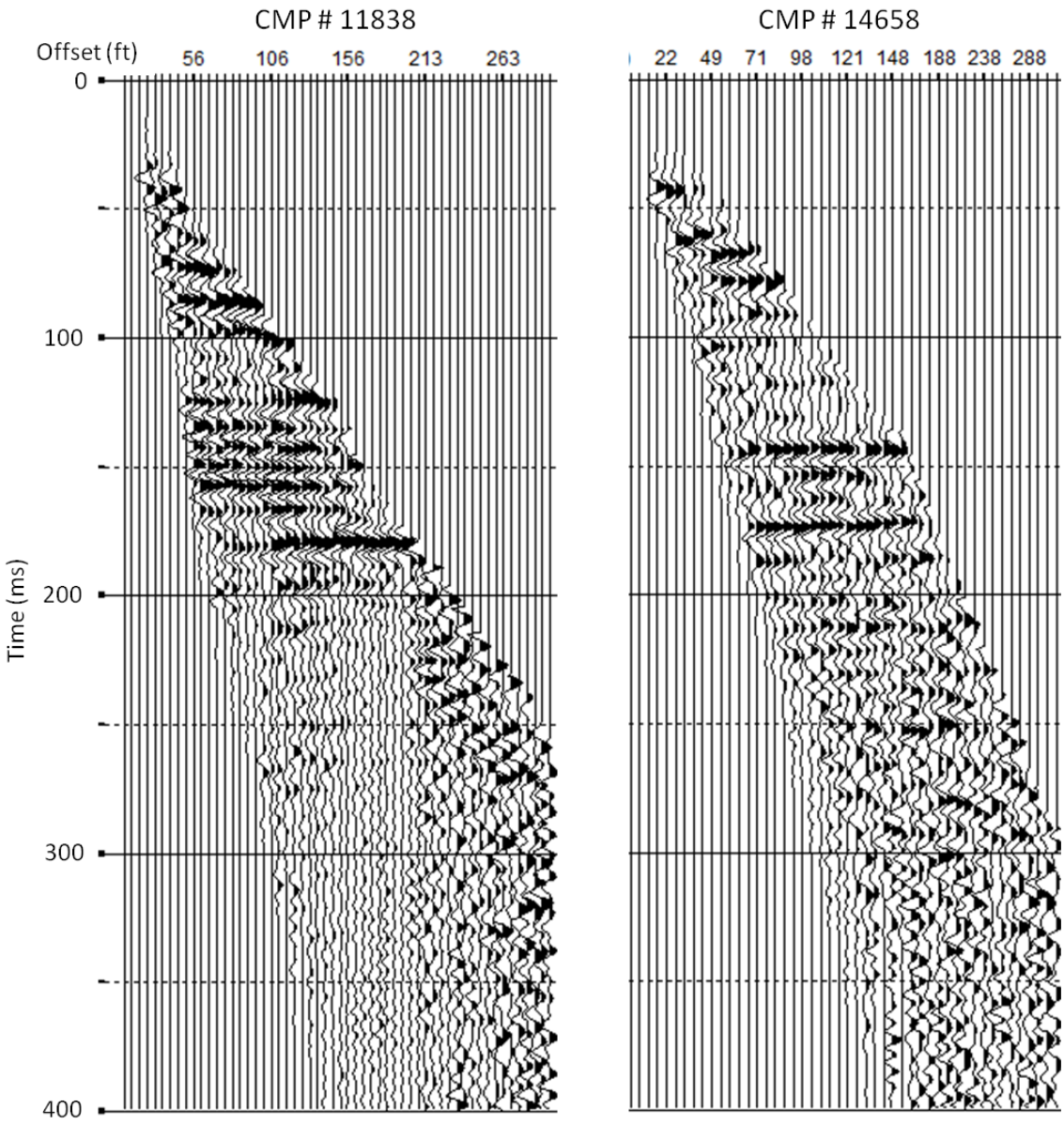

Figure 22: Fully processed CMP gathers with NMO and static corrections applied.

related to differentially compacted fill and distorted rock layers made it impossible to obtain the accuracy in the velocity function required for a more robust migration method (Figure 23). A single velocity was used for the migration which limits its effectiveness in collapsing diffractions and moving dipping events to the correct locations. This may also lead to artifacts in the stacked section due to incorrect migration velocities at varying depths. Low stacking velocities common in the near surface has been shown to lower the need of migration (Black et al., 1994). Specifically on this data set, migration appears to refocus energy near the base of the salt in and around collapse structures and improve the lateral coherency of sub salt reflections.

Fold and Resolution

As is the case with most shallow high-resolution seismic reflection data, the redundancy of subsurface coverage (fold) across optimum offsets is highly time-varying after processing (noise editing, NMO stretch) (Liberty and Knoll, 1998). Based on acquisition parameters this data set would be reported to possess a maximum of 60 fold, indicated by the 60 traces on the CMP gather (Figure 22). However, estimation of fold as defined by contribution by non-zero traces in the CMP would suggest the typical fold coverage ranges from 6-35 increasing with depth (time) between the target window of 25-200 ms on the U.S. 50 data set.

Vertical resolution of seismic reflection data is often defined by the ¼ wavelength criterion (Widess, 1973) relating the resolution potential to the dominant wavelength. Dominant frequency of this data is approximately 120 Hz in the upper 200 ms with a theoretical (1/4 wavelength) vertical bed resolution on the order of 4-6 m but more realistically 8-12 m using the ½ wavelength rule. Based on the Rayleigh's criterion in measuring the minimum distance

between separate distinguishable objects, the horizontal resolution of this broadband data is determined by the Fresnel zone radius:

$$r = \sqrt{\frac{VZ}{2f}}$$

where r is the Fresnel radius, Z is the depth to the horizon, V is the velocity, and f is the dominant frequency (Ebrom et al., 1996). The Fresnel zone radius at the depth of the Hutchinson Salt Member would be approximately 40 m. Migration may improve the horizontal resolution by collapsing the Fresnel zone to approximately the dominant wavelength (Stolt and Benson, 1986; Yilmaz, 1987).

Post Processing

Acoustic Impedance Inversion

To better delineate near surface instability, bridging zones and the solution altered salt interval, acoustic impedance inversions were calculated near Brandy Lake along this seismic profile (Figure 24). Acoustic impedance inversion attempts to remove the wavelet from the reflection series and reconstruct the impedances of the rock layers (Lindseth, 1979). This removes the complexities of the wavelet within the seismic bandwidth and presents the data as values that represent changes in rock properties. This method should allow for improved stratigraphic interpretations and a better delineation of the salt interval and tuning affected interbedded insoluble layers than that of the amplitude data.

The results of this approach were not beneficial for multiple reasons. First, low frequency information is required by the inversion process to estimate reflectivity (Ferguson and

Margrave, 1996) and these data were recorded to specifically reduce low frequency content. Preservation of the low frequency on high resolution data rarely enhances the final stacked image. Low frequency information can be supplemented on data like these by stacking velocities and well logs (Lindseth, 1979). With a significant portion of the low frequency bandwidth missing (> 30 Hz) in these data, apriori information driven inversions result in products more controlled by initial models and less by the seismic data itself. The significant amount of near surface velocity and static variability related to subsidence created instability and limited the accuracy in the initial impedance estimation and the overall results.

Horizon Flattening

Significant pull down effects were identified in reflections beneath subsidence related to Brandy Lake and recent road deformation on the time stacked sections (Figure 25). This time drop is the result of velocity variability caused by rock subsidence in overlying layers and does not reflect true structure beneath the salt. Time section estimates of subsidence and removed rock salt would be unreliable unless compensation for velocity changes is accounted for (Miller, 2002). To compensate for velocity variability relating to compaction it is reasonable to flatten along the interpreted Lower Wellington top reflection near the base of the salt (165 ms). Horizon flattening is a tool used in the petroleum industry generally to observe features and structure that may have existed in the geologic past below the flattened horizon (Bland et al., 2004); however, in this near surface scenario it is used to compensate for velocity variability above the target horizon. Though horizon flattening cannot replace a rigorous velocity function, the current velocity estimation tools make it a significant challenge, if not impossible, to obtain the precision needed within such complex subsidence structures. The horizon flattened section

refocused the energy above the salt interval likely providing a more structurally accurate image of subsidence beneath Brandy Lake.

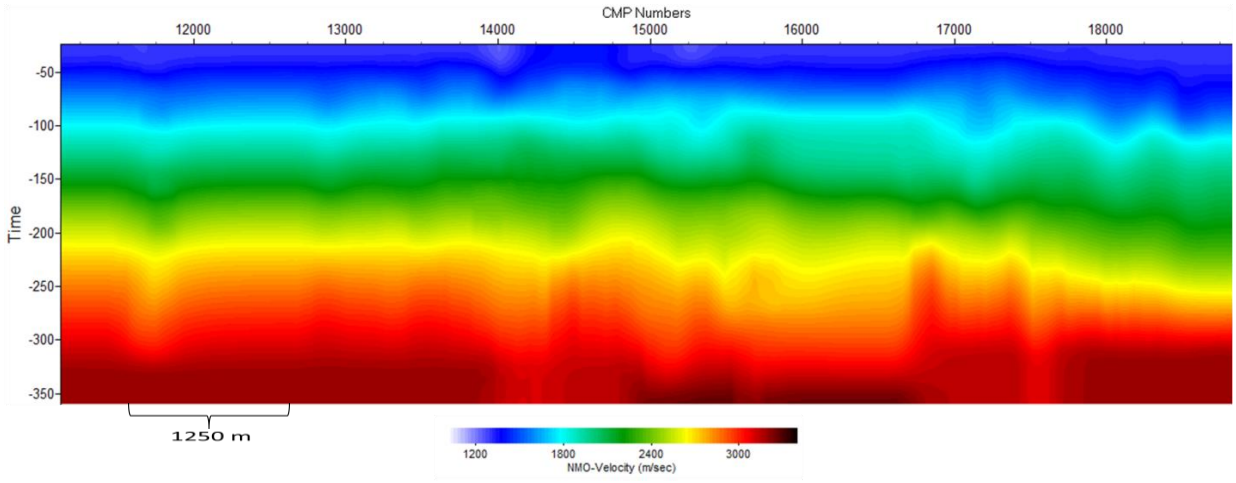

Figure 23: Plotted and smoothed velocity function of the entire seismic line used for the NMO corrections during the processing flow. Notice the lateral variability in velocity particularly on the eastern side of the line that is related to surface subsidence.

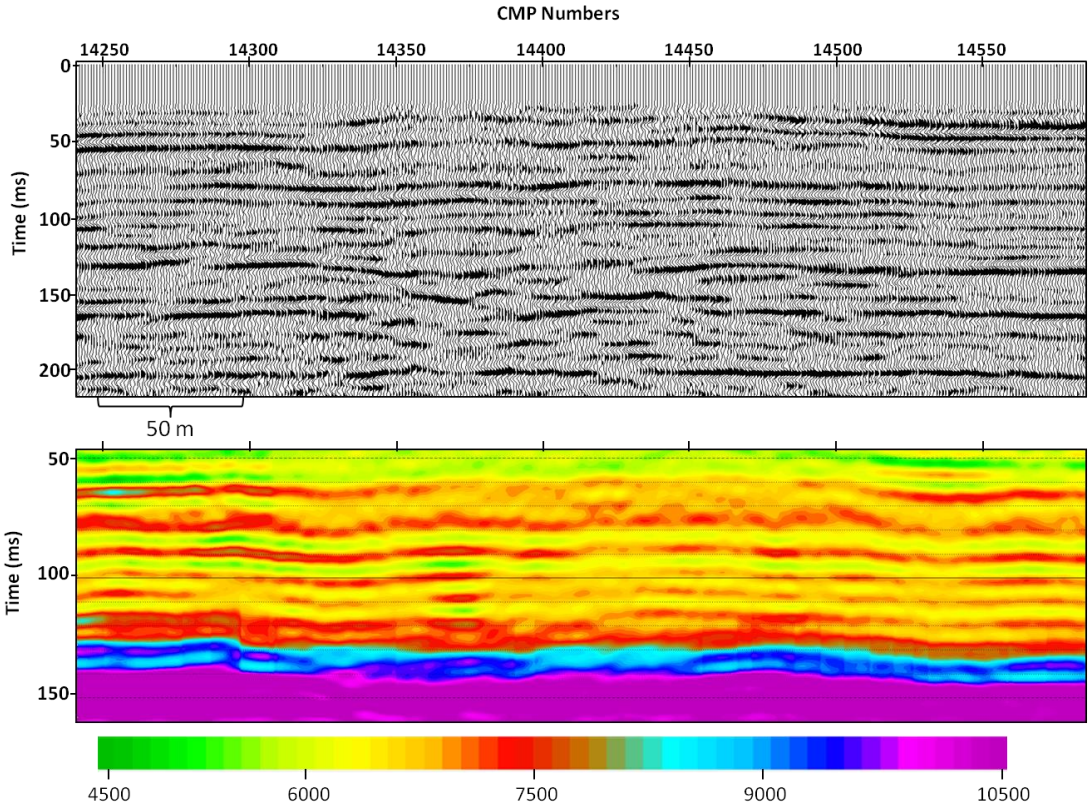

Figure 24: (top) Seismic reflection profile of sinkholes related to road deformation west of Brandy Lake. (bottom) Acoustic impedance inversion of the Permian bedrock above the salt interval. Near surface velocity and static variability create instability and reduce the accuracy of the inversion.

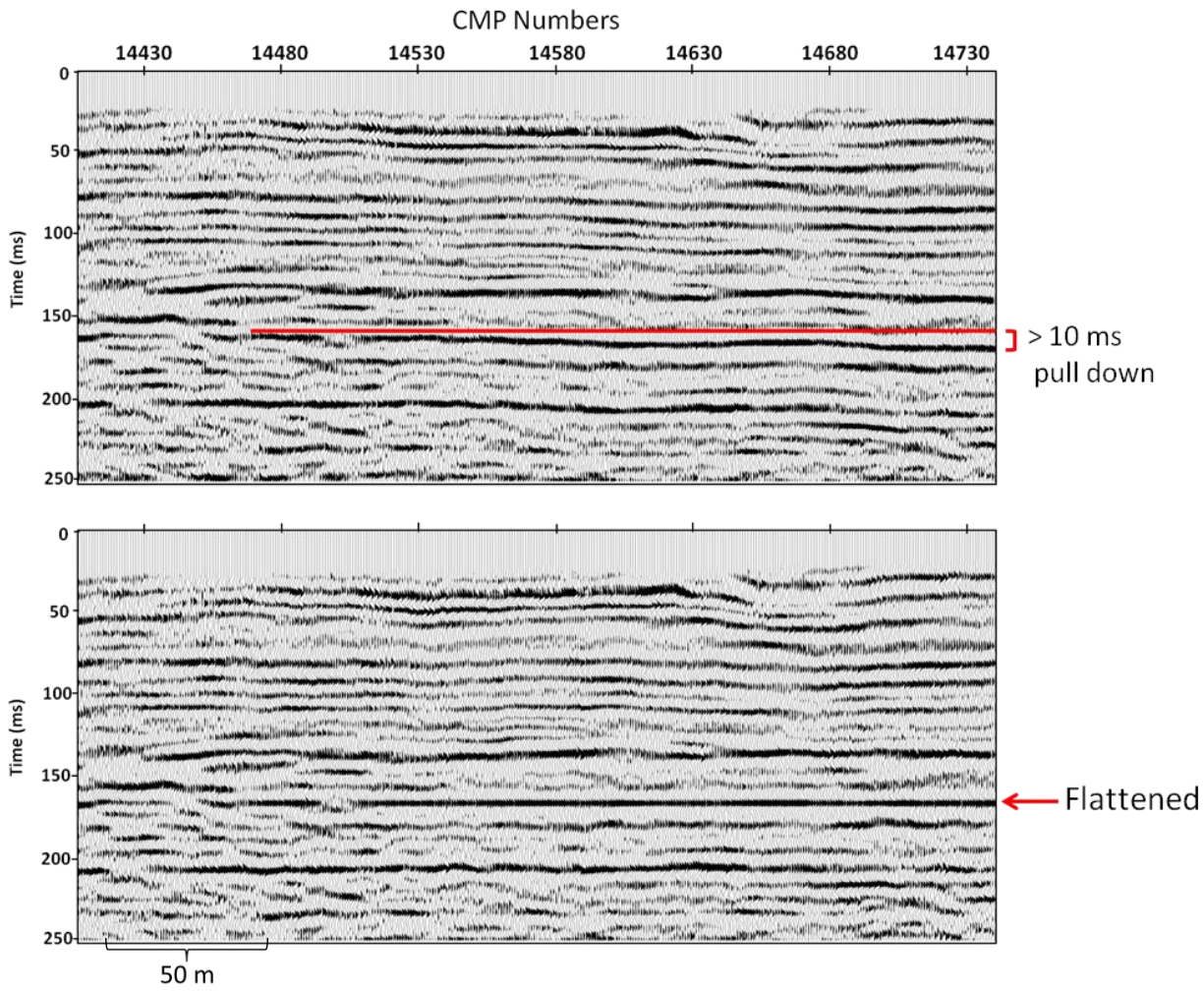

Figure 25: Subsalt pull-down anomalies are the result of velocity variability and are not true structure. Flattening along a subsalt horizon can help to compensate for velocity variability relating to differential compaction within subsidence structures and provide a more structurally accurate image of the subsurface.

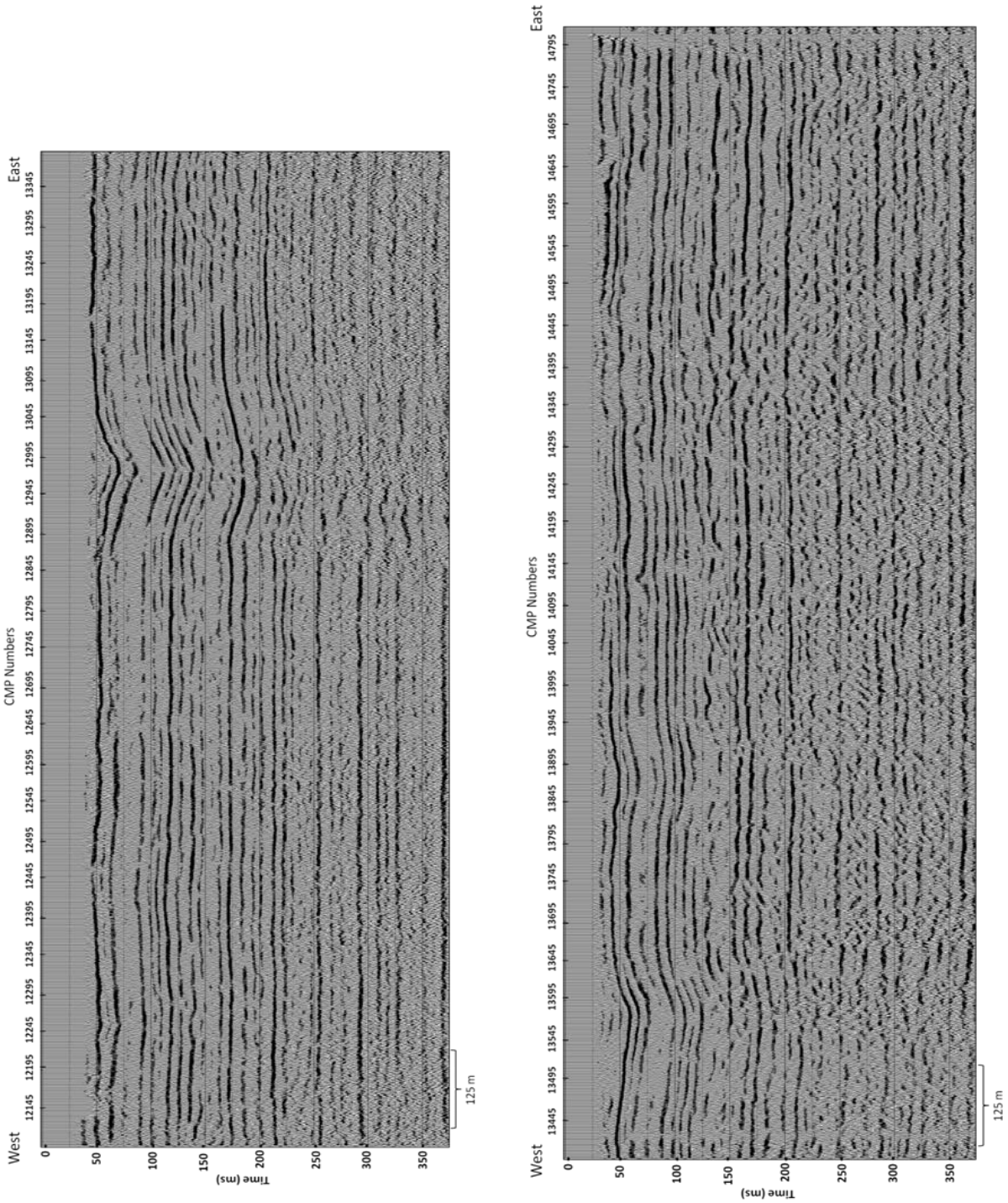

Figure 26: Unmigrated CMP stack sections from U.S. Highway 50 imaging the natural dissolution front.

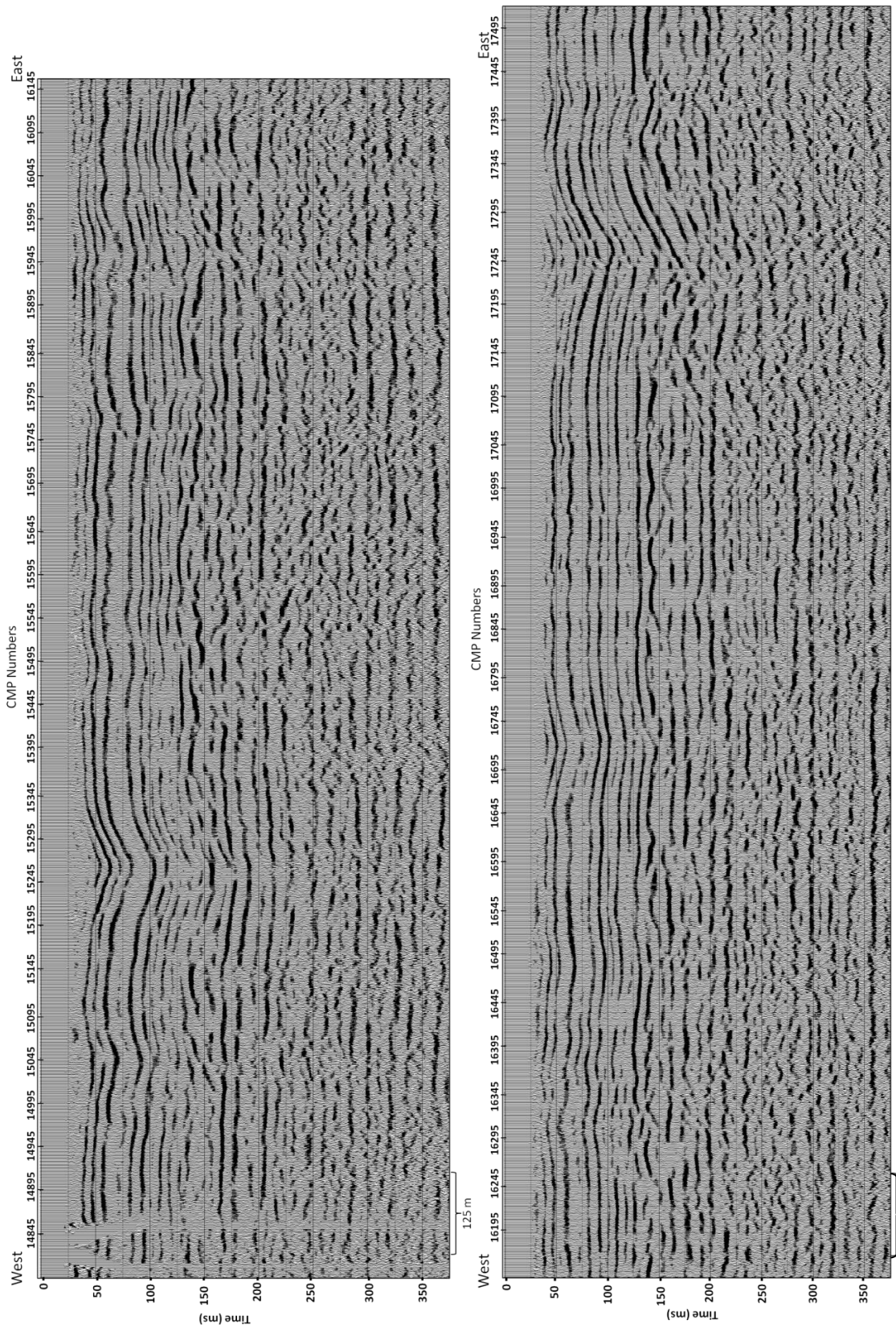

Figure 27: Unmigrated CMP stack sections from U.S. Highway 50 imaging the natural dissolution front.

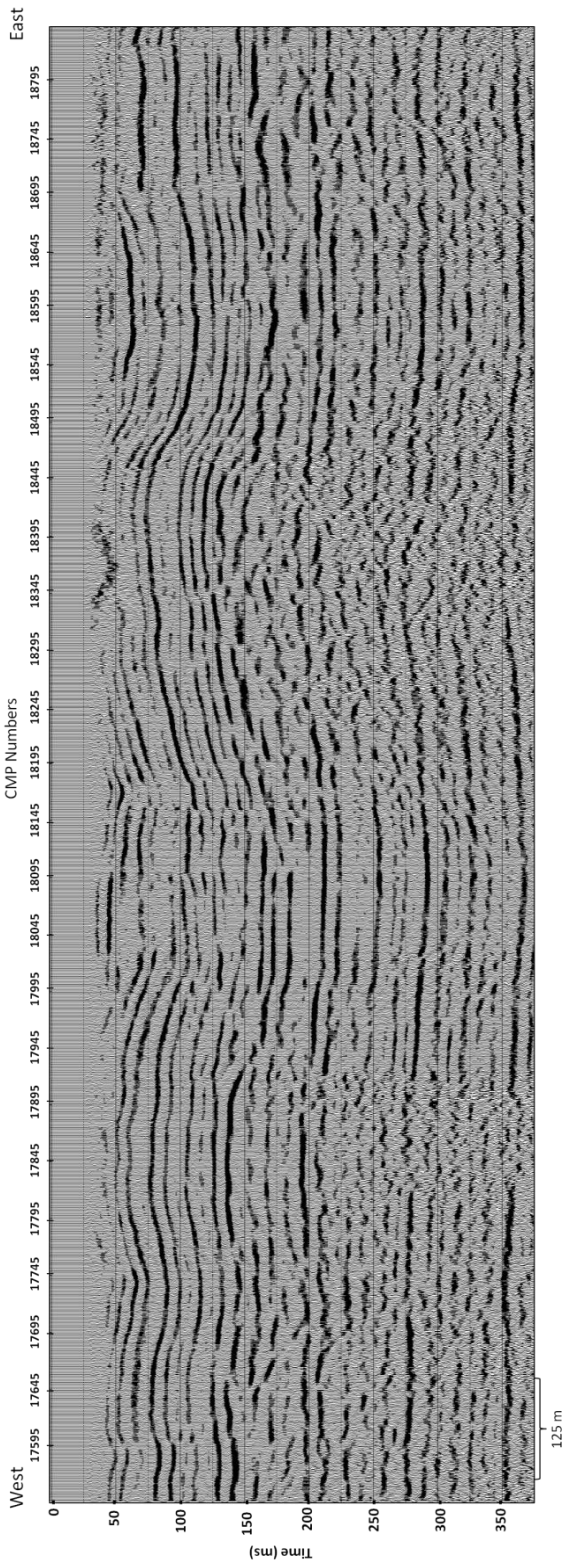

Figure 28: Unmigrated CMP stack sections from U.S. Highway 50 imaging the natural dissolution front.

Results and Interpretation

All interpretable reflections in the upper 200 ms on the stacked section directly correlate to reflection hyperbolae on the shot gathers. All times indicated in this interpretation are in two-way travel time. Beginning along the western side of the CMP stacked section a strong reflection event near 50 ms is interpreted as the bedrock (approximately 40 m depth) and represents the top of the Ninnescah shale (Figure 29 and 30). The reflection from the top of the Wellington Formation is interpreted near 90 ms (approximately 85 m depth) and the reflection from the top of the Hutchinson Salt arrives at approximately 135 ms (approximately 130 m depth). The lower Wellington has been described as the "anhydrite beds" (Ver Wiebe, 1937) due to the many cyclical anhydrite layers interbedded within the shale interval. The approximate base of the salt can be identified by the high amplitude reflections returning from the cyclic anhydrite beds that begin near 170 ms (approximately 200 m depth) indicative of the transition into the lower Wellington, making the salt interval approximately 70 m thick. The Chase Group reflection is interpreted near 225 ms (approximately 270 m depth).

An isochron was created from the interpreted top of the salt horizon and base of the Wellington horizon using Hampson and Russell software (Figure 31). The isochron possesses features that are consistent with the observed subsidence structures on these seismic data. The pattern of dissolution illustrated on the isochron is not representative of a gradual stepwise thinning of the salt interval but reveals a highly complex, sporadic dissolution progression along this cross section of the salts eastern margin. Anomalous thinning of the salt interval occurs across the entire extent of the profile. Beginning approximately 3 km west of the borehole inferred dissolution front (Watney, 2003), the salt interval begins to gradually thin reaching a thickness of approximately 40 m at the front (Figure 31). Dissolution zones increase in width

and depth (vertical salt removal) to the east resulting in broad subsidence structures along the eastern margin of the profile.

Critical to mapping dissolution along the eastern margin of the salt is identifying how solution altered and native salt appear on the CMP stacked seismic section. An interpreted interval of undisturbed salt with several unique localized dissolution features is imaged along the initial 2 km of the CMP stacked section (Figure 29). Undisturbed salt is rare along this seismic profile and is valuable in understanding the reflection signature along the shale/salt contact. The close proximity of solution altered salt also provides a unique opportunity to compare reflection characteristics and geometry of the overburden and salt. Centered on CMP 12550 a subsidence feature spans approximately 200 meters (Figure 30). Reflections from within the salt interval have a synform shape that is often characteristic of naturally induced subsidence events (Miller, 2002) and drape is present in the Permian rock over the dissolution altered salt volume. Immediately to the east, beneath CMP 12715 is an interpreted undisturbed salt interval based on the flat lying geometry of both the salt and the Permian overburden (Figure 30). The wavelet characteristics within the undisturbed salt interval have lower amplitude when compared to that of the disturbed salt interval. Amplitude is a principal seismic characteristic for identifying solution altered zones beneath continuous spans of roof rock or interbedded layers because of its direct relationship to acoustic impedance (Miller, 2007).

Possible scenarios along the dissolution front that could result in solution altered rock are void development beneath the insoluble shale caprock, paleo-void development, salt creep or flowage, void development within the salt interval along insoluble layers, or possibly dissolution prior to deposition of the upper Wellington shales (Miller, 2007). Amplitude and reflection

geometry is used in this research as a tool in a general capacity to distinguish between disturbed and undisturbed rock salt.

Understanding seismic artifacts, geometric distortions and localized compressional-wave velocity variability associated with these subsidence features is important to an accurate seismic interpretation. Bed terminations, faulting, and synform curvature in overburden beds can produce diffractions and geometric distortions within stacked seismic sections. "Pull downs" in two way travel time along reflections within subsidence features can be the result of localized variability in material velocity and are expected based on seismic subsidence models (Anderson et al., 1995) (Figure 32b). Velocity variability related to these subsidence structures can also result in sub-salt reflections having a subdued expression of the sinkhole. Diffractions and distorted reflections ("bow tie" distortion and misplaced reflections) can result from terminated beds and small radius curvature of synforms within the salt and Permian overburden (Figure 32c).

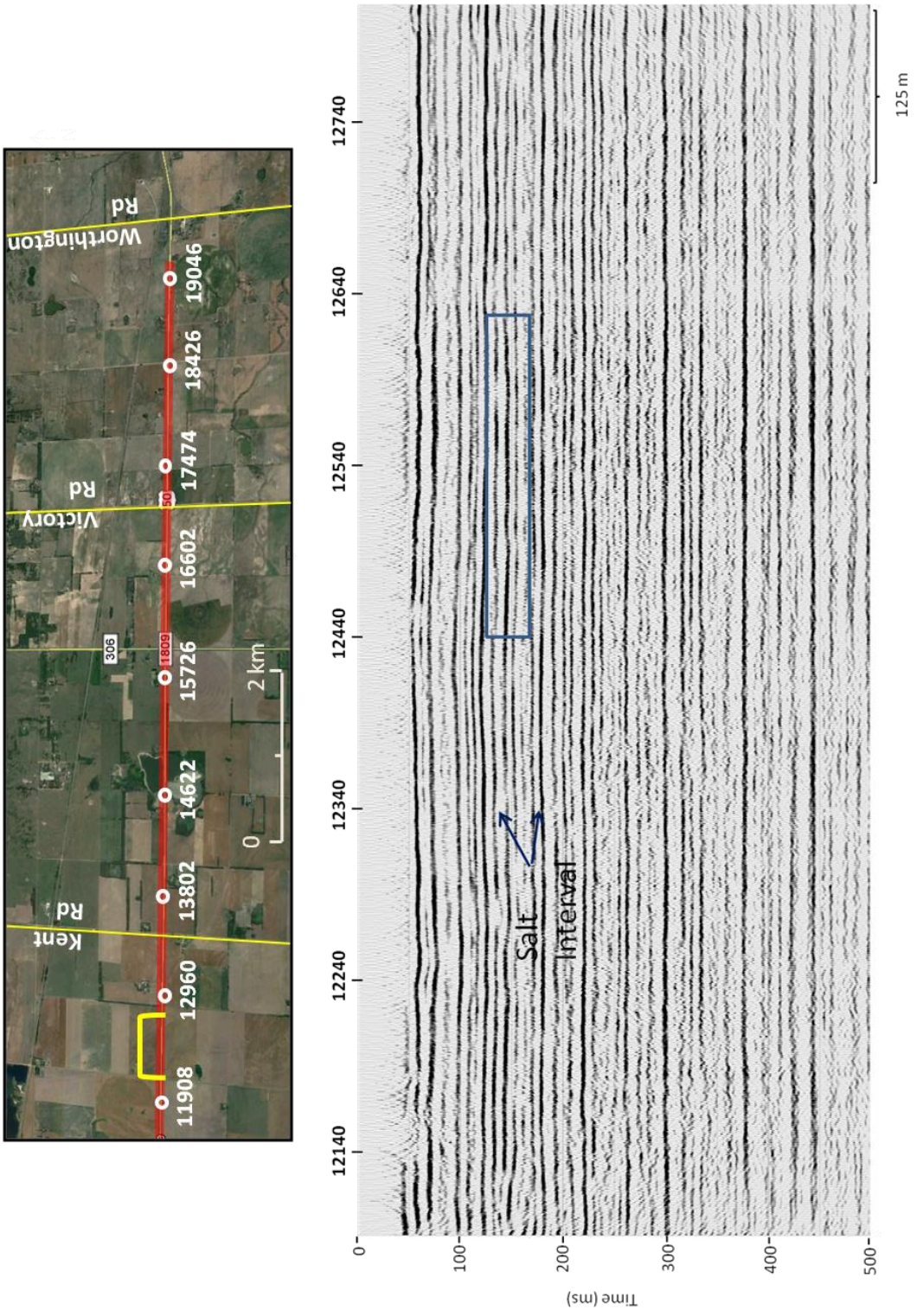

Figure 29: Migrated stacked section of relatively undisturbed salt interval west of Kent Rd. The flat geometry of beds both above and below the salt are prominent. An increase in signal quality is observed in areas of undisturbed salt. Blue box indicates a subtle subsidence feature (Figure 30)

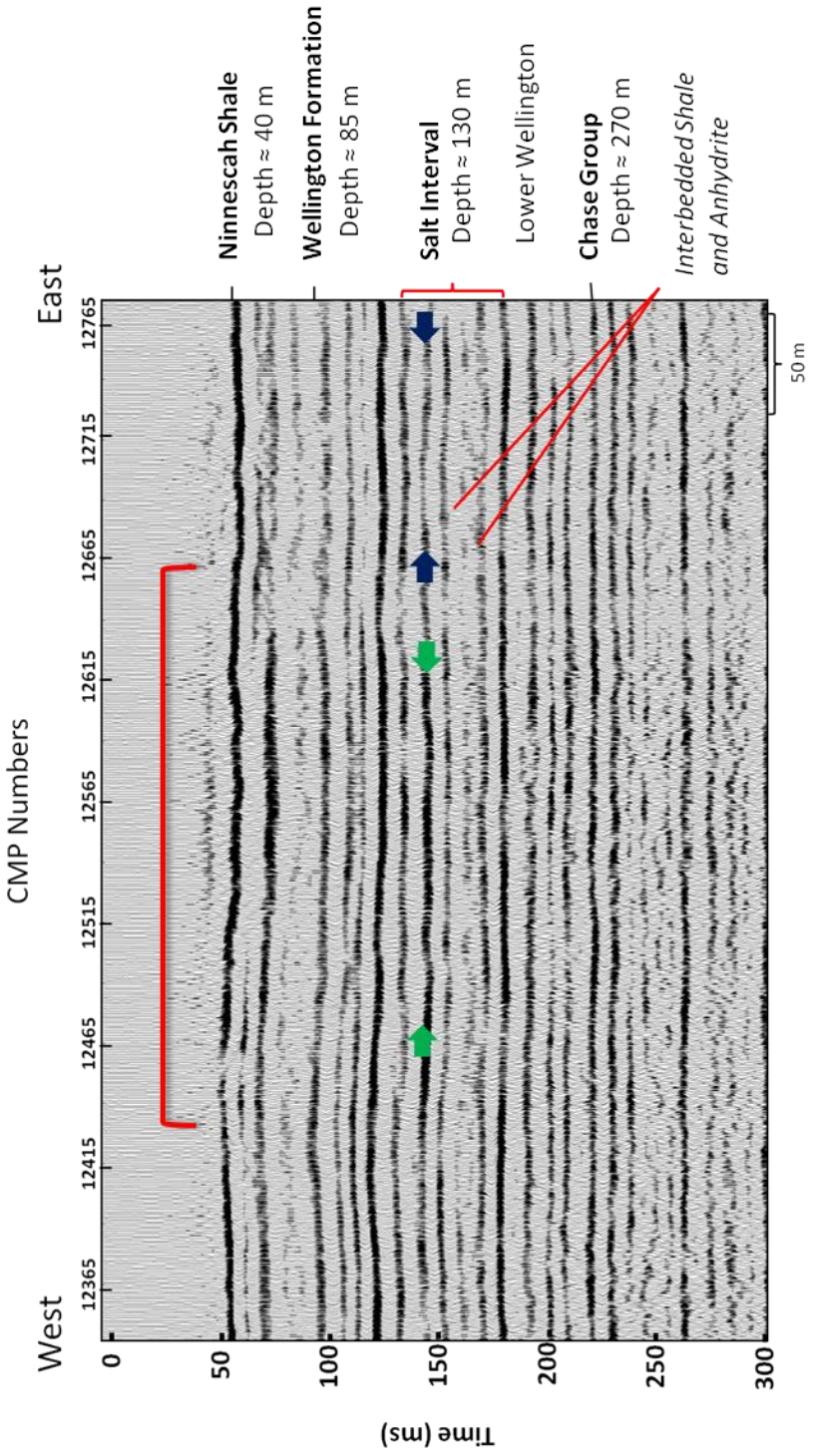

Figure 30: Migrated section of subtle paleo-subsidence feature (no surface expression). A clear increase in amplitude is associated with the solution altered zone near the top of the salt interval (green arrows) compared to the undisturbed salt reflection characteristics below CMP 12715 (blue arrows). Interpreted Permian units and approximate depth indicated on the right.

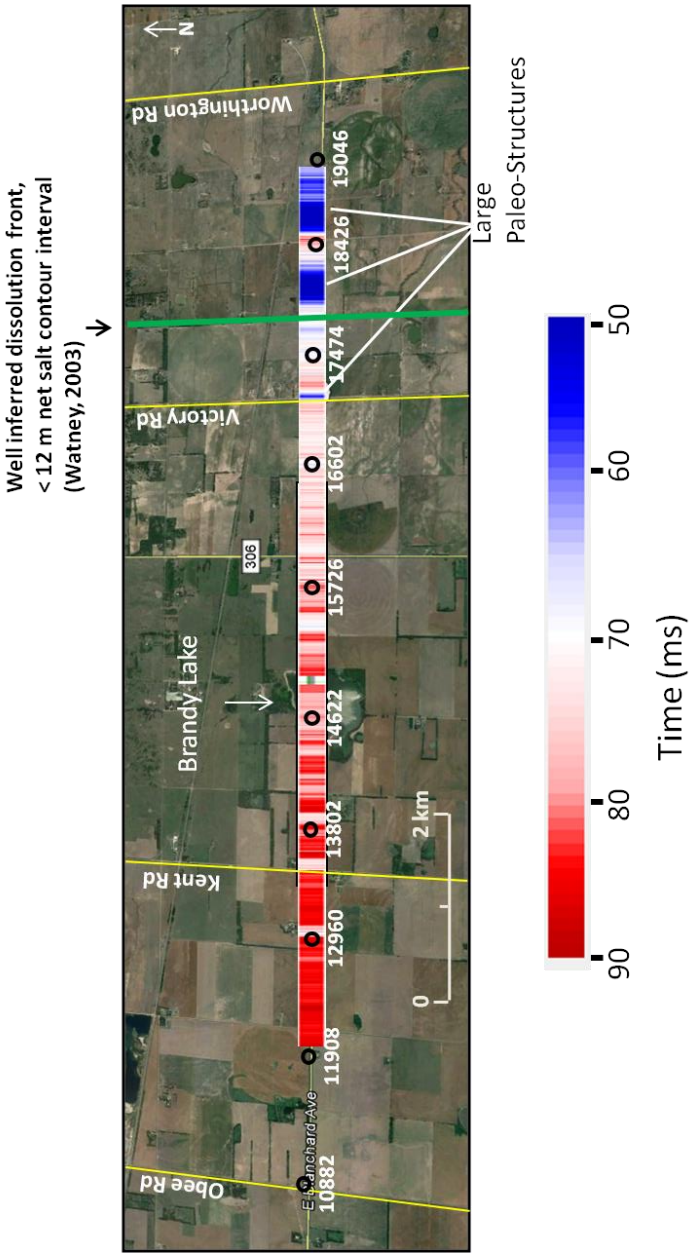

Figure 31: Isochron of interpreted top of salt and base of Wellington indicating the dissolution progression approaching the dissolution front. This reveals a highly complex and discontinuous dissolution pattern along the eastern margin.

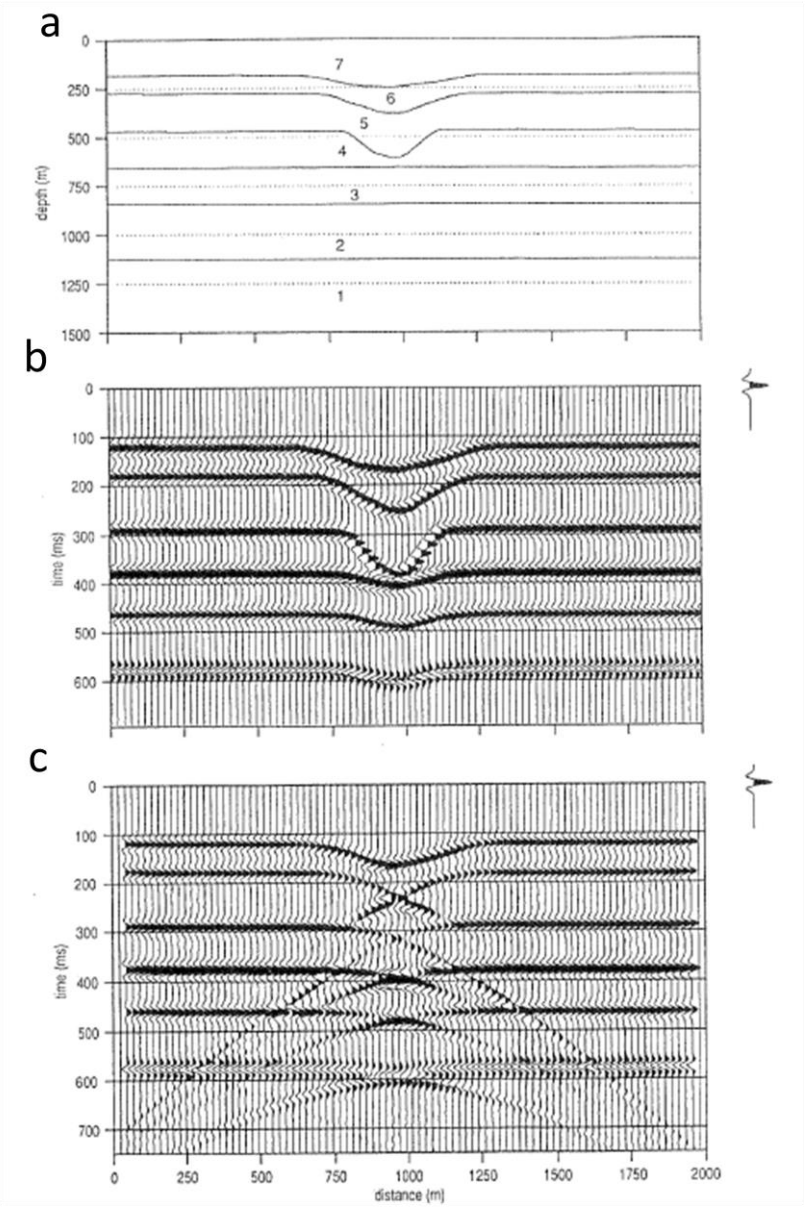

Figure 32: (a) Cross-section of typical subsidence feature with 3 flat beds beneath the structure. (b) synthetic seismogram indicating the time delays observed beneath the synform relating to subsidence. (c) Synthetic seismogram with diffracted energy from wavefield distortion (Anderson, 1995)

Interpretation of the Eastern Dissolution Margin

As expected, the concentration of subsidence events increases within proximity of the eastern margin of the Hutchinson Salt. More than a dozen inadvertently imaged paleo subsidence structures are clearly identifiable on the 2008 CMP stacked section. On this 2-D profile, these features begin approximately 8 km to the west of the eastern edge of the salt.

The pattern of leaching along this cross section of the eastern margin can be characterized as laterally (east – west) discontinuous and sporadic (Figure 33). This is illustrated by several paleo-subsidence features that have no surface expression identified over the western most 2 km of the CMP stacked section (centered near CMPs 12550, 12970, 13565, and 13865). These structures are identified by synform or "bowl-shaped" depressions indicated by a gentle sag or dip in reflections above the salt. The subsidence features are characterized by the anomalous thinning of the approximately 70 m thick salt interval, with the vertical extent of leaching variable within each sinkhole. Away from the center of the subsidence structure the rock salt returns to a thickness of approximately 70 m. The characteristics of the overlying Permian rock appear relatively undisturbed between each feature with normal flat lying deposition above spans of undisturbed salt that range from 50 – 200 m in width.

These localized single episode subsidence features provide evidence to suggest that dissolution along the eastern margin is extending away from the defined front, along dissolution created fluid pathways. It is unlikely that isolated episodes of leaching are occurring in the main body of the Hutchinson salt as leaching requires both an inlet and outlet for gravity driven fluid flow. If unsaturated water was able to vertically penetrate the salt and no exit pathway existed, leaching would immediately halt and brine would remain dormant along the base of the water column. The discontinuous pattern of dissolution along these seismic data suggests dissolution

corridors are intruding into the salt interval from the eastern margin, providing the necessary fluid pathways for leaching to occur.

Immediately east of these subsidence features the reflection characteristics (geometry and amplitude) near the top of the salt dramatically change, becoming what seismically appears to be a highly rugged salt topography (Figure 34). These reflections are suggestive of a high energy environment indicated by a lack of geometric consistency and bed terminations along interbedded insoluble layers within the upper salt beds. These characteristics are interpreted to be the result of leaching along the top of the salt interval. More aggressive or localized leaching and potential void/rubble zones are seismically indicated by increased time delays/drape (Figure 36, A). Despite the highly altered salt interval, less than 5 ms of drape is observed in the Permian reflection (110 ms) directly above this dissolution zone (between CMP 13965-14265) in response to over 12 ms of drape along the top of salt. This 250 m span is immediately adjacent to recently active subsidence west of Brandy Lake. Despite its proximity, this is interpreted as the remnants of a paleo dissolution network or channel system because of the lack of surface expression above visible drape in the Permian bedrock (Figure 34, A). However, the potential for reactivation of leaching and apparent bridging within the shale overburden present a future risk to the road surface at this location.

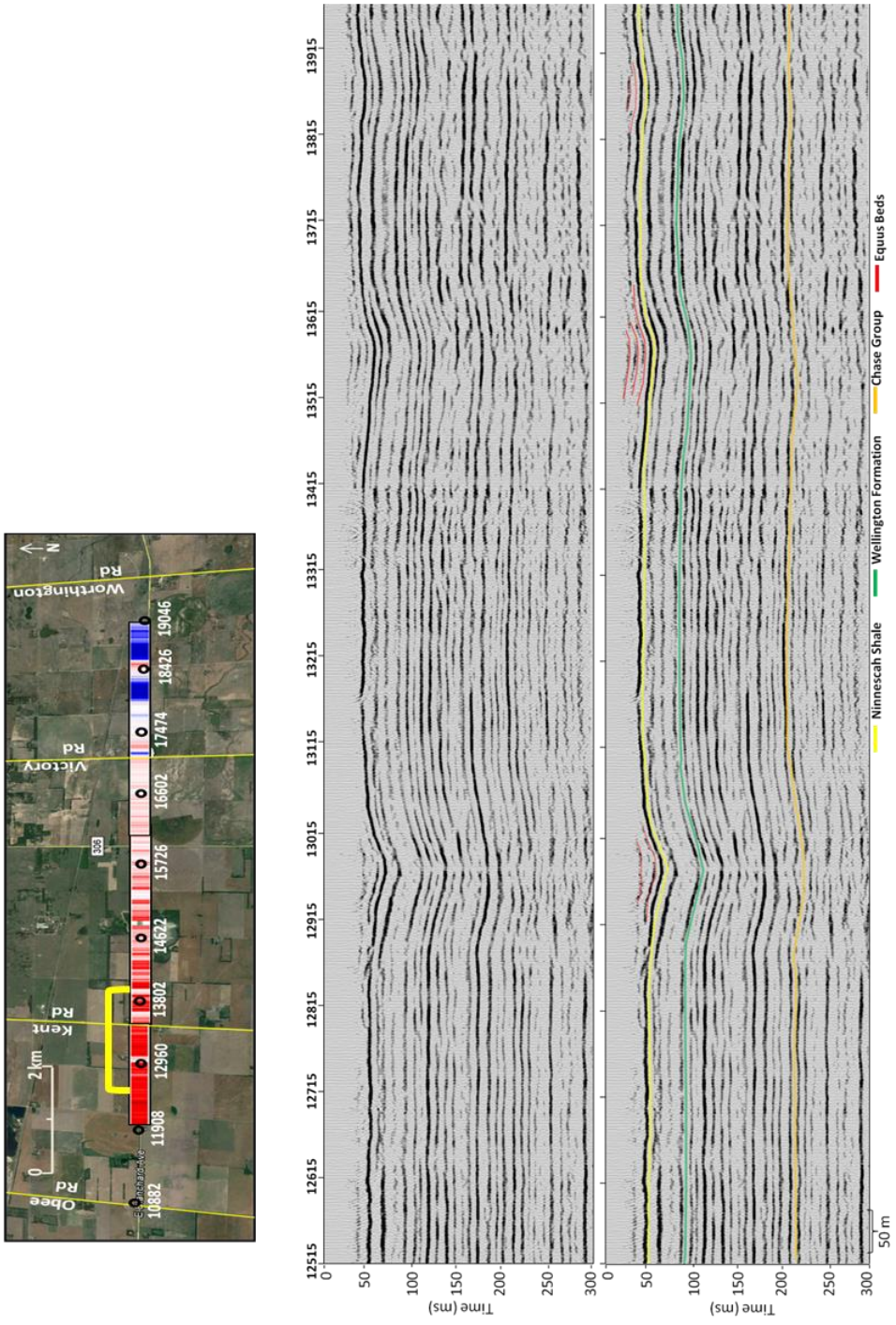

Figure 33: Multiple sinkholes are identified approximately 8 km from the dissolution front. These paleosinkholes can be identified by their bowl shaped depressions. Thinning of the salt appears to be laterally discontinuous along this east-west cross section. These features are likely the result of dissolution corridors intruding westward from the eastern salt front.

Interpretation of the Brandy Lake sinkholes

Seismic imaging reveals nearly 400 meters of Permian rock disturbed by subsidence beginning immediately west of the Brandy Lake – Hwy 50 transect (CMP 14625) (Figure 4 and 35). GPS data collected in 2008 in conjunction with the seismic acquisition allowed an estimated correlation with the 2009 Lidar data (Herrs, 2010). Multiple episodes of subsidence appear to be the cause of recent road deformation and the continued expansion of the surface expression that makes up Brandy Lake. Interpretation of the failure progression of these subsidence features can be limited as the horizontal resolution of the data causes over sampling of discrete data points along reflectors resulting in trace-to-trace smearing of small vertical offsets on CMP stacked sections. Failure interpretation of these features is dependent on geometry and determined from observable offset, subtle changes in rock layer slopes and amplitude variability (Miller, 2007)

Distinct geometries indicate at least four unique subsidence features centered on CMP 14335, 14405, 14485 and 14535 are imaged west of Brandy Lake (Figure 35). All four of these sinkholes span some portion of the surface expression delineated by LiDAR data. The highest magnitude of subsidence is centered on CMP 14535 and is characterized by a subtle drape in the Permian overburden (CMP 14500-14580). Obvious pull down effects in reflections beneath subsidence features centered over CMP 14485, 14535 and extending beneath Brandy Lake begin near CMP 14470 on the time stacked section. These are the result of velocity decreases caused by changes in bulk density during subsidence and do not represent true structure. To compensate for this, these features are interpreted on horizon flattened CMP stacked sections (Figure 36).

The current geometry of the surface expression that makes up Brandy Lake suggests it has experienced multiple episodes of subsidence. This seemingly complex sinkhole formation

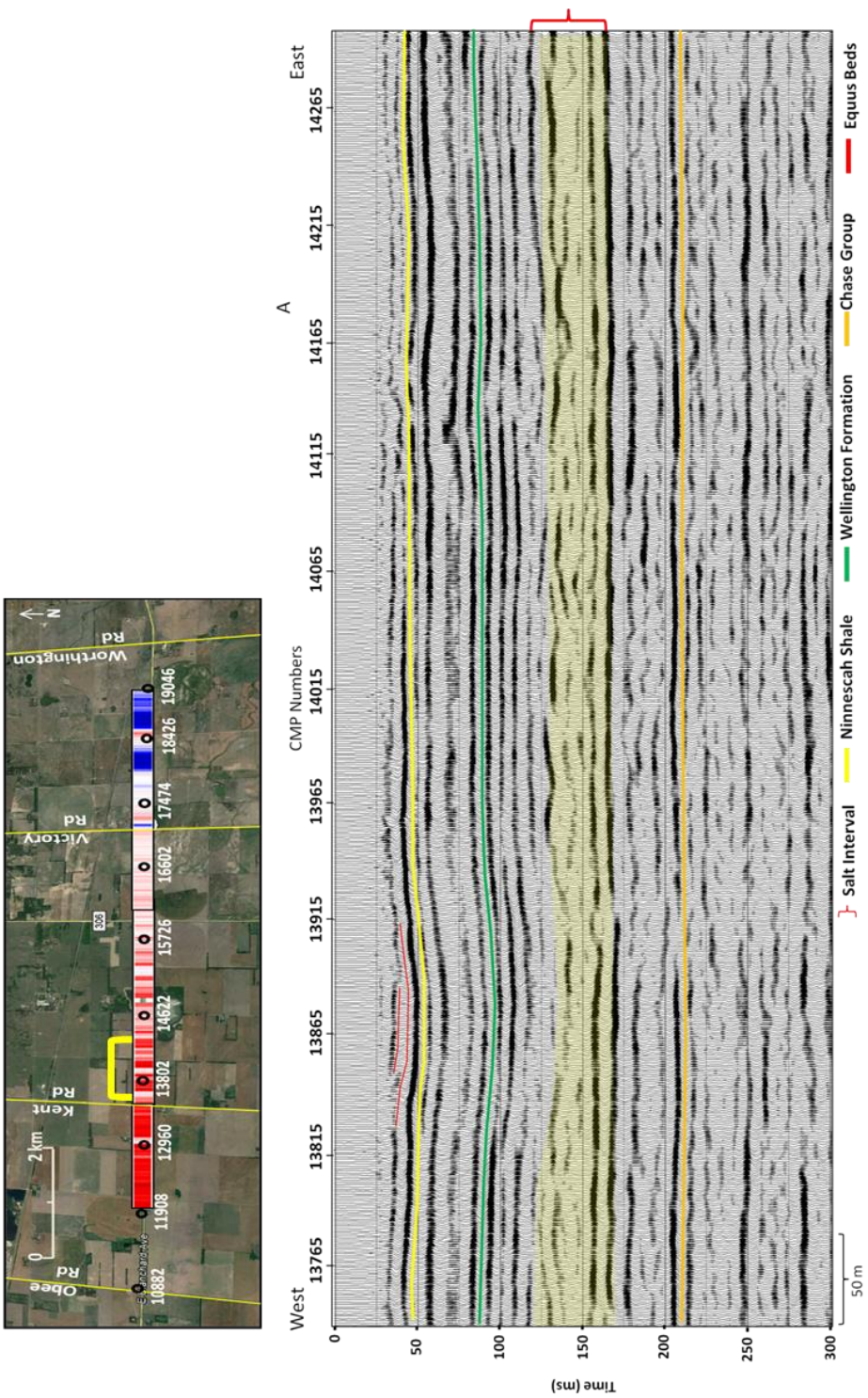

Figure 34: Geometrically distorted salt reflections indicate leaching has occurred along the top of the salt interval. Potential void/rubble zones are indicated by increased time delays (A). Currently minimal subsidence has occurred across this dissolution zone. Bridging in the Permian above the salt interval (A) could indicate future risk of road subsidence.

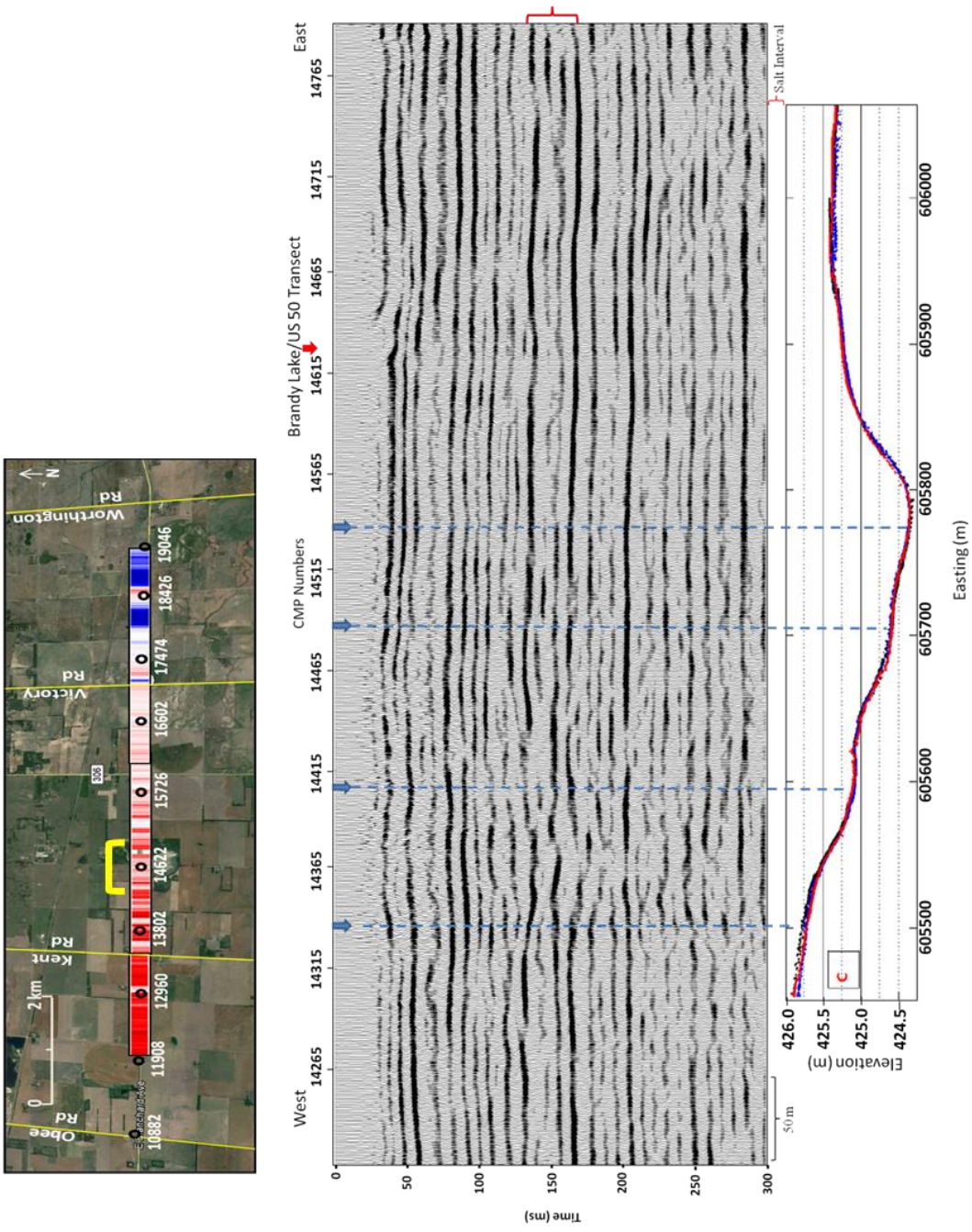

Figure 35: Migrated CMP stacked section correlated with elevation data. Four unique subsidence structures correspond to the "stepping" deformation pattern indicated by LiDAR data. The onset of Brandy Lake along this transect is identified by the red arrow. Notice pull-down effects beneath the salt interval (130 ms) begin near CMP 14470. These are the results of velocity variability and are not real structure.

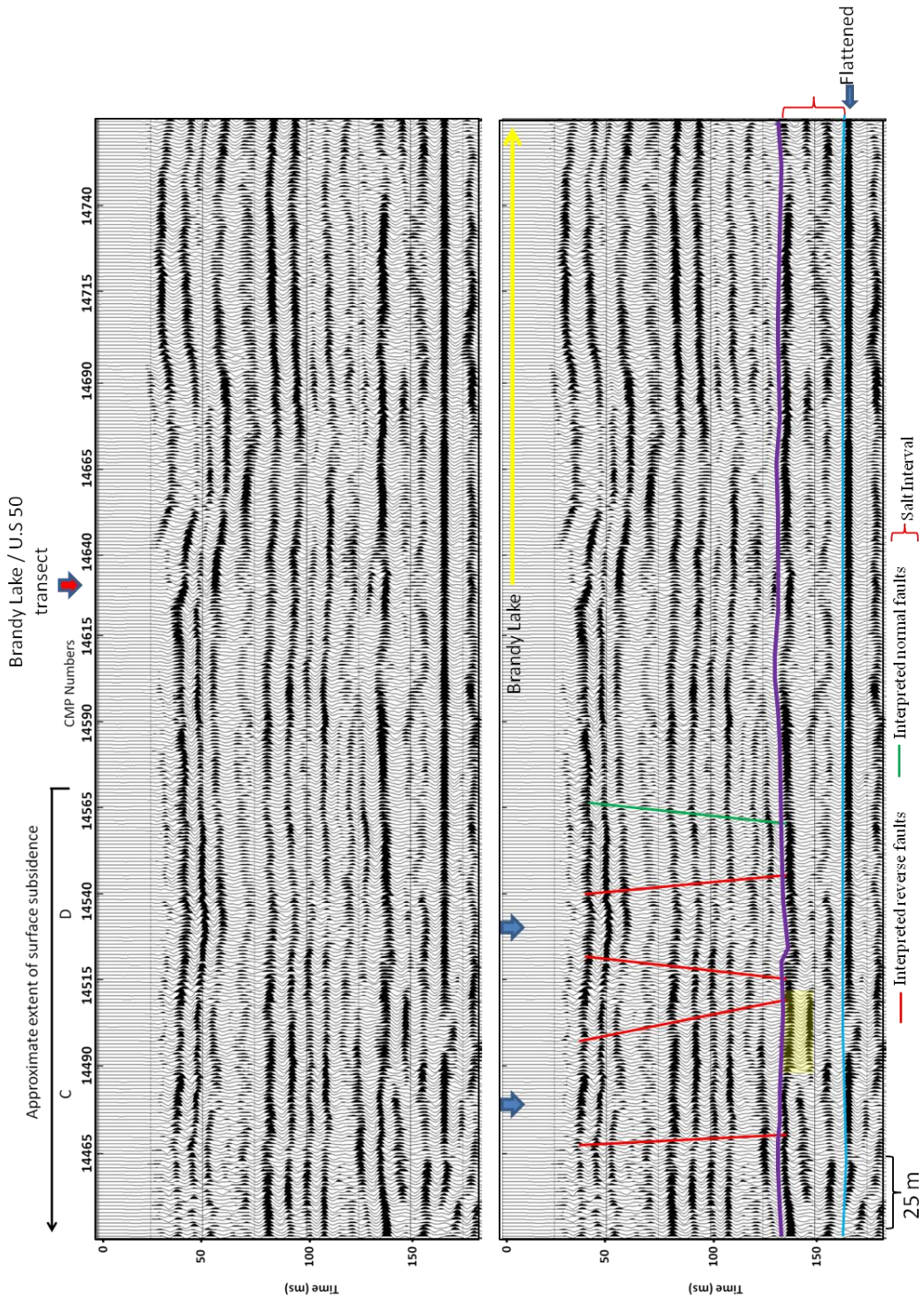

Figure 36: (D) Maximum surface subsidence of 1.25 m is centered beneath subtle synform depression. A reactivation or continuation of leaching has occurred immediately to the west forming a second sinkhole (C). (C) Corresponds to over 1 m of surface deformation. Subsidence that has resulted in the western 150 m of Brandy Lake is centered beneath CMP 14670. Leaching is suspected to be horizontally driven westward along the upper salt interval from dissolution zones that currently make up Brandy Lake

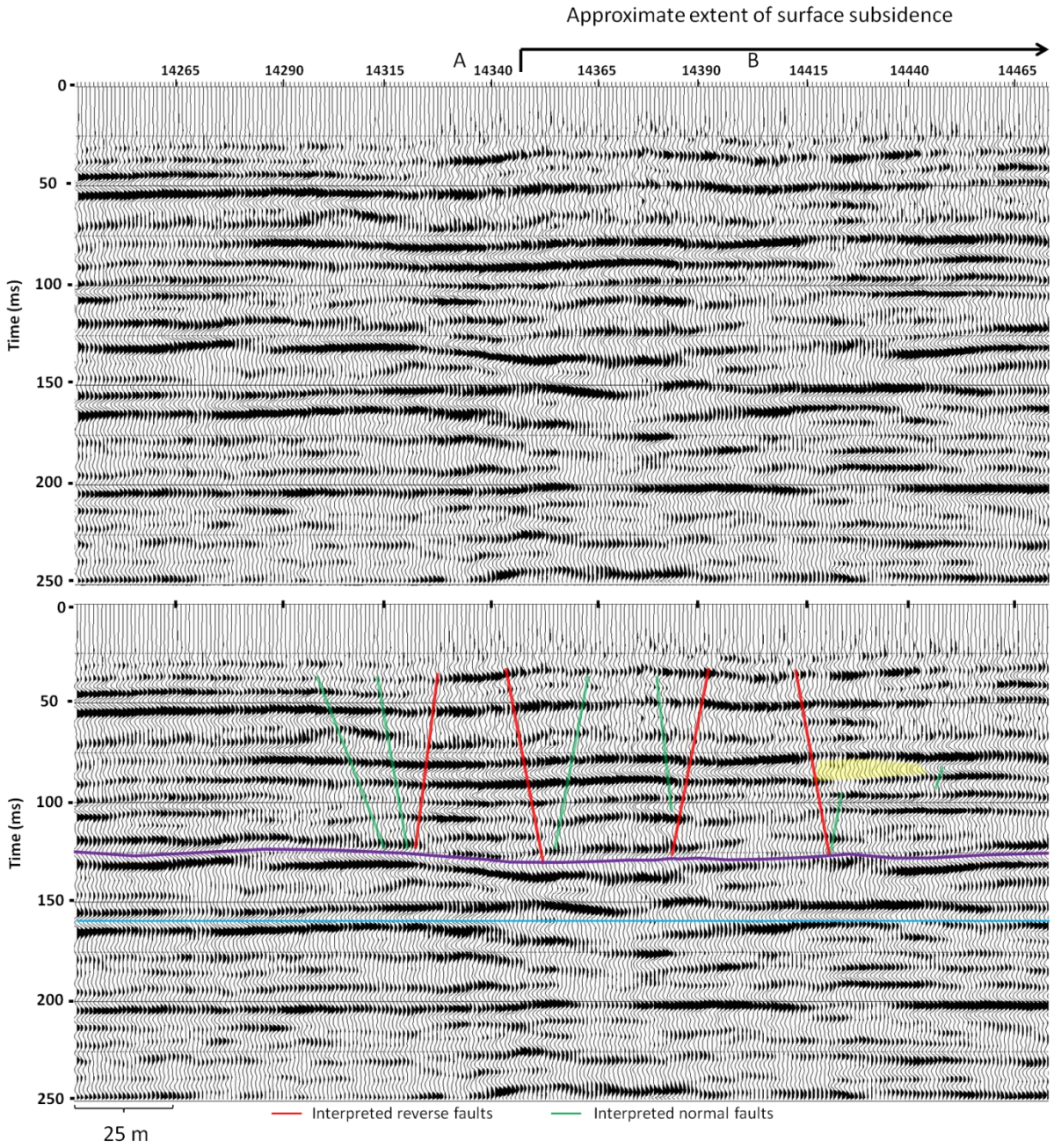

Figure 37: Interpretation of failure mechanics of subsidence structures that have resulted in deformation of U.S. 50. Subsidence structure entered over (B) corresponds to 0.75 m of road deformation. The subsidence structure immediately to the west (A) likely formed prior to roadway development based on its lack of current surface expression. Interpretation is speculative but consistent with subsidence mechanics and other features interpreted along the front. Yellow indicates potential bridging.

may be the result of intermittent unsaturated water access or changes in hydrology that diverted (e.g. subsidence) continuous fluid access resulting in different solution fronts. Unfortunately minimal fold coverage due to limitations during acquisition restricts the full exposure of the subsurface beneath the lake along this 2-D profile. An asymmetrical depression centered near CMP 14670 appears to make up the western 150 m of the lakes current surface expression (Figure 36). Drape in the Upper Wellington reflection (80 ms) results in nearly 8 m of depth depression across the feature. Beneath this sinkhole a well defined leached salt interval is identified by a subtle synform depression near the shale/salt contact. Dissolution appears to have expanded horizontally along the upper salt beds with failure eventually resulting in the current 8 m down dropped overburden (Figure 36). Reflection characteristics indicate minimal unsaturated water is penetrating deeper into the salt. Time to depth estimates based on the NMO velocities on the horizon flattened section suggest there is at least 55 m of an undisturbed salt interval remaining beneath this feature and approximately 60 m beneath most of Brandy Lake.

Unsaturated fluid flows appear to continue to intrude west into the salt interval from dissolution zones that formed Brandy Lake. A broad trough like depression is visible on the flattened reflection profile between CMP 14500 and 14580 (Figure 36, D). At the center of the trough is an interpreted failure cone which corresponds to the highest magnitude of surface subsidence at 1.25 m. Thinning of the salt interval is evident beneath this feature and suggestive of leaching guided along the base of the shale/salt caprock. Leaching likely resulted in a vertically thin void between CMP 14500-14580 that eventually failed. Further complicating this section is what appears to be a second subsidence structure immediately to the west (Figure 36, C). This feature has an unusual migration pathway with the disturbed area of overburden rock extending slightly offset from the salt, with a subtle synform depression centered beneath CMP

14480 where 1 m of surface subsidence exists. Leaching in the salt interval is characterized by a lower frequency and higher amplitude reflection with slightly chaotic arrivals that may indicate active or recently active leaching (Figure 36, C).

The westernmost features are characterized by subtle bowl shape geometries in the Permian overburden (Figure 37). Combined these two features span approximately 200 m. The original sinkhole margins of both subsidence features formed along reverse oriented fault planes during periods of brittle stress release consistent with the tensional dome model (Davies, 1951). Extensional failure appears to have resulted in the radial expansion of the initial failure, forming a broad trough shaped depression. Despite its migration to the surface, less than 20 cm of surface subsidence has occurred along the eastern flank of the westernmost feature since the highway was constructed (Figure 37, A). The minimal surface expression suggests this feature likely formed prior to roadway development with surface subsidence the result of continued settling in the overburden. Failure is suspected to have been recent (1990's) within the sinkhole centered on CMP 14405 based on the magnitude of subsidence which reaches 0.75 m near the center of the failure cone (Figure 37, B). The salt interval is not well defined beneath this feature and drape in the overburden is minimal (< 3 ms). Apparent bridging along the eastern edge of this feature is a potential zone for continued slumping and settlement.

These CMP stacked sections were used to uniquely identify the complex dissolution pattern beneath recent road deformation. Recently active unsaturated fluid flows appear to have intruded into the upper salt beds resulting in expansion of previous dissolution zones that formed Brandy Lake to the north and the east. This has resulted in a complex dissolution system and the formation of 3 subsidence features with sinkhole development along U.S. 50 occurring over a 20-30 year span (Herrs, 2010). Even though subsidence was dormant over the 1 year time lapse

Lidar survey, this area will likely undergo variable subsidence rates through incremental gravity slumping and compaction within these subsidence features. The most significant risk to the road surface is the high likely hood of active or reactivation of leaching in the future.

Interpretation of the Eastern Dissolution Margin (cont.)

Reflections from the Hutchinson salt indicate a progressively more rugged and distorted salt topography 5 km from the dissolution front (Figure 38). Geometric distortion and increased reflection amplitudes from the salt interval (130 ms) indicate discontinuous but extensive dissolution zones along the shale/salt contact. It is likely that leaching has occurred along a significant portion of the upper salt beds within this section. The Permian overburden is characterized by more localized short-wavelength synform depressions creating a karst type topography along the bedrock. More vertical dissolution zones are still laterally discontinuous and separated by spans of thicker but highly altered salt. The salt interval thins to 40 m beginning approximately 3 km west of the borehole inferred dissolution front.

The eastern most 2 km of the seismic reflection profile is dominated by 3 large (width > 400 m) paleo-subsidence structures centered near CMP 17250, 18100, and 18590(Figure 39 and 40). Some of these features posses unique characteristics that provide clues to the dissolution process of the front. First, the salt interval appears to be extensively or fully leached beneath the subsidence features. Second, flat lying Pliocene – Pleistocene deposits above the sinkholes indicate periods of subsidence dormancy ranging from the Tertiary to recent. Lastly, current surface subsidence or anomalous thinning of the Equus Beds suggests reactivation of subsidence. The first of these features is at the intersection of Victory Road and U.S. 50 (Figure 39). This site has been heavily investigated prior to this study due to recent and currently active subsidence

along the road surface (Miller, 2002; Miller, 2007; Rice, 2009; Herrs, 2010). The remaining two paleo superstructures are to the east and span the final 2 km of the seismic line (Figure 40).

At least two episodes of subsidence can be identified in the Victory Road sinkhole (Miller, 2002; Rice, 2009) (Figure 41). The bowl shaped depression defining this feature is centered on CMP 2400 with the original subsidence volume likely extending between CMP 2440 – 2350. Flat lying Equus Bed deposits 20 m thick beneath CMP 2380 indicate the original subsidence volume has been dormant since at least Pliocene or early Pleistocene deposition (Figure 42). Reactivation of subsidence began along the western flank of this feature in the 1990's and can clearly be delineated by the subtle synform depression within the Ninnescah Shale and Wellington group between CMPs 2520-2460 (Miller, 2002).

One of the largest features along this seismic line spans over 700 m (Figure 43). The top of the Hutchinson salt can be identified by the high amplitude reflection near 130 ms. The salt interval itself resembles a wedge narrowing towards the subsidence volume and flattening beneath the subsidence feature. This suggests either a fully removed salt interval or a stoppage of vertical dissolution along an insoluble bed within the salt. The Equus Beds geometry suggests a complex dissolution history with multiple time periods of subsidence. Laterally coherent deeper Equus bed reflections appear to thicken across the west side of the feature (CMP 18000-18130). Thickening may be associated with dormancy and reactivation of subsidence. If the onset of dissolution and the resulting subsidence occurred prior to deposition of the deeper Equus beds, then they would thicken over the feature (Figure 42). The apparent thinning and drape in all observable Equus beds centered on CMP 18165 is a result of re-activated growth into areas without subsidence prior to their deposition. Based on this observation, subsidence within

this feature likely predates Pliocene deposition making the onset of dissolution at this feature at least as early as the Tertiary (Lane and Miller, 1965).

Flat reflections make up the final 150 m of the seismic section with Permian bedrock nearing an estimated 60 m in depth and an approximately 20 m thick Hutchinson Salt interval (Figure 40). This is consistent with research from Bayne (1956), indicating Permian bedrock depth just over 60 m 2 km north of this section of the seismic line.

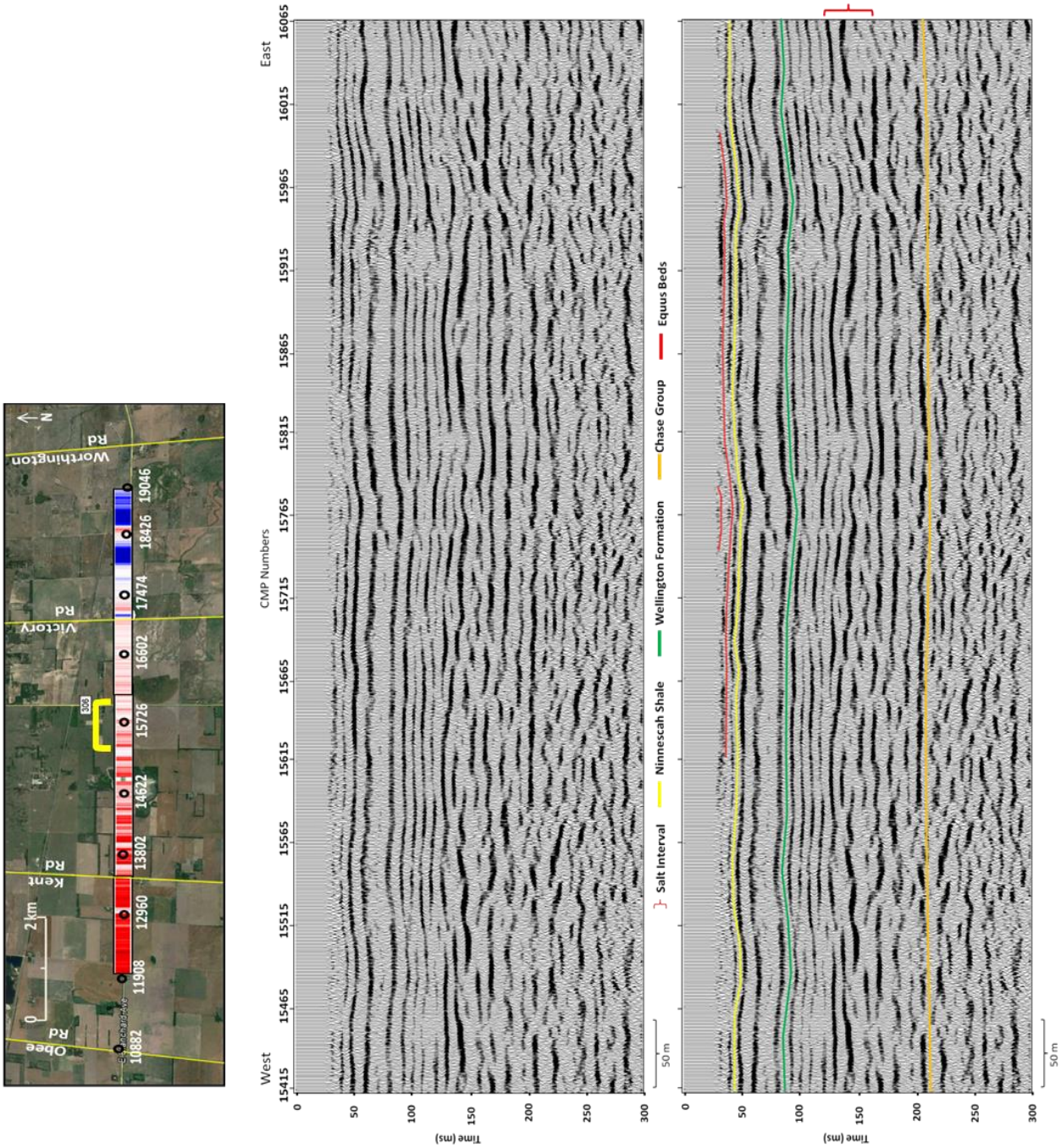

Figure 38: Migrated CMP stacked section of the subsurface 5 km west of the dissolution front. A highly deformed overburden representing an almost karstic topography that conforms to the rugged salt interval. The observable increase in deformation along the western 5 km of the dissolution front is a result of laterally extensive leaching along the upper salt beds.

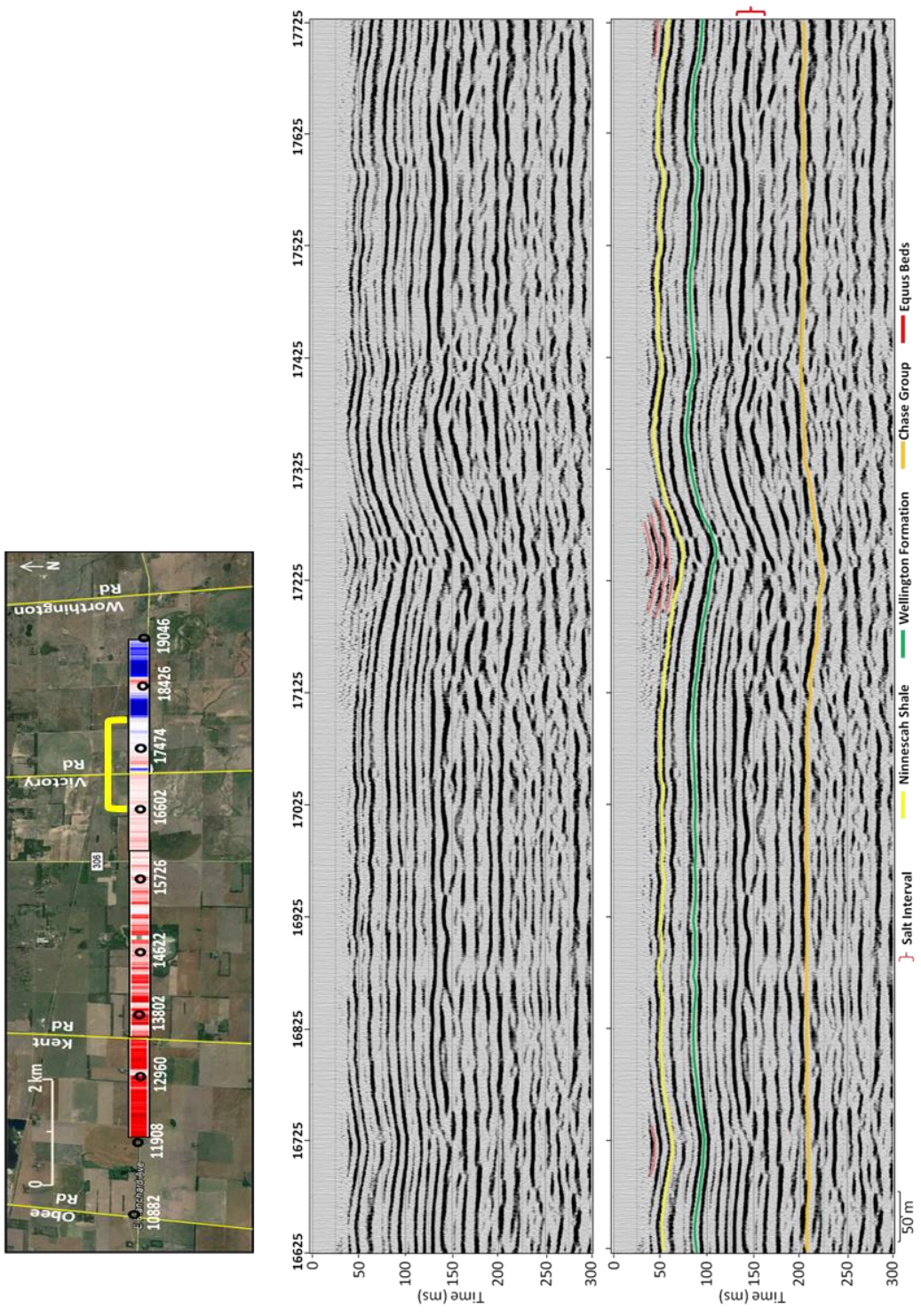

Figure 40: A migrated CMP stacked section of the subsurface less than 2 km west of the dissolution front. A large paleo-structure is centered over CMP 17250. Recent reactivation along the western flank of this feature has deformed the road surface at the intersection of U.S. Highway 50 and Victory Road. salt interval is approximately 40 m thick outside of this feature.

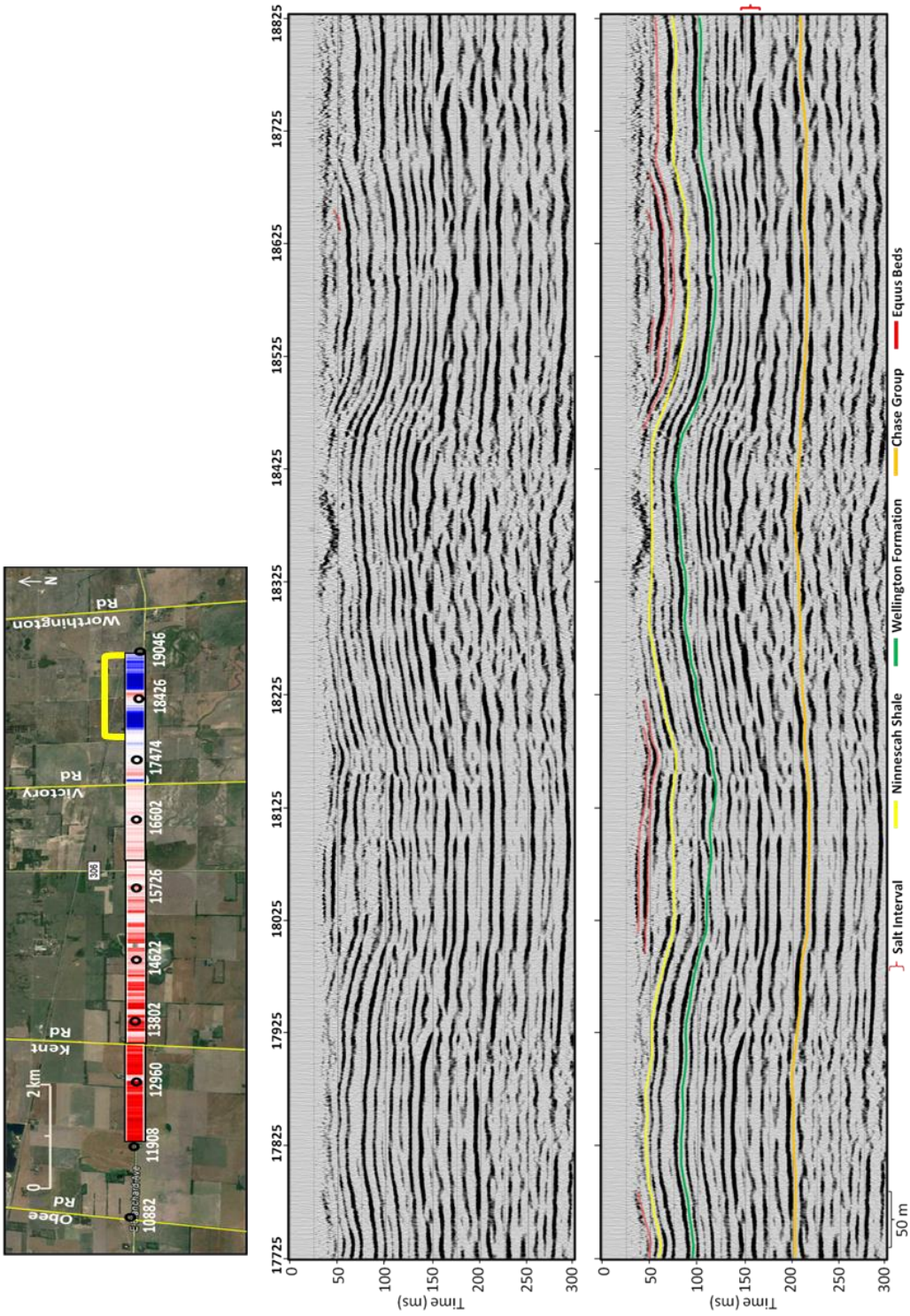

Figure 41: Migrated CMP stacked section of two large paleo- superstructures that are imaged immediately east of the bore hole inferred dissolution front and span approximately 2 km of the seismic survey.

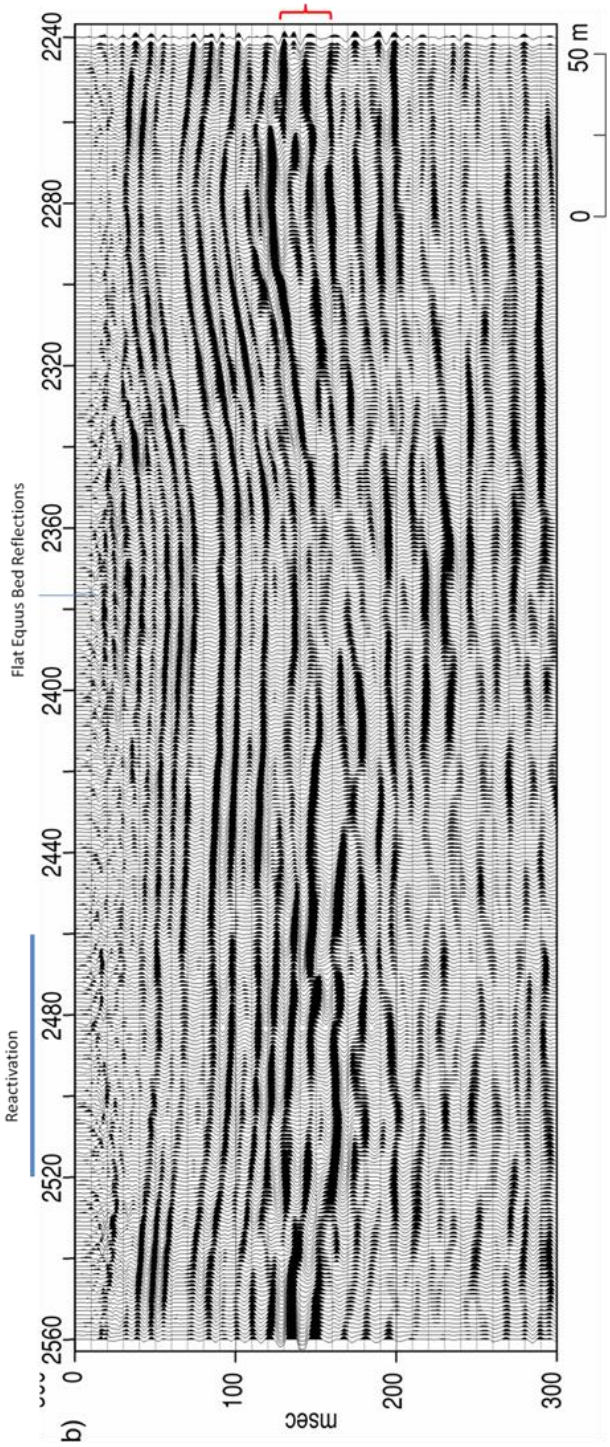

Figure 42: Subsidence feature near Victory Road – U.S. 50 intersection (modified Miller, 2002). This large paleo root spans almost 400 m and was imaged due to recent reactivation along its western flank. 20 m of Flat Equus bed deposits below CMP 2380 suggests dormancy in this feature since early Pliocene-Pleistocene deposition

.

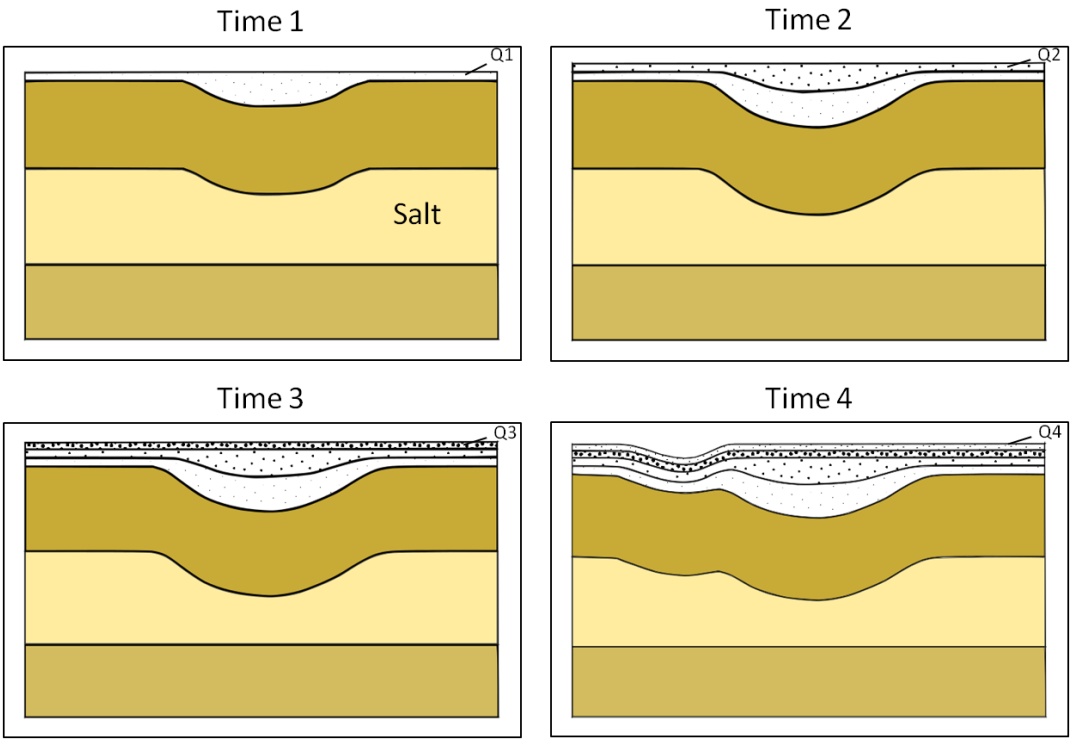

Figure 43: Cartoon of possible Pliocene-Pleistocene Equus beds and Quaternary deposition (indicated by Q1-Q4) in regards to dormant and reactivated subsidence features. Anomalous thickening of the Equus bed and/or Quaternary deposits over the feature indicates subsidence prior to its deposition. Flat lying deposits indicate dormancy of the subsidence structure.

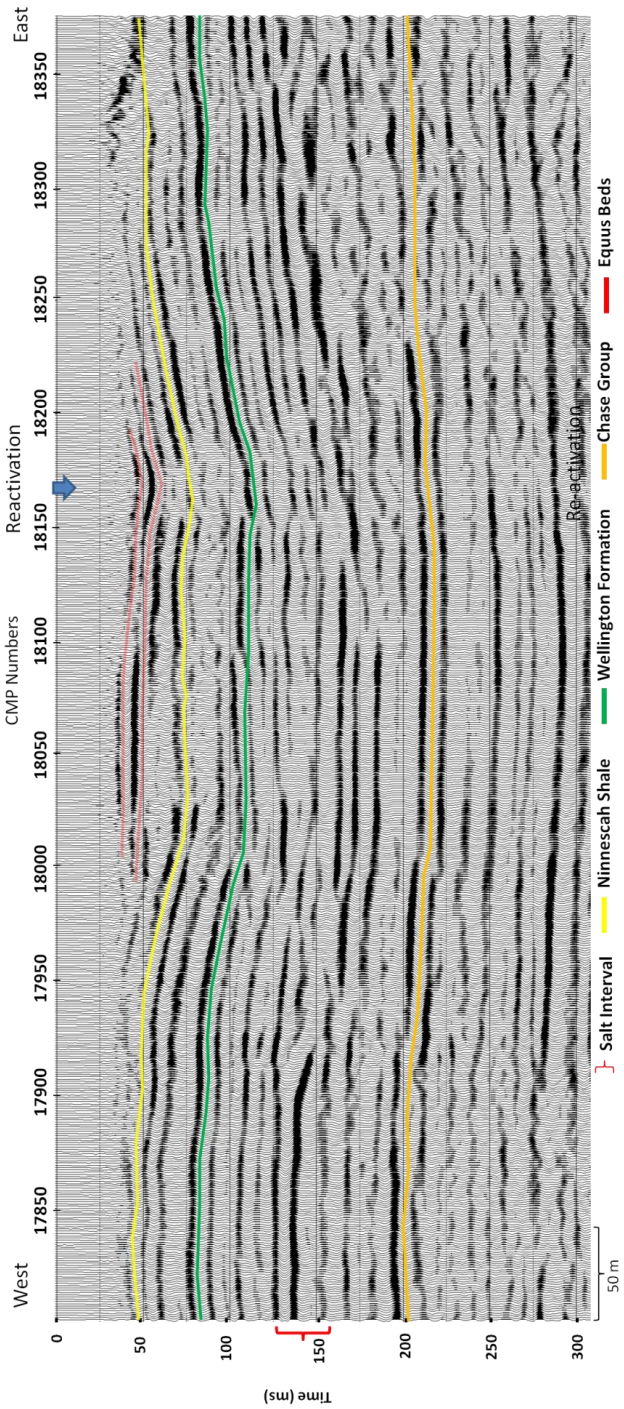

Figure 44: Migrated CMP stacked section of paleo-Superstructure imaged along the eastern dissolution front. Multiple growth episodes can be clearly identified by thinning and thickening of Equus Beds. A reactivation of subsidence along the eastern flank of this feature is clearly identified beneath CMP 18160.

Discussion/Conclusion

Key Observations and Dissolution Model

These 22 km of seismic reflection data represent a high resolution snapshot of the rapidly (in geologic time) changing natural dissolution margin, east of Hutchinson. Leaching and associated subsidence along the dissolution front, on a local scale, may appear random when viewing it in an anthropogenic time frame and piecing the processes together from surface subsidence; however from a regional prospective it progressed westward over the last 2 million years at a relatively consistent rate (~0.3 cm/yr) (Walters, 1978; Watney and Paul, 1980). Though regionally the front has migrated westward at a consistent rate, these seismic reflection sections indicate localized processes are highly sporadic and lack predictability within tens of km of the high gradient front. These observations suggest that the eastern dissolutional margin of the salt is not undergoing a continuous, gradual (east-west) dissolution front nor does it appear to be heavily driven by fault zones as previous models have suggested.

Correlating the regional scale progression inferred by low-resolution well-log data with the high resolution imaging of local scale processes provided by seismic reflection data, gives a more complete model that accounts for dissolution front observations across all scales (Figure 44). The dissolution "front" should actually be characterized as a complex network of dissolution flow paths that principally branch westward into the salt interval from the eastern margin. Several of the key observations from stacked seismic sections produced as part of this study support this interpretation and include:

1) **Paleosinkholes inadvertently imaged on the 22 km seismic profile are identified up to 20 km west of the eastern dissolution front**. – Anomalous thinning of the salt

interval and discontinuous subsidence features ranging up to 20 km west of the dissolution front indicates that unsaturated water has had access into the salt interval and that brine is finding fluid pathways out of the system. This is significantly further from the eastern margin then can be explained by a simple ramp-style dissolution front. The identification of these features is strong evidence to support the suggestion that dissolution corridors are intruding westward into the salt interval and extending up to at least 20 km. These corridors also provide the necessary fluid pathways for saturated fluids to flow out of the system, whereas vertical fractures could provide a pathway for fluids to enter but gravity would inhibit escape.

2) **There is no seismic evidence of a gradual ramp-style main dissolution front.** - The eastern 2 km of the seismic profile is composed of discontinuous, broad subsidence structures that are separated by 40+ m thick spans of remnant rock salt. Dissolution zones appear to increase in width and depth (leached salt) towards the east. Progression of this pattern suggests expansive dissolution zones increasing in width to the east with decreasingly intermittent spans of remnant rock salt. This has created a highly erratic eastern "face" of the salt that has been commonly referred to as the front. This process also accounts for spans of remnant rock salt encountered by boreholes east of the dissolution front (Spinazola et al., 1985)

3) **Periods of dormancy followed by re-activation of leaching indicates time varying fluid pathways and intermittent unsaturated water access.** – Fluid flows are intermittent along the eastern margin of the salt. Over time, these varying fluid pathways enlarge dissolution corridors and have formed expansive dissolution networks along

eastern margin. If these pathways grow beyond roof rock strength failure occurs and it is likely a sinkhole will form.

4) **Natural dissolution is relatively confined to the eastern margin of the Hutchinson salt**. – If geology based-fluid pathways such as faults and fractures zones are a main driver of the natural dissolution process, then dissolution would be prominent throughout the main body of the Hutchinson salt where these features exist. However, natural dissolution appears to be relatively confined to within 20-30 km of the eastern margin (Walters, 1978). Faults can be a vertical fluid conduit but greatest fluid movement typically would be immediately after rupture. No evidence of faulting has been identified across any active or paleo subsidence structure along the natural dissolution front. It is possible that previously interpreted fracture zones (Anderson, 1994; Watney et al., 2003) are not providing the permeability through the thick Permian shale for fluid to access the salt. Alternatively, if unsaturated water is accessing the salt through fracture zones and leaching does occur, this process will become stagnant without an exit because saturated fluids must flow downward or horizontally due to gravity. These features may be guiding the dissolution progression once impinged upon by the interpreted dissolution corridors but are not a main driving force of the progression of the dissolution front.

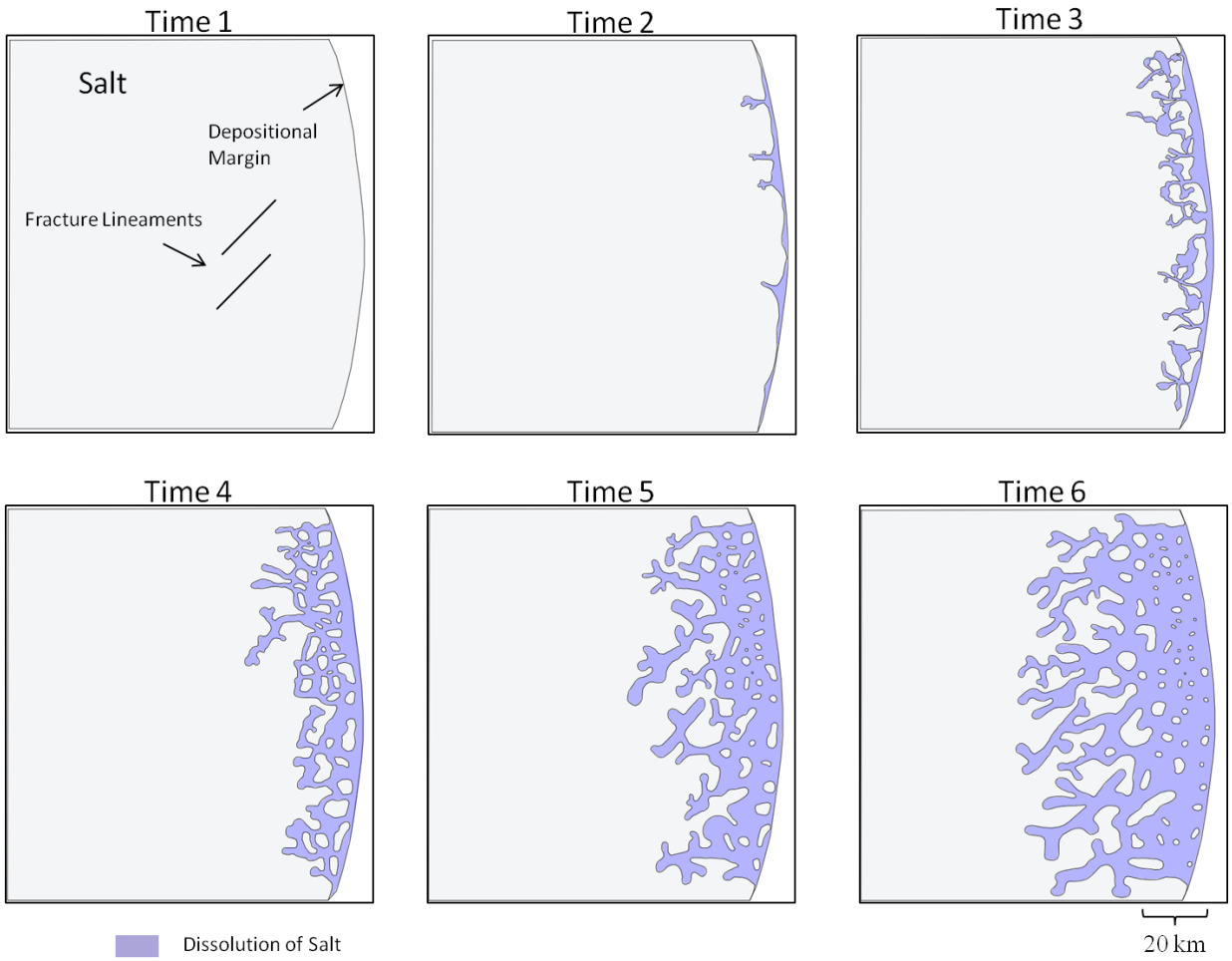

Figure 45: Cartoon of possible natural dissolution front progression. Continued dissolution along the depositional margin of the salt creates complex system of dissolution channels. Intermittent access to fresh waters from east of the salt face allows dissolution to progress horizontally into the salt interval. Paleo-subsidence channels provide outlets for saturated water to flow out of the system. Faults and fracture zones may guide dissolution once impinged upon by dissolution channels.

Along with these observations, the processes imaged beneath Brandy Lake are indicative of the dissolution front and consistent with the interpretation that leaching is extending westward into the salt interval along dissolution channels. Brandy Lake is interpreted to be one of these dissolution corridors horizontally intruding into the salt body. Previous subsidence that has occurred along this dissolution corridor has likely been masked by continued deposition of Quaternary sediment. Recently active subsidence along its western flank is clearly delineated on these seismic data and indicates leaching is continuing to encroach into the salt interval in a highly irregular fashion from the adjacent dissolution zones that make up Brandy Lake. The seismic data indicate that leaching is also occurring along the upper salt beds at this site, consistent with the gravity drive system.

The progression of the dissolution front suggests unsaturated water is accessing the salt face from the east or from above and penetrating westward into the salt interval. Dissolution is also controlled by regional hydrodynamics where changes in pressure gradients, new fresh water inlets, fluid chemistry and overburden collapse at one location are accounted for somewhere else in the system (Miller, 2007). This results in the utilization of new or dormant fluid pathways and accounts for the expansion of paleo-dissolution channels by the intrusion of unsaturated water into previously undisturbed salt beds, growing the dissolution system (e.g. Brandy Lake, Victory Road).

The seismically observed subsidence structures and highly altered salt interval along this cross section indicate that a real threat of unanticipated surface subsidence exists throughout the eastern margin of the salt. Paleo subsidence features and/or an altered salt interval are more prone to leaching. The pattern of dissolution along the eastern margin of the salt is highly complex and not a realistically mappable system, however improved models of the progression

of the front from continued research can help better define regions more susceptible to risk in the future.

Future

Many questions still exist in regards to the onset and progression of the natural dissolution front. Besides this study, local scale research regarding timeframes, growth rates, and extent of the dissolution progression along the eastern margin of the salt have been relatively limited. Even this study only provides a single linear profile along the 150 km long (north – south) dissolution front. 3-D seismic reflection and its suite of attributes is the logical next step and a seemingly appropriate tool for fully delineating the complexities related to 3-D subsidence structures and dissolution systems relating to the front. 3-D seismic reflection data would also provide a more structurally accurate image as it is not as susceptible to out of plane energy and can utilize full 3-D migration processing methods.

Further research is needed on the utility of acoustic impedance inversions for near surface subsidence investigations. However, two necessities for utilization of acoustic impedance inversion methods in this near surface setting are maintaining low frequency signal in the seismic data, and borehole logs that provide seismic-well tie points for accurate wavelet extraction and initial impedance models. In many near surface seismic investigations, the cost of these requirements will often outweigh any potential benefits.

References:

Anderson, N.L., J. Hopkins, A. Martinez, R.W. Knapp, P.A. Macfarlane, and W.L. Watney, 1994, Dissolution of bedded rock salt: A seismic profile across the active eastern margin of the Hutchinson Salt Member, Central Kansas: Computers and Geosciences , 889-903.

Anderson, N.L., R.W. Knapp, D.W. Steeples, R.D. Miller, 1995, Plastic deformation and dissolution of the Hutchinson Salt Member in Kansas, in Anderson, N.L., and Hedke, D., Eds., Geophysical atlas of Kansas: Kansas Geol. Surv. Bull., 237, 66-70.

Anderson, N. L., W.L. Watney, P.A. Macfarlane, and R.W. Knapp, 1995, Seismic signature of the Hutchinson Salt and associated dissolution features: Kansas Geological Survey, Bulletin 237, 57-63.

Anderson, N.L., A. Martinez, J. Hopkins, and T. Carr, 1998, Salt dissolution and surface subsidence in central Kansas: A seismic investigation of the anthropogenic and natural origin models. Geophysics , v 63, p 366-378.

Anderson, R.Y., and D.W. Kirkland, 1980, Dissolution of salt deposits by brine density flow. Geology, v 8, p 66-69.

Anderson, R.Y., 1981, Deep-Seated Salt Dissolution in the Delaware Basin, Texas and New Mexico: New Mexico Geological Society, Special Publication no 10, p 133-145.

Baker, G.S., 1999, *Processing Near-Surface Seismic-Reflection Data—A Primer*: Society of Exploration Geophysicists, Course Notes Series No. 9, R. Young, ed.

Bayne, C. K., 1956, Geology and ground-water resources of Reno County, Kansas: Kansas Geological Survey, Bulletin 120.

Beck, B.F., A.J. Pettit, and J.G. Herring, eds., 1999, Hydrogeology and engineering geology of sink-holes and Karst-1999: A.A. Balkema.

Bland, S., P. Griffiths, and D. Hodge, 2004, Restoring the seismic image with a geological rule base: First Break, v 22, no 4.

Black, R., D.W. Steeples, and R.D. Miller, 1994, Migration of shallow reflection data: *Geophysics*, v. 59, p 402-410.

Black, T.J., 2003, Evaporite Karst in Michigan: Oklahoma Geological Survey Circular 109, p 315-320.

Boone, S., M. Monier-Williams, R. Turperning, T. Morgan, K. Tandon, B. Bryans, 2008, Identification and Interpretation of Solution Mining Features in Bedded Salt Deposits on a Crosswell Reflection Profile: SEG expanded abstract, p 1407-1410.

Brittle, K. F., L.R. Lines, and A.K. Dey, 2001, Vibroseis Deconvolution: a synthetic comparison of cross correlation and frequency-domain sweep Deconvolution: Geophysical Prospecting, v 49, p 675-686.

Brown, A. R., 2004, Interpretation of three-dimensional seismic data, 7th Ed. AAPG Memoir no. 42. Tulsa: Association of Petroleum Geologists.

Carmichael, R.S., 1989, *CRC Practical Handbook of Physical Properties of Rocks and Minerals*: Boston, CRC Press, p 741.

Chopra, S., and K. Marfurt, 2005, Seismic Attributes - A Historical Perspective, Geophysics, 70, 3so-28so.

Coruh, C., and J.K. Costain, 1983, Noise attenuation by Vibroseis whitening (VSW) processing: Geophysics, v 48, no 5, p 543-554.

Davies, W.E., 1951, Mechanics of cavern breakdown: National Speleological Society, v 13, p 6-43.

Dellwig, L.F., 1971, Study of salt sequence at proposed site of the national radioactive waste repository at Lyons, Kansas;. In Final Report, Geology and Hydrology of the proposed Lyons, Kansas Radioactive Waster Repository Site: Kansas Geological Survey, Subcontract No. 3484.

Doll, W.E., and C. Coruh, 1995, Spectral Whitening of impulsive and swept-source shallow seismic data. [Exp. Abs.] SOC. Explor. Geophys., p. 398-401.

Ebrom, D.A., S.A. Markley, and J.A. McDonald, 1996, Horizontal resolution before migration for broadband data [exp. abs.]: Society of Exploration Geophysics, p. 1430-1433.

Ege, J.R., 1984, Formation of solution-subsidence sinkholes above salt beds: U.S. Geological Survey Circular 897, p 1-11.

Fatima, M., L.B. Kumar, P. Rao, and D. Sinha, D., 2010, Improving resolution with Spectral Balancing-A case study, 8th Biennial International Conference and Exposition on Petroleum Geophysics, Hyderbad.

Ferguson, R.J. and G.F. Margrave, 1996, A simple algorithm for bandlimited impedance inversion: CREWES Research Report, v 8, no 21.

Galloway, D., D. Jones, and S. Ingebritsen, 2000, Land Subsidence in the United States: United States Geological Survey.

Ge, H., and M.P.A. Jackson, 1998, Physical modeling of structures formed by salt with-drawal: Implications for deformation caused by salt dissolution: AAPG Bulletin, v. 82, p 228-250.

Gogel, T., 1981, Discharge of Saltwater from Permian Rocks to Major Stream-aquifer Systems in Central Kansas: Chemical Quality Series 9.

Herrs, A., 2010, Quantifying Surface Subsidence along US Highway 50, Reno County, KS using terrestrial LiDAR: University of Kansas.

Ivanov, J., R.D. Miller, and J. Xia, 1998, High frequency random noise attenuation on shallow seismic reflection data by migration filtering: Society of Exploration Geophysics [Exp. Abs.], p 870-873.

Johnson, K. S., 1981, Dissolution of salt on the east flank of the Permian Basin in the southwestern U.S.A. Journal of Hydrology, 54, p 75-93.

Johnson, K.S., 2013, Salt Karst and Collapse Structures in the Anadarko Basin of Oklahoma and Texas: 13th Sinkhole Conference, p 103-112.

Kent, D. V., and G. Muttoni, 2003, Mobility of Pangea: Implications for Late Paleozoic and Early Mesozoic Paleoclimate. In P. Letourneau, & O. P. E., The Great Rift Valleys of Pangea in eastern North America, Tectonics, Structure, and Vulcanism, New York: Columbia University Press, v 1, p 11-20.

Klemperer, S.L., 1987, Seismic noise-reduction techniques for use with vertical stacking: An empirical comparison: Geophysics, v 52, no 3, p 332-334.

Knapp, R.W., and D.W. Steeples, 1986a, High-resolution common depth-point seismic reflection profiling: Instrumentation, Geophysics, v. 51, p 276-282.

Knapp, R.W., and D.W. Steeples, 1986b, High-resolution common-depth-point reflection profiling: field acquisition parameter design, Geophysics, v. 51, p 283-294.

Knapp, R.W., D.W. Steeples, and R.D. Miller, 1989, Seismic-reflection surveys at sinkholes in central Kansas: Kansas Geological Survey, Bulletin 226.

Lambrecht, J.L., 2006, Time-lapse high resolution seismic Imaging of a catastrophic salt-dissolution sinkhole in Central Kansas: Kansas Geological Survey Open-File Report No. 2006-23.

Lambrecht, J.L., R.D. Miller, T.R. Rademacker, 2004, Advantages and disadvantage of pre-correlation, pre-vertical stack processing on near-surface, high-resolution Vibroseis data: SEG expanded Abstract, p 1425-1428.

Lane, C.W., D.E. Miller, 1965, Geohydrology of Sedgwick County, Kansas: Kansas Geological Survey, Bulletin 176.

Leonard, R.B., H.K. Kleinschmidt, 1976, Saline water in the Little Arkansas River basin area, south-central Kansas: Kansas Geological Survey, Chem. Quality Series 3, p 24.

Liberty, L.M., and M. Knoll, 1998, Time-varying fold in stacked seismic reflection data: A new quality procedure for shallow high-resolution applications: Proceedings of the Symposium on the Application of Geophysics to Engineering and Environmental Problems (SAGEEP98), p 745-751.

Lindseth, R.O., 1979, Synthetic sonic log – a process for stratigraphic interpretation, Geophysics, v 44, p 3-26.

Merriam, D.F., C.J. Mann, 1957, Sinkholes and related geologic features in Kansas: Transactions of Kansas Academy of Science, v 60, p 207-23.

Merriam, D. F., 1963, The Geologic History of Kansas: Kansas Geological Survey, Bulletin 162.

Miller, R. D., 1992, Normal moveout stretch mute on shallow-reflection data: Geophysics, v 57, no 11, p 1502-1507.

Miller, R.D., A.C. Villella, and J. Xia, 1997, Shallow high-resolution seismic reflection to delineate upper 400 m around a collapse feature in Central Kansas: Environmental Geosciences, v. 4, no. 3, p 119-126.

Miller, R. D., 2002, High Resolution seismic reflection investigation of the subsidence feature on US Highway 50 at Victory Road near Hutchinson, Kansas: Lawrence Kansas.

Miller, R.D., 2003, High-resolution seismic-reflection investigation of a subsidence feature on U.S. Highway 50 near Hutchinson, Kansas; in K.S. Johnson and J.T. Neal, eds., Evaporite karst and engineering/environmental problems in the United States: Oklahoma Geological Survey Circular 109, p 157-167.

Miller, R.D., and R. Henthorne, 2004, High-resolution seismic reflection to identify areas with subsidence potential beneath U.S. 50 Highway in eastern Reno County, Kansas: Proceedings of the 55th Highway Geology Symposium, September 8-10, Kansas City, Missouri, p. 29-48.

Miller, R.D., A. Villella, J. Xia, and D.W. Steeples, 2005, Seismic Investigation of a Salt Dissolution Feature in Kansas: Special Publication: Near-Surface Geophysics, Volume II, Society of Exploration Geophysics, in press.

Miller, R. D., 2007, High-resolution seismic investigation of subsidence from dissolution: PhD. Dissertation, University of Leoben.

Nissen, S.E., W.L. Watney, 2003, Detailed mapping of the Upper Hutchinson Salt and Overlying Permian strata beneath Hutchinson, Kansas: Kansas Geological Survey Open-file Report 2003-66.

Norton, G. H., 1939, Permian redbeds of Kansas. Wichita, Kansas: American Association of Petroleum Geologists.

Pritchett, W. C., 1990, Acquiring Better Seismic Data. New York: Chapman and Hall.

Rice, D., 2009, Applicability of 2-D time-lapse high resolution seismic reflection approach to image natural salt-dissolution and subsidence in central Kansas and improved post-processed vibroseis data characteristics: M.S. Thesis, Lawrence, Kansas: University of Kansas.

Russell, D.J., 1993, Role of the Sylvania Formation in sinkhole development, Essex County: Ontario Geological Survey, Open File Report 5861, p 122.

Shalev, E., V. Lyakhovsky, and Y. Yechieli, 2006, Salt dissolution and sinkhole formation along the Dead Sea shore: Journal of Geophysical Research, v 111.

Sherriff, R.E., 2002, Encyclopedic Dictionary of Applied Geophysics, 4th ed.: Oklahoma Society of Exploration Geophysicists, Tulsa, p 429.

Simm, R., and M. Bacon, 2014, Seismic Amplitude: An interpreter's handbook, Cambridge University Press.

Spinazola, J. M., J.B. Gillespie, and R.J. Hart, 1985, Ground-water flow and solute transport in the Equus beds area, south-central Kansas, 1940-1979, U.S. Geological Survey, Water-Resources Investigations Report 85-4336.

Steeples, D.W., 1980, Seismic reflection investigations of sinkholes in Russell and Ellis counties, Kansas: Progress report to the Kansas Department of Health and Environment and the Kansas Department of Transportation, p 14.

Steeples, D.W., R.W. Knapp, and C.D. McElwee, 1986, Seismic reflection investigations of sinkholes beneath interstate highway 80 in Kansas: *Geophysics*, v. 51, p. 295-301.

Steeples, D. W., and R.D. Miller, 1998, Avoiding pitfalls in shallow seismic surveys. Geophysics, p 1213-1224.

Stolt, R. H., 1978, Migration by fourier transform: Geophysics, 43, p 23–48.

Stolt, R.H., and A.F. Benson, 1986, *Seismic Migration*: Geophysical Press.

Terzaghi, R.D., 1970, Brinefield subsidence at Windsor, Ontario: Third Symposium on Salt, Vol II, Northern Ohio Geological Society, Cleveland, p 298-307.

Urai, J.L., C.J. Spiers, H.J. Zwart, and G.S. Lister, 1986, Weakening of rock salt by water during long-term creep: *Nature*, v 324, p 554-557.

Ver Wiebe, W.A., 1937, Wichita Municipal Univ. Bull., v. 12, no 5.

Walden, A., 1991, Making AVO sections more robust: Geophysical Prospecting, p 915-942.

Walters, R. F., 1978, Land subsidence in central Kansas related to salt dissolution: Kansas Geological Survey, Bulletin 214.

Walters, R.F., 1980, Solution and collapse features in the salt near Hutchinson, Kansas: Geological Society of America, South-central Section, Field Trip Notes, 10 p.

Waltham, T., F. Bell, and M. Culshaw, 2005, Sinkholes and Subsidence: Karst and Cavernous Rocks in Engineering and Construction. Chichester, UK: Praxis Publishing.

Watney, W.L., and S.E. Paul, 1980, Maps and cross sections of the Lower Permian Hutchinson salt in Kansas: Kansas Geological Survey Open-file Report 80-7, 10 p., 6 plates, map scales 1:500,000.

Watney, W.L., J.A. Berg, and S.E. Paul, 1988, Origin and distribution of the Hutchinson Salt (lower Leonardian) in Kansas, In W. A. Morgan, & J. A. Babcock, Permian rocks of the Mindcontinent: Midcontinent SEPM Special Publications no 1, p 113-135.

Watney, W.L., S.E. Nissen, S. Bhattacharya, and D. Young, 2003, Evaluation of the role of evaporite karst in the Hutchinson, Kansas, gas explosions, January 17 and 18, 2001; in K.S. Johnson and J.T. Neal, eds., Evaporite karst and engineering/environmental problems in the United States: Oklahoma Geological Survey Circular 109, p. 119-147.

West, R., K.B. Miller, and W.L. Watney, 2010, The Permian System in Kansas: Kansas Geological Survey, Bulletin 257.

Widess, M.B., 1973, How thin is a thin bed?: *Geophysics*, v. 38, p. 1176-1180.

Xia, J., R.D. Miller, D.W. Steeples, and D. Adkins-Heljeson, 1995, Kansas Geological Survey Map Series, M-41E

Yilmaz, Ö., 1987, *Seismic Data Processing*: Tulsa, Society of Exploration Geophysicists.

Yilmaz, Ö., 2001, Seismic Data Analysis: Society of Exploration Geophysics, 2nd Edition.

Zhang, K., and K. Marfurt, Time-Frequency domain spectral balancing and phase dispersion compensation, University of Oklahoma.